DISSERTATION

ECONOMIC AND ENVIRONMENTAL EVALUATION OF EMERGING ELECTRIC VEHICLE TECHNOLOGIES

Submitted by

Noah Horesh

Department of Mechanical Engineering

In partial fulfillment of the requirements

For the Degree of Doctor of Philosophy

Colorado State University

Fort Collins, Colorado

Summer 2023

Doctoral Committee:

Advisor: Jason Quinn

Thomas Bradley
Shantanu Jathar
Bryan Willson

ABSTRACT

ECONOMIC AND ENVIRONMENTAL EVALUATION OF EMERGING ELECTRIC VEHICLE TECHNOLOGIES

As the transportation sector seeks to reduce costs and greenhouse gas (GHG) emissions, electric vehicles (EVs) have emerged as a promising solution. The continuous growth of the EV market necessitates the development of technologies that facilitate an economically comparable transition away from internal combustion engine vehicles (ICEVs). Moreover, it is essential to incorporate sustainability considerations across the entire value chain of EVs to ensure a sustainable future. The sustainability of EVs extends beyond their usage and includes factors such as battery production, charging infrastructure, and end-of-life management. Techno-economic analysis (TEA) and life cycle assessment (LCA) are key methodologies used to evaluate the economic and environmental components of sustainability, respectively. This dissertation work uses technological performance modeling combined with TEA and LCA methods to identify optimal deployment strategies for EV technologies.

A major challenge with the electrification of transportation is the end of life of battery systems. A TEA is utilized to assess the economic viability of a novel Heterogeneous Unifying Battery (HUB) reconditioning system, which improves the performance of retired EV batteries before their 2nd life integration into grid energy storage systems (ESS). The modeling work incorporates the costs involved in the reconditioning process to determine the resale price of the batteries. Furthermore, the economic analysis is expanded to evaluate the use of HUB reconditioned batteries in a grid ESS, comparing it with an ESS assembled with new Lithium-ion (Li-ion) batteries. The minimum required revenue from each ESS is determined and compared with the estimated revenue of various grid applications to assess the

market size. The findings reveal that the economical market capacity of these applications can fully meet the current supply of 2nd life EV batteries from early adopters in the United States (U.S.). However, as EV adoption expands beyond early adopters, the ESS market capacity may become saturated with the increased availability of 2nd life batteries. Despite the growing interest in EVs, their widespread adoption has been hindered, in part, by the lack of access to nearby charging infrastructure.

This issue is particularly prevalent in Multi-Unit Dwellings (MUDs) where the installation of chargers can be unaffordable or unattainable for residents. To address this, TEA methodology is used to evaluate the levelized cost of charging (LCOC) for Battery Electric Vehicles (BEVs) at MUD charging hubs, aiming to identify economically viable charger deployment pathways. Specifically, multiple combinations of plug-in charger types and hub ownership models are investigated. Furthermore, the total cost of ownership (TCO) is assessed, encompassing vehicle depreciation, maintenance and repair, insurance, license and registration, and LCOC. The study also conducts a cradle to grave (C2G) LCA comparing an average passenger BEV and a gasoline conventional vehicle (CV) using geographical and temporal resolution for BEV charging. The TCO is coupled with the C2G GHG emissions to calculate the cost of GHG emissions reduction. The analysis demonstrates that MUD BEVs can reduce both costs and GHG emissions without subsidies, resulting in negative costs of GHG emissions reduction for most scenarios. However, charging at MUDs is shown to be more expensive compared to single-family homes, potentially leading to financial inequities. Additional research is required to assess the advantages of public charging systems and commercial EVs.

While home charging is typically the primary option for EVs, public charging infrastructure is necessary for long-distance travel and urgent charging. This is especially important for commercial vehicles, which rely on public charging to support their operational requirements. Various charging systems have been proposed, including Direct Current Fast Charging (DCFC), Battery Swapping (BSS), and Dynamic Wireless Power Transfer (DWPT). This work includes a comparison of the TCO and global warming potential (GWP) of EVs of various sizes, specifically examining the charging systems utilized to determine precise location-specific sustainability outcomes. Nationwide infrastructure deployment simulations are conducted based on the forecasted geospatial and temporal demand for EV charging from 2031 to 2050. The TEA and LCA incorporate local fuel prices, electricity prices, electricity mixes, and traffic volumes. To account for the adaptability of variables that highly influence TCO and GWP, optimistic, baseline, and conservative scenarios are modeled for EV adoption, electricity mixes, capital costs, electricity prices, and fuel prices. The change to TCO by switching from ICEVs to EVs is shown to vary across scenarios, vehicle categories, and locations, with local parameters dramatically impacting results. Further, the EV GWP depends on local electricity mixes and infrastructure utilizations. This research highlights the dynamic nature of EV benefits and the potential for optimal outcomes through the deployment of multiple charging technologies.

In conclusion, this research underscores the significance of strategically deploying EV charging infrastructure and utilizing retired EV batteries for grid energy storage. Instead of posing a challenge at end of life, these batteries are shown to be a solution for grid energy storage. The study also highlights the economic advantages of different charging infrastructure types for EVs and their role in driving EV adoption, resulting in potential GHG emissions reductions and consumer savings. Ultimately, widespread EV adoption and decarbonization of electrical grids are pivotal in achieving climate goals.

ACKNOWLEDGEMENTS

I would like to thank my esteemed committee members—Dr. Thomas Bradley, Dr. Shantanu Jathar, and Dr. Bryan Willson—for providing their support and expertise. I would like to express my deepest gratitude and appreciation to my research advisor, Dr. Jason Quinn, whose unwavering guidance and support have been invaluable throughout my graduate journey. I am also grateful to the entire Quinn research group and my collaborators at Argonne National Laboratory and ASPIRE ERC for their endless feedback. Lastly, I am deeply thankful to my family and friends for their constant support, encouragement, and belief in me as I pursued this degree.

Funding support for Chapter 2 was provided by the Department of Energy Advanced Research Projects Agency-Energy (ARPA-E) award number DE-AR0001045. Funding support for Chapter 3 was provided by the National Science Foundation Non-Academic Research Internships for Graduate Students (INTERN) under award number 1941524 and the Vehicle Technologies Office, Office of Energy Efficiency and Renewable Energy, United States Department of Energy. Funding support for Chapter 4 was provided by the National Science Foundation under award number 1941524. Opinions, findings, conclusions, or recommendations expressed here are those of the author(s) and do not necessarily reflect the view of the U.S. Department of Energy or the National Science Foundation.

TABLE OF CONTENTS

CHAPTER 1: INTRODUCTION

In pursuit of national climate goals, the United States (U.S.) White House has set a target for electric vehicles (EVs) to account for 50% of vehicle sales by 2030 [1]. This ambitious target aims to reduce greenhouse gas (GHG) emissions from the transportation sector, which contributed to 29% of U.S. GHG emissions in 2019 [2]. Achieving this target necessitates a significant transformation of both the electric grid and the transportation system. To support this transition, there is a critical need for technological solutions that facilitate strategic charging infrastructure deployment and address end-of-life challenges. These solutions must establish a sustainable future for both sectors, and their effectiveness can be evaluated through Techno-Economic Analysis (TEA) and Life Cycle Assessment (LCA).

The widespread use of lithium-ion (Li-ion) batteries in EVs and grid storage is driven by their lightweight design, high energy density, low self-discharge, and reliable performance [3,4]. Li-ion batteries are expected to remain the preferred battery chemistry in the near future, and ongoing research and development (R&D) efforts are focused on improving Li-ion battery chemistries to develop the next generation of battery technologies [5–7]. However, it is projected that the world's lithium reserves can only produce batteries for approximately one billion EVs with a capacity of 40 kilowatt-hours (kWh) each. Therefore, to sustainably meet the projected demand for EVs and grid storage, recycling or reusing EV batteries will be necessary [8]. The increasing demand and limited supply of Li-ion batteries will have remarkable impacts on various supply chains, particularly in managing EV batteries at the end of their 1st life. The retired EVs of early adopters have recently given rise to the need for effective strategies to handle these batteries.

The end of the 1st life for EV batteries occurs when the State of Health (SOH) of the battery reaches approximately 80%. At this point, the batteries can no longer reliably meet the high-performance criteria required for use in EVs. However, they can still be potentially reused for less demanding applications or recycled. While Li-ion recycling will likely be necessary, research by Olsson et al. (2018) suggests that reuse and subsequent recycling are complementary processes that extend the resource cycle more effectively than recycling alone [9]. To address this challenge, Original Equipment Manufacturers (OEMs) have initiated 2nd life battery businesses and have begun selling batteries to 2nd life enterprises. However, minimal work has been done to evaluate the economic viability of utilizing 2nd life EV batteries in grid applications. As more grid applications seek to reduce the costs of energy storage, targeted R&D, based on TEAs of innovative technological solutions such as 2nd life battery reconditioning, are needed to cost-effectively utilize the increasing supply of 2nd life batteries resulting from broader EV adoption.

Early EV adoption has predominantly been limited to residents of single-family homes, partly due to their higher household incomes and access to charging infrastructure [10]. Battery electric vehicles (BEVs), the most popular type of EV currently [11], rely solely on stored electrical energy from charging. Thus, charging infrastructure is needed to limit range anxiety at several vehicle destinations such as homes, public, and workplaces [12,13]. In California, home charging was found to be the primary charging location for 94% of EV owners living in single-family homes [14]. However, only 48% of California's EV owners living in Multi-Unit Dwellings (MUDs) primarily charged their vehicles at home due to limited access to home chargers [14]. Deploying chargers at MUDs presents unique challenges, including outdated or inadequate electrical service and high capital costs for MUD residents [14–16], many of whom have low-to-moderate incomes [10,14]. To overcome the financial barriers faced by residents from installing EV charging infrastructure, it is necessary to explore solutions that can reduce charging costs and shift the upfront investment burden to potential investors, such as private companies, utilities, and property owners. TEA can used to evaluate the charging costs associated with various ownership models and charger types for MUD charging hubs. Thus, the economic feasibility of different combinations can be assessed, enabling a comprehensive evaluation of charger deployment options.

While home charging remains the primary option for personal vehicle owners, public charging infrastructure is essential, particularly for those without access to home charging or requiring additional range during their journeys [12,13]. Unlike home charging, which typically occurs at the vehicle's destination, public charging typically occurs between vehicle destinations and thus interrupts the vehicle's trip [12]. As vehicle electrification expands to include medium and heavy-duty classes, which have larger battery capacities than light-duty vehicles [17–19], it becomes imperative to explore charging technologies that can reduce charging durations and enhance convenience.

Traditional charging technologies involve physically connecting the vehicle to a plug while stationary, with power levels typically ranging from 1.9 to 50 kilowatts (kW), resulting in lengthy charging times. However, advancements in charging systems offer alternatives that can dramatically reduce these durations. Direct Current Fast Charging (DCFC) enables vehicles to be charged with up to 350 kW of power while stationary, substantially reducing the time required for charging. Battery Swapping (BSS) eliminates real-time charging by replacing the depleted battery with one charged in advance using a traditional charger [20]. Dynamic Wireless Power Transfer (DWPT) enables vehicles to charge while driving on high traffic density roadways using 50 kW pads embedded in the pavement [21]. Each of these charging systems possesses distinct parameters and characteristics [22–24], and it is essential to assess their economic viability and environmental impact through TEA and LCA to ensure their sustainability before widespread deployment.

Previous TEA and LCA studies of EVs have highlighted the importance of EV usage and battery production in terms of GHG emissions and total cost of ownership (TCO) [22,25]. The cost of EV usage primarily stems from charging, which varies depending on the location and charger type, emphasizing the importance of evaluating the economics of charging systems [26]. Additionally, the emissions associated with EV usage depend on the grid mix that supplies electricity to the charger [27]. Literature has shown substantial variations in GHG emissions reductions across different U.S. state grid mixes, ranging from 10% to 87% in 2020 [28]. Furthermore, considering that grid mixes are non-uniform and GHG emissions vary throughout the day, it is important to consider the time-of-day that the EV charges [29]. The choice of charging system also impacts usage emissions, and the size of the vehicle's battery can differ between charging systems. Notably, DWPT charging enables the use of smaller batteries, resulting in reduced costs and emissions associated with battery production [24]. Moreover, the total GHG emissions from battery production, on a per kWh discharged basis, can be lowered by providing a 2^{nd} life to the batteries.

This dissertation aims to address the aforementioned challenges faced by the transportation system and electric grid resulting from vehicle electrification. The scope of this work spans the entire value chain of EV systems, including an assessment of the economic viability of 2^{nd} life battery systems and a detailed evaluation of home and public charging infrastructure through integrated TEA and LCA. By using TEA and LCA methodologies, this research seeks to gain a comprehensive understanding of EV technologies from both economic and environmental perspectives. The outcomes of this work will serve as valuable guidance for decision-makers and support future R&D efforts for EV technologies.

CHAPTER 2: TECHNO-ECONOMIC ANALYSIS OF A NOVEL METHOD TO RECONDITION SECOND LIFE ELECTRIC VEHICLE BATTERIES[1]

2.1 Introduction

In 2019 there were 2.8 million (M) EVs produced globally, and EVs are expected to be a quarter of market sales by 2030 [30]. This surge in EV adoption emphasizes the expanding market for EV batteries and underscores the importance of exploring opportunities for their 2nd life usage. By leveraging the potential of 2nd life applications, the lifecycle of EV batteries can be extended, contributing to resource efficiency and sustainability in the EV industry.

While OEMs have begun developing 2nd life battery applications, minimal work has been done to evaluate the economic viability of using 2nd life EV batteries in grid applications. Mathews et al. (2020) determined a utility scale solar-plus-storage system would be profitable if 2nd life batteries are sold for <60% of the price of a new battery [31]. Neubauer and Pesaran (2011) determined area regulation to be profitable while electric service power quality, wind generation grid integration, short duration transmission and distribution upgrade deferral, and voltage support will likely be profitable [32]. Song et al. (2019) found 2nd life batteries used in wind farms currently not economical [33]. Other studies determined residential demand management coupled with photovoltaics would be profitable [34], [35]. Heymans et al. (2014) found that load leveling would only be profitable under favorable conditions [36].

[1] This chapter was published as a peer-reviewed journal article: Horesh N, Quinn C, Wang H, Zane R, Ferry M, Tong S, Quinn J. Driving to the future of energy storage: Techno-economic analysis of a novel method to recondition second life electric vehicle batteries. Applied Energy 2021;295:117007. https://doi.org/10.1016/j.apenergy.2021.117007.

While these studies have investigated the market potential for 2nd life ESS, these studies simply leveraged prior estimates for battery acquisition costs and performance. This is a major assumption and does not accurately capture the market price and performance of 2nd life batteries considering technology advancements focused on reconditioning of batteries.

Cready et al. (2003) quantified the battery resale price and repurposing costs for used Nickel Metal Hydride EV battery modules, and the results show that labor dominates the cost of repurposing [37]. A study by Neubauer et al. (2015) estimated the costs to repurpose EV Li-ion battery modules, however, the resale price was simply calculated by multiplying the price of a new battery by the health factor of the 2nd life battery [38]. While various studies have estimated the cost of a repurposed 2nd life battery systems, to our knowledge none have evaluated the cost of using reconditioning techniques to improve the performance of a 2nd life ESS.

Second life battery reconditioning represents an exciting opportunity to improve the performance and thus the value of 2nd life batteries. This research chapter evaluates the economics to recondition batteries using a novel reconditioning process that uses a Heterogeneous Unifying Battery (HUB) system to improve SOH uniformity of the cells in each battery module without the need to deconstruct the battery module. The HUB reconditioning process economics were modeled using two different scenarios: reconditioning with grid services (RGS) and reconditioning through energy shuffle (RES). The economics of the HUB reconditioning methods are directly compared to the traditional repurposing process which sorts battery modules to produce battery packs with similar SOHs. This work determines the resale price after HUB reconditioning or repurposing batteries and then expands the system boundary of the economic analysis to include energy or power services that leverage the 2nd life batteries. The economics of the 2nd life batteries are compared to new Li-ion batteries used for power and energy services. Specifically, the cost and performance of the 2nd life and new Li-ion batteries for multiple power and energy applications are considered. The work includes a sensitivity analysis to support strategic investment in R&D to drive the technology towards commercialization. The novelty of the work includes the economic evaluation of 2nd life battery reconditioning that enables improved performance as compared to repurposing with an extended system boundary used to evaluate the viability of grid ESS.

2.2 Methods

This work includes a battery performance model coupled with techno-economic analysis (TEA) methodology to evaluate the economic viability of two novel HUB reconditioning pathways (RGS and RES) as well as a direct comparison to traditional repurposing. The RGS scenario performs grid services at certain times in the day to charge and discharge the battery modules which is required for reconditioning. The RES scenario constantly shuffles energy between two battery banks reducing the time for reconditioning.

Two system boundaries were used to evaluate the technology; the first determined the minimum battery selling price for a 2nd life battery and the second expanded the system boundary to determine the minimum required revenue from a grid ESS that uses 2nd life batteries. All scenarios and methods assumed relevant expenses and revenue streams to operate a facility in California. California was chosen since it has an expanding battery storage market and the most EV sales in the U.S. since 2011 [39], [40].

2.2.1 TEA Overview

2.2.1.1 System Boundary and Scenarios

Figure 1 shows a framework and description of the scenarios, economics, sensitivity analysis, and market potential developed. The economic analysis included two system boundaries: 2nd Life Resale and Grid ESS. The resale system boundary was limited to the scenarios of reconditioning or repurposing of batteries to define the required resale price of 2nd life batteries. The grid ESS system boundary included all aspects of the resale system boundary and extended the economic assessment to also include the use of 2nd life batteries in an ESS to provide either power or energy grid services. Repurposing was used for comparison in both the 2nd life resale and grid ESS system boundary scenarios while a new Li-ion battery scenario was used as a comparison to the reconditioned batteries in the grid ESS system boundary. A sensitivity analysis was performed for the energy market ESS to identify high impact inputs of each battery type. Also, the market potential of the ESS with different battery types was determined based on the revenues and market sizes of energy and power applications.

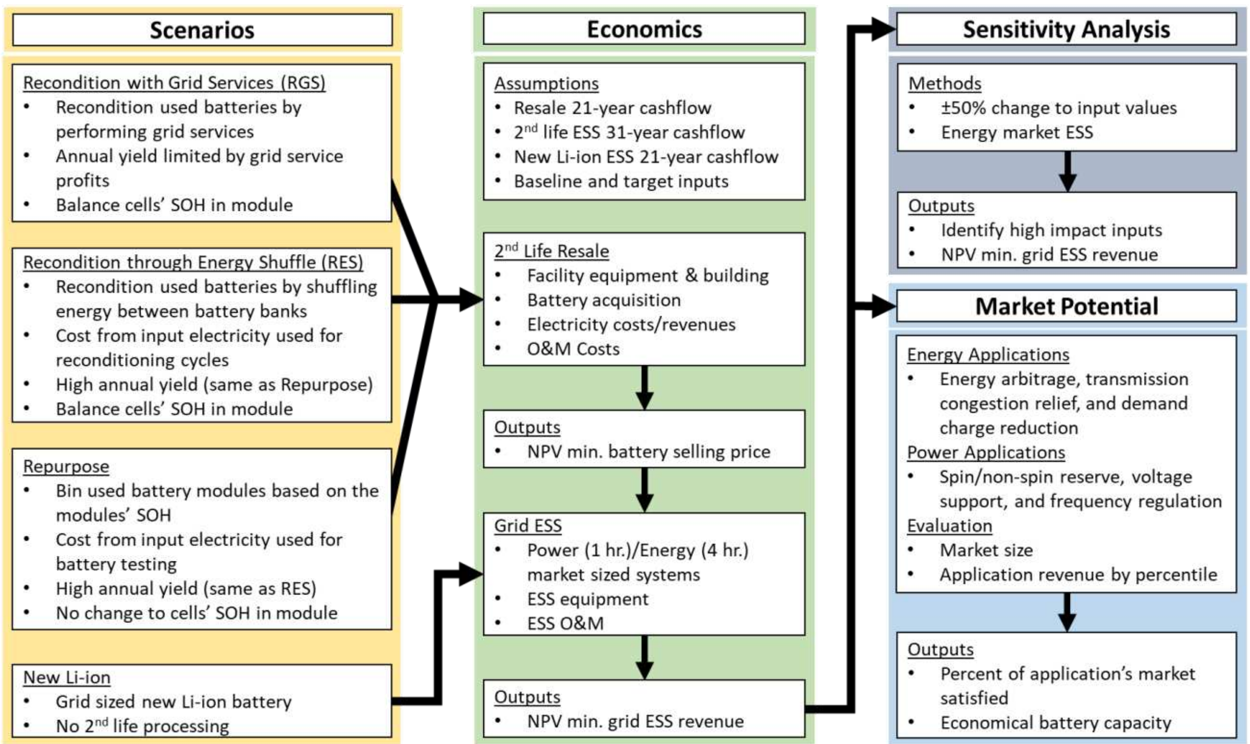

Figure 1: Flow diagram of the scenarios used to evaluate the economics of 2nd life battery resale and grid ESS. The resale scenario was for 2nd life batteries that use the processing methods of RGS, RES, and repurpose. The ESS scenario was for new and 2nd life batteries that were used in either power markets or energy markets. The sensitivity analysis was for energy market ESS that have new Li-ion, RGS, RES, or repurposed batteries. The economic outputs from the ESS were used to determine the market potential of each of the battery types.

As shown in Figure 1, three 2nd life battery processing scenarios were modeled: RGS, RES, and repurpose. The economics of these methods are presented in the subsequent sections of 2.2.2 Recondition with Grid Services (RGS), 2.2.3 Recondition through Energy Shuffle (RES), and 2.2.4

Repurpose. Each of these methods had specific operational parameters that characterized the key performance of the process with a summary presented in Table 1.

Table 1: Key performance parameters for 2nd life battery processing scenarios RGS, RES, and repurpose.

Assumption	RGS	RES	Repurpose	Units
Annual Battery Yield	122 (Eq. 1)	219 (Eq. 1)	219 (Eq. 2)	MWh
Battery Acquisition Price	35 [38]	35 [38]	35 [38]	$/kWh
C-rate	0.5 (a)	0.5 (a)	0.5 (a)	1/h
Viable Product	99% [38]	99% [38]	99% [38]	%
Reconditioning/ Repurposing Cycles	300 (a)	300 (a)	2 (a)	Cycles
Cycles per Day	3.35 (b)	6 (c)	-	Cycles/day
Roundtrip Efficiency	90% [31]	90% [31]	90% [31]	%
DC-DC Converter/ BMS Cost	500 (a)	500 (a)	-	$/kW
Electricity Purchase Price	0.16 [41]	0.14 [42]	0.16 [41]	$/kWh
Warranty	5% [38]	5% [38]	5% [38]	%
Adapter Tub Price	100 (a)	100 (a)	-	$/kWh
Facility Size	2,463 (T. A2)	2,463 (T. A2)	1,620 (T. A2)	m^2

(a) Developer input (b) Based on CAISO RTM energy arbitrage from 2018 [43] (c) 4-hour cycles and 24-hour operation

All methods evaluated both a baseline and target scenario. The baseline scenario represented the best estimates for a system built in 2019. The target scenario represented potential improvements to the system based on preliminary findings from R&D efforts. The assumptions in Table 1 were for the baseline scenarios and the assumptions for the target scenario for each method are shown in Table A1. The target scenarios include potential reductions in the reconditioning cycles, labor task times, warranty, transportation distance, hardware costs, and acquisition price.

The annual battery yield (Table 1) of each method was used to compute the variable operational costs and annual revenue from battery sales. The annual battery yield of the two HUB reconditioning methods varied depending on the number of reconditioning cycles that could be achieved each day due to the system operation. The annual battery yield (Y) was calculated (Eq. 1) based on the facility reconditioning capacity (C_{rec}), number of reconditioning cycles needed (N), and average number of reconditioning cycles per day (n).

$$Y = C_{rec} * 365 * n/N \qquad (1)$$

The annual battery yield of the repurposing method (Y) was set equal to the annual battery yield of the RES method for comparison. Repurposing was assumed to take three days (t). The facility repurposing capacity (C_{rep}) was calculated using Eq. 2.

$$C_{rep} = Y * t/365 \qquad (2)$$

2.2.1.2 TEA Methodology

Capital costs, operational costs, grid revenue, and annual battery yields from the facility were used as inputs into a yearly discounted cash flow rate of return (DCFROR) analysis. This methodology is consistent with previous repurposing studies that quantified the cost of repurposing [37], [38]. The DCFROR used n^{th} plant assumptions which most notably assumed an internal rate of return (IRR) of 10%, a 35% tax rate, and debt financing at 50%. The capital costs included all of the expenses incurred in year zero of the cashflow during the 1-year build period which included the facility building, grid connection equipment, and facility equipment expenses. The operational costs consisted of the expenses incurred after year zero while the facility was in operation for years 1 through 20. The operational costs did not account for changes to market prices over time. The DCFROR analysis calculated the minimum battery selling price by adjusting the required revenue from the 2^{nd} life battery resale such that a Net Present Value (NPV) of zero was achieved in the 21-year cashflow. The minimum battery reselling price was computed for the HUB reconditioned and repurposed batteries. The economic analysis for the grid ESS determined the required revenue in a 31-year cashflow for the ESSs instead of a selling price for the batteries. For both system boundaries, the reconditioning and repurposing facilities were assumed to operate for 20-years. Thus, a 31-year cashflow was used for the grid ESS to account for the batteries processed in the final year of the facility that were then used in ESSs; the batteries processed in the final year of the facility were retired from the grid ESS 10 years later (Table 2). The new Li-ion battery scenario used a 21-year cashflow that also computed the required revenue from the ESS. Each grid ESS was assumed to operate for 20 years for both 2nd life and new Li-ion ESSs. All expenses were converted to 2019 values using producer price indexes.

2.2.2 Recondition with Grid Services (RGS)

We assumed that OEMs disassemble battery packs and extract modules prior to acquisition. Once the modules were acquired and transported to the reconditioning facility, the modules underwent the reconditioning process to balance the SOH of the cells within the modules without deconstruction. The HUB system used a modular DC-DC power converter matrix with isolated series output connections to achieve fully independent control of energy flow to each of the battery cells [44]. This provided model-based control that drove each battery's SOH towards uniformity. The energy flow required for reconditioning was used to perform grid services in the energy arbitrage market.

2.2.2.1 Capital Costs

The capital costs of the reconditioning facility consisted of the facility building ($2.4M [45], [46], [47], [48]), grid equipment ($3.1M [49], [50]), and facility equipment ($9.2M [47], [51], [52], [53]). To determine these costs, a commercial sized facility with a reconditioning capacity of 30 MWh-nameplate was assumed. The electronics power rating (P) was computed (Eq. 3) based on the reconditioning capacity (C), average usable battery capacity (U), and C-rate (R) (Table 1).

$$P = CUR \qquad (3)$$

A detailed breakdown of the analysis for the facility size (Table A2), facility building (Table A3), grid equipment (Table A4), and facility equipment (Table A5) is presented in Appendix A.

2.2.2.2 Operational Costs

Electricity

The aim of using grid services to complete reconditioning cycles was to gain a net profit from charging and discharging the batteries. Energy arbitrage was chosen as the grid service since it had the appropriate C-rate and load profile for reconditioning batteries. The grid profits were estimated to be 0.02 $/kWh per cycle or $820K annually for energy arbitrage in the California Independent System Operator (CAISO) Real-Time Market (RTM) using 2018 historical pricing data; details of our study are provided in Appendix A [43]. This estimate accounted for the grid participation fees and efficiency losses for a ½ C-rate system. The auxiliary electricity used for lighting and HVAC (heating, ventilation, and air conditioning) was assumed to be supplied by Pacific Gas and Electric rather than from CAISO and the A-10 Tariff (0.16 $/kWh) was used and thus resulted in an annual cost of $82K [41].

All Other Costs

The remainder of the operational costs were transportation (90 thousand (K) $/year [54], [55]), battery acquisition (35 $/kWh-nameplate [38]), variable labor (6.31 $/kWh-nameplate or 772K $/year [56], [57]), fixed labor (457K $/year [57], [58], [59], [60]), insurance (80K $/year), and warranty (5% of resale price [38]). Appendix A includes details on the costs of transportation (Table A6), labor (Table A7), and facility operations.

2.2.3 Recondition through Energy Shuffle (RES)

The RES scenario used the same process as in 2.2.2 Recondition with Grid Services to cycle the batteries to get a unified SOH. The primary difference was that the energy used for reconditioning was supplied by the utility and discharged to another battery bank rather than back to the grid. The energy taken from the utility resupplied the energy that was lost due to charging and discharging losses from shuffling energy between battery banks.

2.2.3.1 Capital Costs

The same building costs ($2.4M) and facility equipment costs ($9.2M) were used as in the Recondition with Grid Services scenario (section 2.2.2). The grid equipment ratings were reduced relative to the Recondition with Grid Services scenario since the only power drawn from the grid for reconditioning was to replenish the energy lost due to charging and discharging efficiencies. With lower ratings, the grid equipment costs were $574K.

2.2.3.2 Operational Costs

Electricity

The electricity used for reconditioning to charge the batteries from the grid was an expense since the energy was not discharged back to the grid like in 2.2.2 Recondition with Grid Services. The levelized cost of electricity for a continuous load was estimated to be 0.14 $/kWh with the Pacific Gas and Electric E-20 tariff (higher load) and the annual electricity cost was estimated to be $808K annually [42]. The electricity cost included the electricity used for both auxiliary and reconditioning loads. The auxiliary load (72K $/year) was the same as in the Recondition with Grid Services scenario (section 2.2.2) but this scenario used a less expensive E-20 tariff for electricity charges. The annual reconditioning load (L) was calculated using Eq. 4 based on the reconditioning capacity (C), average usable battery capacity (U), roundtrip efficiency (E), and average number of reconditioning cycles per day (n) (Table 1 and Table 2).

$$L = CU(1 - E)n365 \qquad (4)$$

All Other Costs

The other operational costs were similar to that of the Recondition with Grid Services scenario (section 2.2.2) since the same battery acquisition (35 $/kWh-nameplate), fixed labor (457K $/year), insurance (80K $/year), and warranty costs (5% of resale price) were assumed. The energy shuffle method had a higher battery yield (Table 1) which increased the total variable costs. The average discounted transportation costs were estimated to be $107K per year, and the variable labor costs were estimated to be 6.31 $/kWh-nameplate or $1.4M annually.

2.2.4 Repurpose

The repurposing method did not change the SOH of individual cells in modules. Rather, the repurposing method sorted modules by their SOHs and then the similar SOH modules were combined to make a "new" 2nd life battery pack. The repurposing method required the battery module to be inspected, tested, and then binned by SOH. The battery modules were inspected to check the integrity of the module prior to charging and discharging. The modules that passed the initial inspection were then characterized by charging and then discharging the modules at a ½ C-rate. The modules were subsequently binned by sorting and then placing them in a battery pack. The pack was then packaged by connecting the contacts and inspecting the pack. The battery pack was tested for quality assurance with a full charge and discharge cycle at a ½ C-rate.

2.2.4.1 Capital Costs

For comparison purposes, the facility processing capacity was calculated to be 1.8 MWh (Eq. 2) in order to have the same annual yield as the RES scenario (Table 1). The capital costs included the facility building ($1.7M) and facility equipment ($3.9M). It was assumed that grid equipment was not needed since the repurposing facility drew low power and did not perform grid services.

2.2.4.2 Operational Costs

Labor

The operational costs were similar to the reconditioning methods (Sections 2.2.2 and 2.2.3) with minor changes presented in Appendix A. The variable labor cost was estimated to be 10.17 $/kWh-nameplate or $2.2M annually [56], [57]. The fixed labor was estimated to be $470K annually [58], [59], [60], [61].

All Other Costs

The same costs as section 2.2.3 were used for transportation (107K $/year), battery acquisition (35 $/kWh-nameplate), insurance (80K $/year), and warranty (5% of resale price). The same A-10 electricity rate (0.16 $/kWh) that was used for section 2.2.2 auxiliary loads was used based on the total electricity load [41]. The electricity costs were from the lights, battery testing, and HVAC, and the total electricity costs were $100K annually.

2.2.5 Energy Storage System (ESS) Revenue

An alternative to computing the selling price of the battery module was to compute the required revenue from the battery in a 2nd life grid ESS. The scenarios considered were RGS, RES, repurpose, and new Li-ion. The ESSs with 2nd life batteries were compared to a new Li-ion battery ESS used for grid applications to determine the competitiveness of each technology. The high impact assumptions for each scenario's estimates are in Table 2.

Table 2: Major assumptions of ESS with scenarios of RGS, RES, repurpose, and new Li-ion

Assumption	**RGS**	**RES**	**Repurpose**	**New Li-ion**		**Units**
				Today	**2030**	
Battery Module Price	NA	NA	NA	209 [49]	110 [62]	$/kWh
Battery Life	10 [38]	10 [38]	10 [38]	10 [63]	10 [63]	Years
Power Applications ESS Cost	449 [49]	449 [49]	449 [49]	449 [49]		$/kW
Energy Applications ESS Cost	743 [49]	743 [49]	743 [49]	743 [49]		$/kW
ESS Life	20 [64]	20 [64]	20 [64]	20 [64]		Years
C-rate Power Applications	1 [65]	1 [65]	1 [65]	1 [65]	1 [65]	1/h
C-rate Energy Applications	0.25 [65]	0.25 [65]	0.25 [65]	0.25 [65]	0.25 [65]	1/h
Individual System Size	4 [65]	4 [65]	4 [65]	4 [65]	4 [65]	MW
Initial SOH/Usable Capacity	80% [66]	80% [66]	80% [66]	100%	100%	%
Depth of Discharge	50% [38]	50% [38]	50% [38]	80% [63]	80% [63]	%
Annual Operating Cost	10 [63]	10 [63]	10 [63]	10 [63]	10 [63]	$/kW

The assumptions in Table 2 are for the baseline scenario. The target scenario assumptions for the ESS are shown in Table A8. The ESS target scenario included all inputs from the resale target scenario (Table A1). The target scenario was based on improvements from R&D and projections for ESSs in 2025. Specifically, the target scenario reduced the ESS capital cost, ESS operating cost, battery acquisition prices, and increased the depth of discharge (DOD).

2.2.5.1 Energy Storage System Costs

Capital Costs

The ESS costs (Table 2) were determined for power and energy applications estimated by Fu et al. (2018) [49]. The ESS costs were defined as all ESS costs except for the battery. For power applications, the ESS was sized for a 1-hour discharge duration or 4-MW (4-MWh) [65],[67], and the ESS was estimated to cost 449 $/kW or $1.8M per ESS [49]. The power applications considered were spin/non-spin reserve, voltage support, and frequency regulation. A description of each power application can be found in Balducci et al. (2018) [67]. For energy applications, the ESS was sized for a 4-hour discharge duration or 4-MW (16-MWh) [65],[67], and the ESS was estimated to cost 743 $/kW or $3.0M per ESS [49]. The energy applications considered were energy arbitrage, transmission congestion relief, and demand charge reduction. A detailed breakdown of costs for the power and energy ESSs are shown in Table A9.

Operational Costs

Each ESS was assumed to have a yearly operating cost of 10 $/kW [63]. The ESS operational costs also included a disposal cost of 5 $/kWh-nameplate for the batteries removed from the ESS. Upon disposal, the batteries were recycled by a separate business.

2.2.5.2 Second Life Batteries

The grid ESS cashflow expanded upon the resale cashflows from RGS, RES, and repurpose. The cashflows from the resale scenario were expanded upon by adding the costs to build and operate the ESSs. A new 2nd life ESS was assumed to be built while the batteries continued to be processed. Each ESS was assumed to have debt financing as described in 2.2.1.2 TEA Methodology. Once the batteries were processed, they were transported to the ESS site. The batteries were then installed in the ESS and connected to the grid to perform grid services; the ESS grid services were different than the grid services performed for RGS. The reconditioned batteries were expected to have a longer life than repurposed batteries; however, since there was limited aging data for reconditioned batteries, the reconditioned batteries and repurposed batteries were assumed to have the same aging behavior. The batteries were projected to last for 10 years in a moderate climate such as Los Angeles [38]. Each ESS was assumed to last for 20 years of service with the first set of batteries replaced by recently processed batteries after 10 years of service [64]. ESSs were built until the first set of 2nd life batteries needed to be replaced. Thus, new ESSs were built from years 1 through 10. Then in years 11 through 20, the initial batteries were swapped with batteries that were recently processed. The ESSs and second set of batteries were then decommissioned in years 21 through 30. The total ESS capacity from years 0 through 30 was determined as the sum of the capacities multiplied by the DOD (Table 2) of the ESSs at each respective time. The maximum capacity of all the ESSs was 1.6 GWh which occurred from years 11 to 20. The ESS capacity over time is shown in Figure A1.

2.2.5.3 New Li-ion Battery

A yearly DCFROR analysis was used for a new Li-ion battery. The ESS cost and assumptions from 2.2.5.1 Energy Storage System Costs were used. The new Li-ion batteries were assumed to cost 209 $/kWh in year zero of the cashflow [49]. The batteries were assumed to last 10 years with an 80% DOD before needing replacement [63]. A new Li-ion battery was then be swapped in for a projected cost of

110 $/kWh in 2030 [62]. The required revenue for power and energy applications was then calculated based on this cashflow.

2.2.5.4 Market Potential

The required revenue for the 2nd life ESSs from grid applications were compared to the current market revenue from power and energy applications to assess the economic viability. The potential capacity (P_{cap}) from each application that could satisfy the minimum revenue of an ESS at a given revenue value was calculated by Eq. 5 using the market capacity (M) and percentile of revenue (R_{per}).

$$P_{cap} = M(1 - R_{per}) \qquad (5)$$

For each application, the potential capacity represents the portion of the market capacity with a revenue value equal to or greater than the revenue value at the given percentile. Balducci et al. (2018) provided a range of revenues from numerous energy storage valuation studies in terms of the minimum (0th percentile), 25th percentile, mean, 75th percentile, and maximum (100th percentile) [67]. The mean was assumed to be a reasonable approximation of the median. The percentiles of revenue that were not specified in Balducci et al. (2018) were linearly interpolated between the given percentiles.

2.2.6 Sensitivity Analysis

A sensitivity analysis was performed to identify high impact inputs in the TEA model and demonstrate how changes to these high impact inputs impacts the economics of the battery storage systems evaluated. Specifically, a sensitivity analysis of all baseline inputs of the ESS scenarios for RGS (105 inputs), RES (105 inputs), repurpose (96 inputs), and new Li-ion (24 inputs) were completed for energy applications. The 2nd life ESS scenarios included inputs from both the resale and expanded system boundaries. The sensitivity analysis varied each input independently by ± 50% and then recorded the respective result. A ± 50% variation to the inputs was deemed appropriate to encapsulate the uncertainty of the high impact inputs such as battery life which has been estimated to be between 5 [66] and 16 years [31].

2.3 Results and Discussion

The results from this work are presented in three sections: 2^{nd} Life Battery Resale Price for RGS, RES, and repurpose processing methods; Grid ESS where 2^{nd} life batteries processed and integrated into an ESS for grid applications; and Sensitivity Analysis to support future research direction.

2.3.1 2^{nd} Life Battery Resale Price

The minimum viable resale price based on the DCFROR analysis for 2^{nd} life batteries (excluding battery performance) is shown in Figure 2 for the RGS, RES, and repurpose processing methods. A baseline and target scenario are evaluated for each of the three processing methods and the red diamonds denote the minimum viable resale price. Repurposing and RGS are found to be the most economical pathway for 2^{nd} life battery processing under the baseline and target scenarios respectively. However, the repurpose scenario only provides a 10% advantage in the baseline scenario and assumes that the repurposed batteries would have equal lifetime performance as the HUB reconditioned batteries. The baseline and target results for 2^{nd} life battery resale are further discussed in 2.3.1.1 and 2.3.1.2.

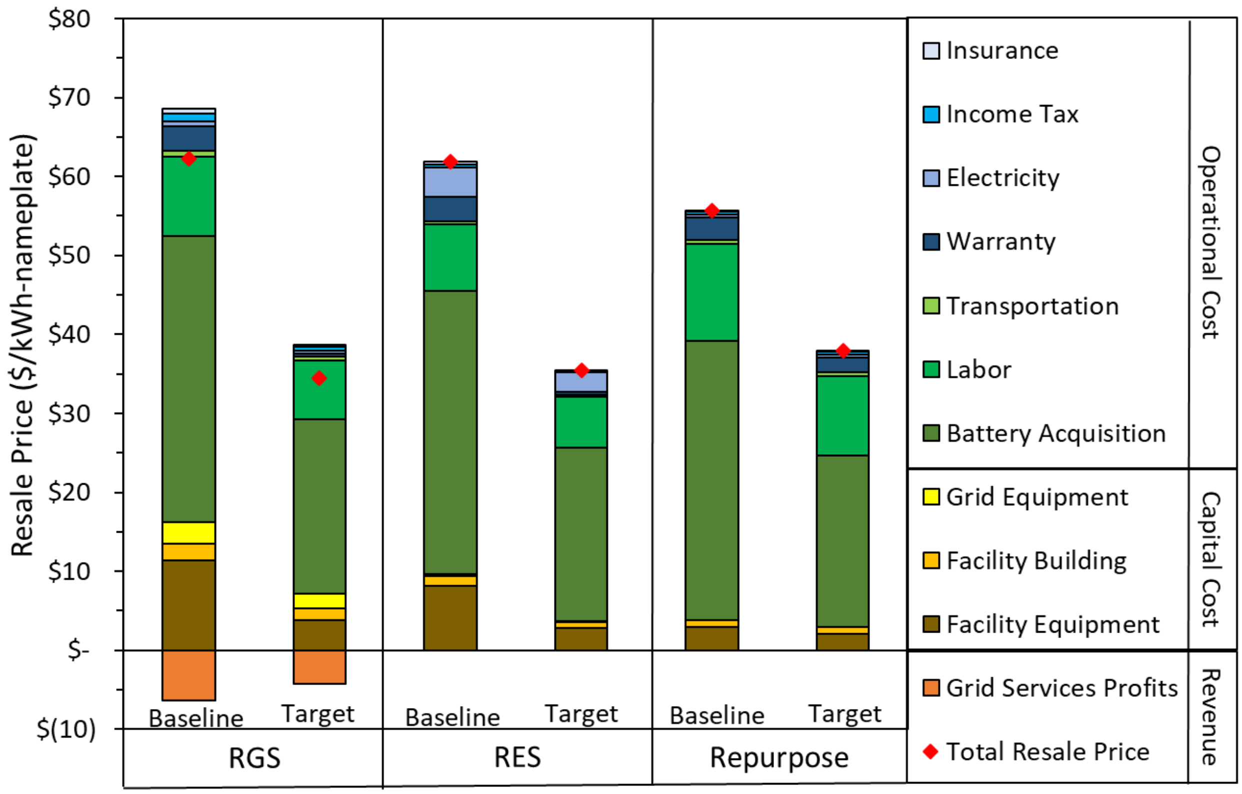

Figure 2: Baseline and target resale prices per kWh-nameplate for the recondition with grid services, recondition through energy shuffle, and repurpose scenarios.

2.3.1.1 Baseline Scenario

The baseline resale prices for RGS, RES, and repurposing are 62.21, 61.89, and 55.65 $/kWh-nameplate respectively. The RES method has a higher annual yield (219 MWh) than RGS (122 MWh). The higher throughput for RES is due to the ability to continually recondition the batteries (charge and discharge) without the need to wait for optimal times to participate in the energy arbitrage market to maximize grid profits (Table 1). While the systems are assumed to be continually cycled, proper charging levels are maintained to protect the system electronics from overheating. The repurposing method was modeled to have the same annual yield as the RES method of 219 MWh (Table 1). With a higher battery yield due to reduced time in the facility, the RES and repurposing processes distribute the fixed capital and operational costs across the resale price of more batteries due to a higher annual yield thus reducing these impacts.

The baseline resale price of RES is lower than RGS, however, the repurposing method has the lowest baseline resale price of all the scenarios (55.65 $/kWh-nameplate). The resale price does not account for the potential battery life improvement and reliability from reconditioning. Repurposing has high labor costs while the HUB reconditioning processes also have high capital costs due to the facility equipment, facility building, and grid equipment. The high labor cost of the repurposing method is due to the labor intensity of the repurposing process. The impact of the high labor cost for the repurposing method is approximately equal to the impact of the high capital cost in the RES method. In the DCFROR analysis, an annual operational cost of $1M from years 1 to 20 is equivalent to a capital cost of $9M in year 0. Thus, there is a trade-off between increasing capital costs to reduce operational costs and vice versa which is demonstrated by the reconditioning and repurposing scenarios.

One major operational difference between reconditioning and repurposing is that reconditioning is an energy intensive process and repurposing is not. The RGS method eliminates electrical operational costs required for battery reconditioning cycles by participating in the energy arbitrage market. Using historical CAISO data, the simulated grid service revenues from energy arbitrage are 6.40 $/kWh-nameplate of battery or 0.02 $/kWh of profit per cycle for RGS. Since the RES method does not participate in grid services, our model assumes a 10% energy loss during each reconditioning cycle that must be resupplied at a cost of 0.14 $/kWh (Table 1) to maintain system functionality. The total cost of electricity used for reconditioning cycles for the RES method is 3.36 $/kWh-nameplate. Thus, the difference between the RGS profits and RES costs for reconditioning cycles is a substantial 9.76 $/kWh-nameplate. The RGS method does not generate enough revenue from grid services to offset the opportunity cost of waiting to perform reconditioning cycles. The opportunity cost is defined as the time the batteries are idle when they could be actively reconditioned through energy cycling. This opportunity cost results in a lower annual yield and therefore fewer battery sales. As a result, the RGS method has the highest resale price for the baseline scenario.

Under the baseline scenario, the RGS method could be competitive with the RES method if the revenue from grid services increases. The baseline resale price of RES is 61.89 $/kWh-nameplate. For the baseline RGS to have the same resale price as the baseline RES, the grid services would need to profit $857K annually which is a mere 4% increase to the baseline revenue assumption. This value could be surpassed by stacking the grid services of frequency regulation and energy arbitrage [68]. This is not included in the primary analysis of the RGS method due to uncertainties on the compatibility of frequency regulation with the SOH balancing process and participating in these two markets simultaneously.

The estimated resale prices of each of these methods can be compared to the resale prices of prior EV battery repurposing studies [37], [38]. Repurposing batteries consists of testing and repackaging modules without balancing the cell SOH in modules [38]. Based on 2nd life battery health factors, Neubauer et al. (2015) calculated the resale price of repurposed batteries to have equivalent values to new EV Li-ion batteries [38]. Neubauer et al. (2015) estimated the resale price of batteries after repurposing to be between 44 $/kWh and 180 $/kWh [38]. Cready et al. (2003) estimated the resale price of repurposed batteries to be 145 $/kWh [37]. Cready et al. (2003) used a bottom up approach to determine the resale price which consisted of a repurposing cost of 64 $/kWh and an acquisition price of 81 $/kWh. These studies, like ours, show battery acquisition and labor to be the largest contributors to the resale price. These studies also show capital costs to be a minor contributor to resale price like ours. Our analysis determines the repurposing battery resale price to be 55 $/kWh under the baseline scenario. Thus, all the methods analyzed in our study are shown to be on the lower-end of estimated repurposing costs primarily due to a lower acquisition price associated with recent reductions to new Li-ion EV battery prices. The target scenario is shown to have lower repurposing costs than all the previous studies considered above.

2.3.1.2 Target Scenario and Future Reductions

The target scenario improves the battery economics by reducing the reconditioning cycles, labor task times, warranty, transportation distance, hardware costs, and acquisition price based on expected improvements to the process through research and commercialization. The majority of reductions for all methods is due to the acquisition price decreasing from 35 $/kWh-nameplate (Table 1) in the baseline scenario to 21.50 $/kWh-nameplate in the target scenario (Table A1). The target RGS scenario (34.41 $/kWh-nameplate) and target RES scenario (35.51 $/kWh-nameplate) are less than the target resale price of repurposing (37.93 $/kWh-nameplate), primarily due to fewer reconditioning cycles needed for SOH balancing. With fewer reconditioning cycles, the battery yield (Eq. 1) is increased, consequently reducing the impact of fixed capital and operational costs through a higher annual yield. As a result, RGS has a lower resale price than RES.

There are several improvements that could be made to the reconditioning process to further decrease the price in the future. Decreasing the number of cycles required to balance battery module SOH by improving balancing schemes would lower the price substantially for the RGS and RES methods. Reducing the number of cycles to 50% of the assumed values in the target scenario results in a battery resale price of 31 and 30 $/kWh-nameplate for RGS and RES. The capital costs could be reduced by decreasing hardware costs from manufacturing. Little reduction to the transportation cost would be achievable as this analysis already assumes a class 8 freight truck could be filled to its full capacity with batteries. Each method would increase in price if the current transportation regulation is used which has a maximum battery weight of 333 kg per truck [54]. The increase in resale price due to transportation for the baseline RGS, RES, and repurpose methods would be 6.67, 6.87, and 7.33 $/kWh-nameplate, respectively [69], [70], [71]. This assumes that cargo vans are used as the transportation vehicle instead of a class 8 freight truck. Lastly, as mentioned in the previous paragraph, a reduction in battery acquisition cost ultimately has the largest impact (Figure A2).

New EV Li-ion batteries are estimated to cost 195 $/kWh in 2020 so the 2nd life batteries (RGS 62 $/kWh) would have a resale price less than a new Li-ion battery today [7]. However, new EV Li-ion batteries could optimistically cost as little as 50 $/kWh in 2030 [7]. Therefore, there is uncertainty on the competitiveness of 2nd life batteries in the future. With a lower new Li-ion battery price in the future, the acquisition price of the 2nd life batteries would likely decrease [38]. Assuming the acquisition price of 2nd life batteries decreases linearly as a fraction of the price of new Li-ion batteries, the resale price of the 2nd life batteries would decrease as shown in Figure A2. In 2030, the new Li-ion baseline price is estimated to be 75 $/kWh so the 2nd life acquisition price would be 13.50 $/kWh-nameplate representing a 21.50 $/kWh-nameplate reduction compared to the baseline. Each of the baseline 2nd life scenarios with the 2030 acquisition price would continue to have a lower price per usable capacity (Table 2) than a new Li-ion battery in 2030 (Figure A2). With an adjusted acquisition price, a new Li-ion battery would become less expensive than the baseline resale prices of RGS, RES, and repurpose scenarios at a price of 43, 43, and 33 $/kWh of usable capacity, respectively.

Assuming 2nd life batteries to be economical in the future, 2nd life batteries could be used in a variety of applications. If a 2nd life battery is of high enough quality it could go back into an EV [72]. Alternatively, 2nd life batteries could be used for stationary residential, commercial, and utility applications; specifically, 2nd life batteries could be integrated with renewable energy for energy storage in residential and utility settings [31], [73]. Finally, 2nd life batteries could also be used to perform various grid services such as spin/non-spin reserve, voltage support, frequency regulation, energy arbitrage, transmission congestion relief, and demand charge reduction [73].

2.3.2 Grid Energy Storage System (ESS)

The system boundary of the analysis is expanded to evaluate the economic feasibility and competitiveness of using 2nd life batteries in grid energy storage markets. Baseline and target scenarios are completed for the processing methods of RGS, RES, and repurpose. A baseline and target scenario for a new Li-ion battery ESS is used to create a comparison to the 2nd life battery scenarios. The grid applications analyzed for two different ESS systems are power applications and energy applications. The power applications are sized for applications that require high power and a fast discharge rate (1-hour) while the energy applications are sized for applications that require bulk energy and a slow discharge rate (4-hour). The minimum required revenue of each scenario is shown in Figure 3 and discussed in 2.3.2.1 ESS Minimum Revenue. The minimum required revenue of the baseline RES and target RGS scenarios are compared in 2.3.2.2 Market Potential to the revenue potentials of power applications (spin/non-spin reserve, voltage support, and frequency regulation) and energy applications (energy arbitrage, transmission congestion relief, and demand charge reduction). Baseline RES and target RGS are the least expensive reconditioning scenarios. The economically viable applications for the baseline RES scenario include frequency regulation, transmission congestion relief, and demand charge reduction. With improved economics, the target RGS scenario is viable for two additional applications: energy arbitrage and spin/non-spin reserve.

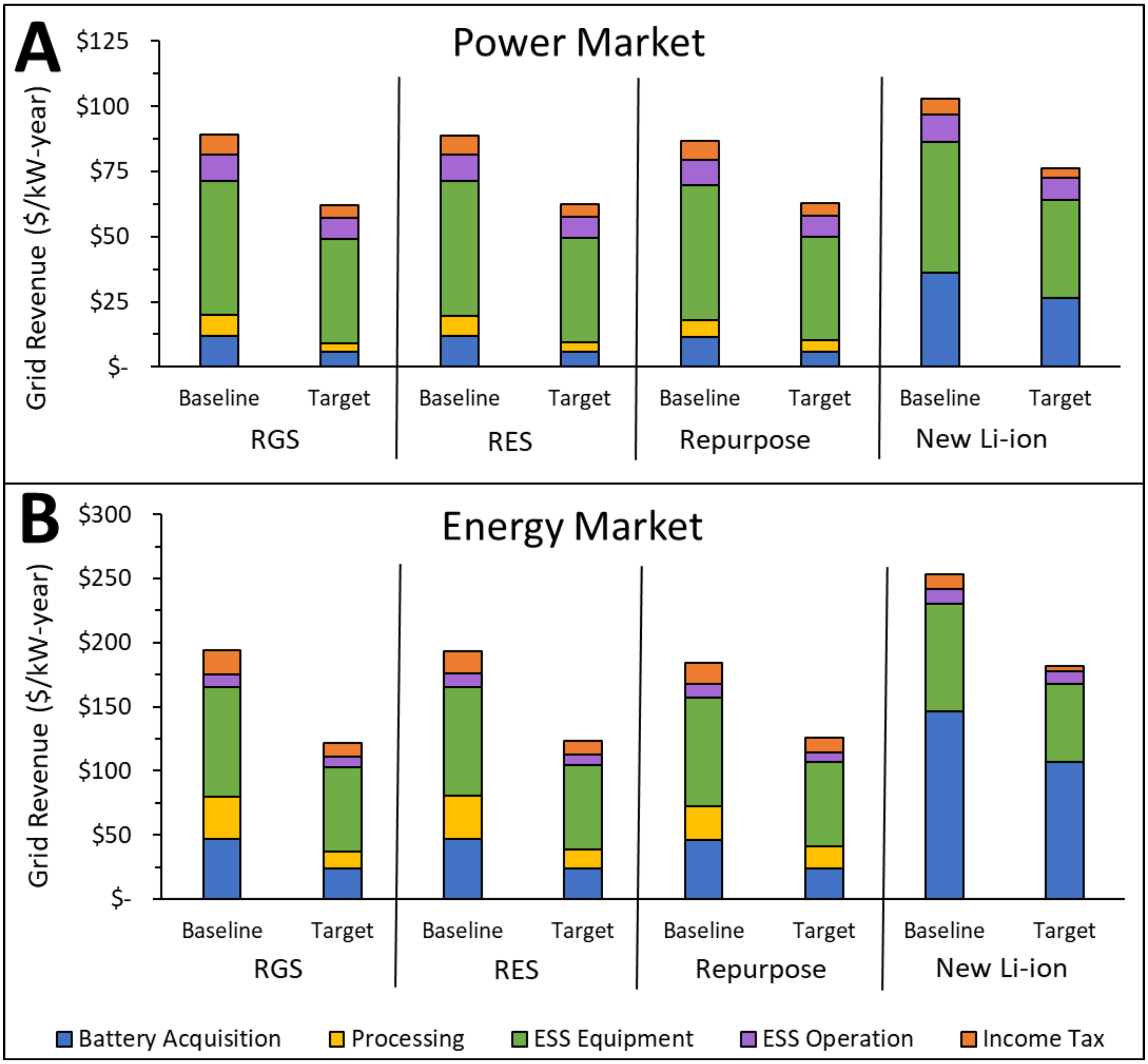

*Figure 3: The required revenue for 2nd life batteries as compared to new Li-ion batteries in (**A**) power markets (**B**) energy markets with baseline and target scenarios.*

2.3.2.1 ESS Minimum Revenue

The baseline RGS, RES, and repurpose scenarios are shown to require less revenue for both power (P) and energy (E) applications (P: 87-89 $/kW-y; E: 184-194 $/kW-y) than the baseline new Li-ion scenario (P: 103 $/kW-y; E: 253 $/kW-y) (Figure 3). This is due to the lower combined costs of 2nd life battery acquisition and processing (P: 18-20 $/kW-y; E: 72-80 $/kW-y) relative to the battery acquisition cost of a new Li-ion battery (P: 36 $/kW-y; E: 146 $/kW-y). The target new Li-ion battery is shown to have a lower grid revenue requirement (P: 76 \$/kW-y; E: 182 \$/kW-y) than all the baseline 2nd life battery scenarios (P: 87-89 \$/kW-y; E: 184-194 \$/kW-y) and a higher grid revenue requirement than all the target 2nd life battery scenarios (P: 62-63 \$/kW-y; E: 122-126 \$/kW-y). Overall, the 2nd life batteries are preferable to new Li-ion batteries. However, as new Li-ion battery prices are reduced, as shown by the target scenario, the answer from this analysis could change. As discussed in 2.3.1 2nd Life Battery Resale, the reduction in 2nd life battery price is smaller than the reduction in new Li-ion battery price implying a reduction in new Li-ion acquisition costs would be greater.

The target scenario for new Li-ion batteries in an energy application (Figure 3**B**) has the largest cost reduction from the battery acquisition cost. However, all other power and energy market target scenarios see the largest reduction from the ESS equipment costs; the ESS equipment costs are assumed to be reduced by 23% in the target scenario [63]. The ESS equipment cost is the largest cost component for the majority of scenarios with the exceptions being for the baseline and target new Li-ion energy market scenarios. The energy market ESS scenarios are dominated by costs assessed on a per unit energy basis such as battery acquisition and processing. Alternatively, the costs assessed on a per unit power basis are more prevalent for the power market ESS as shown by ESS operation.

These results can be compared to benchmarked annual costs found in literature. New Li-ion ESSs deployed in 2018 and 2025 are estimated to have annual costs of 294 \$/kW and 241 \$/kW for 4-hour systems (energy applications) [63]. Our estimate for the new Li-ion baseline scenario (253 \$/kW) is lower than the 2018 benchmark and higher than the 2025 benchmark since we used a longer lifetime of the ESS (20 years) and the same 10 year lifetime of the batteries. This is mainly driven by the assumed longer lifetime in this study (20 years). The new Li-ion target scenario estimate (182 \$/kW) is lower than both the 2018 and 2025 benchmarks.

The results from our study do not account for the value of performance differences among new, reconditioned, and repurposed batteries. A new battery is expected to have the best performance since the cells have a uniform 100% SOH upon deployment of the ESS. EV battery aging has been shown to vary by manufacturer, generating a wide-range of battery performance characteristics [74]. HUB reconditioning aims to balance the SOH of cells and continuously monitor the battery's performance over hundreds of cycles. As a result, HUB reconditioning can produce battery modules with an improved SOH and also a more accurate understanding of the performance characteristics of the battery modules than traditional repurposing can achieve. The performance characteristics of the battery dictate the suitability of the ESS to be used for certain power and energy market applications [66]. The minimum revenue for both power and energy market ESSs are compared to their respective market application revenues in the following section.

2.3.2.2 Market Potential

The ESS minimum revenue for power market ESSs (Figure 3**A**) is compared to the range of market revenues from the applications of spin/non-spin reserve, voltage support, and frequency regulation. The potential market size of the applications in the U.S. is also considered for spin/non-spin reserve, voltage support, and frequency regulation are 6.0-GW, 9.2-GW, and 1.0-GW [65]. The energy applications include energy arbitrage, transmission congestion relief, and demand charge reduction which have market capacities of 18.4-GW, 36.8-GW, and 32.1-GW in the U.S. [67].

The potential capacity of the power and energy applications that could satisfy the minimum required revenue of the ESSs (Figure 3) are shown in Figure 4. Market size data from Eyer & Corey (2010) and revenue data from Balducci et al. (2018) are combined using Eq. 5 [65], [67] and shown in Figure 4. The minimum required revenue from the baseline and target RES method (Figure 3) is plotted by the vertical lines in Figure 4. The market size to the right of the vertical line represents the size of the application's market that could satisfy the revenue requirement of the ESS.

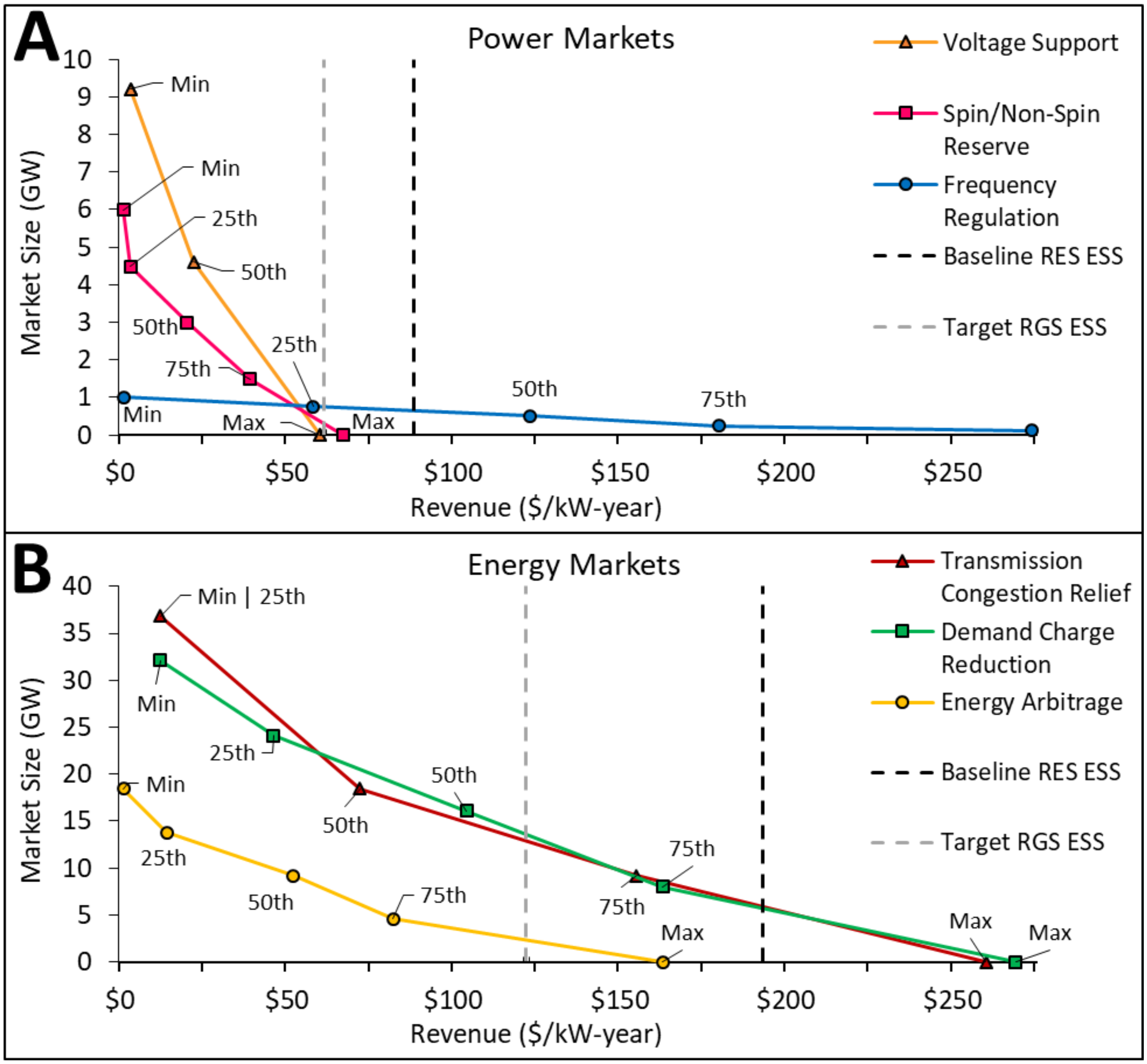

*Figure 4: Market size for applications based on the total market size [65] and percentile of revenue from estimates in literature for energy storage in (**A**) Power Markets and (**B**) Energy Markets [67].*

Power Markets

As shown in Figure 4**A**, frequency regulation is the only power application necessary to satisfy the minimum revenue of the baseline RES ESS. However, at the baseline minimum ESS revenue the capacity of the frequency regulation market (63%) to meet that revenue is only 0.64-GW (0.64-GWh). This analysis modeled the maximum ESS capacity online for the baseline RES method to be 1.6 GWh so the 2nd life batteries could not exclusively be used for frequency regulation or power applications. For the power applications ESS target revenue value (Figure 4**A**), the 2nd life batteries could be used for spin/non-spin reserve and frequency regulation which have potential capacities of 0.27-GW and 0.74-GW. The target ESS scenario has a maximum capacity online of 2.0-GW, therefore the power applications could not satisfy the revenue requirement of the target ESS scenario. The 2nd life capacity of the target scenario could satisfy up to 73% of the frequency regulation market size, 5% of the spin/non-spin reserve market size, and none of the voltage support market size. The 2nd life batteries could also be used for energy applications.

Energy Markets

The energy applications of transmission congestion relief, demand charge reduction, and energy arbitrage each have a higher market capacity than all the power applications combined. As shown in Figure 4B, the minimum revenue for the baseline scenario is 194 $/kW-year which could be satisfied by the energy applications of demand charge reduction (5.7-GW or 22.8-GWh) and transmission congestion relief (5.8-GW or 23.2-GWh). The minimum revenue from the target scenario is 123 $/kW-year which could be satisfied by each of the energy applications. Energy arbitrage, transmission congestion relief, and demand charge reduction have potential market capacities of 2.2-GW (8.8-GWh), 12.8-GW (51.2-GWh), and 13.5-GW (54.0-GWh) at the target scenario's minimum revenue value. The target scenario 2nd life capacity (0.5-GW or 2-GWh) could satisfy up to 0.6% of the total market size (87.3-GW or 349-GWh) for the considered energy applications. The results indicate that the reconditioned batteries in this analysis could have their revenues satisfied by power and energy applications. However, it is also important to consider the total size of the 2nd life EV battery market in the U.S.

Overall 2nd Life Market

The size of the total 2nd life EV market can be approximated based on the cumulative capacity of EVs sold in the U.S. The cumulative capacity of EV batteries sold from 2010 to 2019 is 61.5-GWh in the

U.S. [75]. A fraction of the total capacity of EVs is expected to have a 2nd life. Bloomberg New Energy Finance assumed that about 27% of the EV batteries available in 2025 could be used for 2nd life applications based on their end of 1st life performance [76]. The reconditioning process has the potential to enable a larger portion of available batteries to be used for 2nd life applications due to performance improvement. The size of the 2nd life market will ultimately be dictated by the demand from economical applications.

This analysis assumes that only 2nd life batteries will satisfy the markets for the power and energy applications considered. The total potential capacity of 2nd life batteries that could have their baseline revenue satisfied by the three economical grid applications considered is 46.6-GWh. For the target scenario, the total 2nd life capacity that could be satisfied is 115-GWh from the five economical applications considered. If only 27% of the EV batteries sold from 2010 to 2019 have a 2nd life (16.6-GWh), the baseline and target ESS scenario would have their revenues satisfied by participating in the power and energy markets. If all of the EV batteries sold from 2010 to 2019 have a 2nd life (61.5-GWh), then the target scenario would be able to satisfy all of the batteries' minimum revenues however the baseline scenario would only be able to satisfy 76% of 2nd life batteries' minimum revenues.

The range of application revenues represent the distribution of revenue values determined in literature. The study by Balducci et al. (2018) looked at studies that examined multiple electricity markets such as CAISO, New York Independent System Operator (NYISO), and Midcontinent Independent System Operator (MISO) [67]. Each of these electricity markets have different generation sources, transmission networks, and loads which impact the value of an ESS for certain applications. The potential ESS market size for the applications is also dependent on the generation sources and loads. The revenue differences between electricity markets indicates that 2nd life batteries could be economical in certain markets and not economical in others.

2.3.3 Sensitivity Analysis

Sensitivity analyses of the baseline inputs for RGS, RES, repurpose, and new Li-ion are completed for 3.2 Energy Storage System energy applications. The sensitivity analyses of the TEA inputs are shown in Figure 5 for the 10 most sensitive inputs from each scenario.

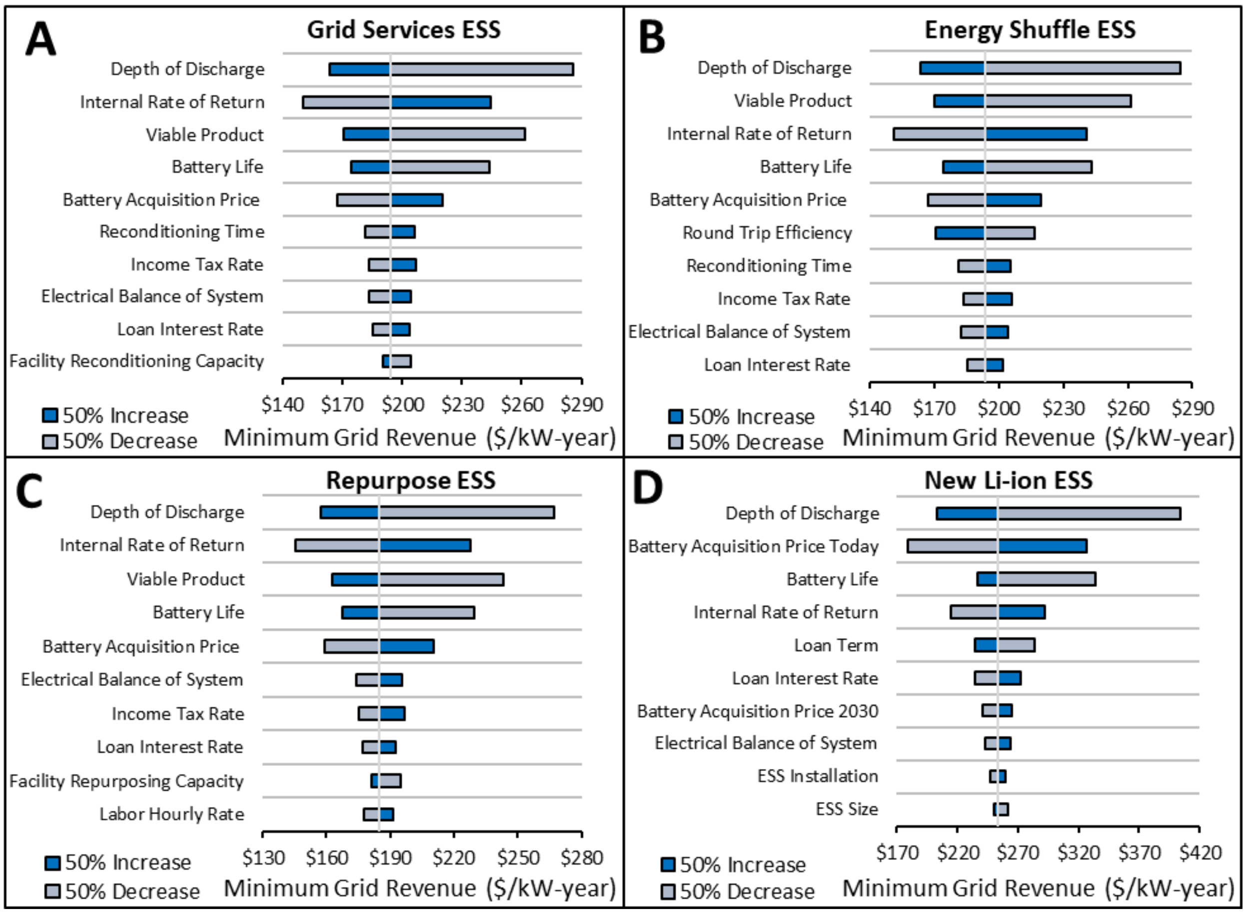

*Figure 5: Sensitivity analysis of the 10 most sensitive model inputs for (**A**) RGS ESS (**B**) RES ESS (**C**) repurpose ESS (**D**) new Li-ion ESS.*

As shown in Figure 5, the DOD is the most sensitive variable for all scenarios. For 2nd life batteries, the DOD is typically operated between 15% to 65% state of charge which is considered best practice [31]. The aging of reconditioned 2nd life batteries is an area of uncertainty so the DOD may have a different optimal operating range than repurposed batteries. The battery life is one of the top four most sensitive variables for each scenario. The lifetime of 2nd life batteries is an area of uncertainty since there is limited aging data on 2nd life batteries. A 50% increase to the battery lifetime is shown to have a much lower impact than a 50% decrease due to the time value of money in the DCFROR analysis. The battery acquisition price is a sensitive variable for every scenario in Figure 5 since it is a high cost in the cashflows. The battery acquisition price also makes the viable product for the repurposing and reconditioning scenarios very sensitive, as shown in Figure 5**A**-**C**. A lower viable product results in more batteries acquired which are disposed rather than used in the ESS. In Figure 5**A**-**B**, the reconditioning time is sensitive since it determines the battery yield. The roundtrip efficiency of the RES scenario (Figure 5**B**) is shown to be sensitive due to its impact on the reconditioning electricity cost from charging and discharging cycles. The sensitivity analysis also shows that decreasing the cost of the ESS installation and electrical balance of system will lower the minimum revenue required. The TEA assumptions, including the internal rate of return, loan term, income tax rate, and loan interest rate, are shown to be sensitive in Figure 5. Therefore, the TEA results would change substantially with different economic assumptions, but the comparisons of the technologies should remain consistent.

2.4 Conclusion

The cost to process batteries for a 2nd life was determined for the methods of RGS, RES, and repurposing with a comprehensive high-fidelity model. The results indicated the RES is likely the most cost-effective reconditioning method. The traditional repurposing approach was shown to be less expensive than reconditioning for the baseline scenario but more expensive for the target scenario. The resale price of reconditioned batteries was determined to be between 34 $/kWh and 62 $/kWh. This range of resale prices was less than the price of a new Li-ion battery today and most estimates for 2030. The 2nd life battery ESSs were shown to be more economical compared to new Li-ion ESSs for both power and energy applications. The 2nd life ESSs were determined to be economically feasible for both power and energy applications with the latter having a much larger potential market size. The combined market size of power and energy applications is expected to be able to satisfy the market size and minimum revenue of 2^{nd} life battery ESSs in the U.S.. R&D should be focused on reducing battery prices, ESS costs, and 2^{nd} life processing costs as well as reducing the uncertainty of 2^{nd} life battery performance.

CHAPTER 3: TECHNO-ECONOMIC AND LIFE CYCLE ASSESSMENT OF MULTI-UNIT DWELLING ELECTRIC VEHICLE CHARGING HUBS[2]

3.1 Introduction

In an effort to achieve national climate goals, in 2021 the U.S. set a target for EVs to reach 50% of vehicle sales by 2030, and subsequently allocated $7.5 billion from the Bipartisan Infrastructure Law to fund the deployment of charging infrastructure [1]. Home charging has emerged as the primary venue for personal EV charging, yet MUDs currently lack the charging infrastructure needed to support EV adoption [14]. Oftentimes, MUD management may need to facilitate charger installations by remedying restrictions such as policies and parking arrangements [77]. Deploying chargers at MUDs can be challenging due to outdated or insufficient electrical service and expensive capital costs for MUD residents [14–16]. Therefore, the deployment of chargers at MUDs using public and private funds will be necessary to not only provide equitable access to home charging but also facilitate the adoption of BEVs [10,14] to lower vehicle GHG emissions [28] from the growing population of 80M multi-unit dwellers in the U.S. [78].

As a result, detailed information on the economics and environmental benefits of MUD charging hubs is needed to strategically deploy the chargers. However, there is minimal information on the levelized cost of charging (LCOC) at MUDs since most studies focus on early BEV adopters who live in single-family homes [10]. A recent national level analysis by Borlaug et al. (2020) overlooked MUDs and found the LCOC to vary by charger power level, region, charger utilization, price of electricity at different

[2] This chapter was published as a peer-reviewed journal article: Horesh N, Zhou Y, Quinn J. Home charging for all: Techno-economic and life cycle assessment of multi-unit dwelling electric vehicle charging hubs. Journal of Cleaner Production 2023;383:135551. https://doi.org/10.1016/j.jclepro.2022.135551.

charging locations (single-family home, workplace, public), and charger capital costs (installation, procurement) [26]. Moreover, Borlaug et al. (2020) determined BEVs charged at single-family homes to be less expensive to fuel than gasoline conventional vehicles (CVs). However, Level 2 (L2) charger installation costs are typically more expensive at MUDs than at single-family homes [16] and vary greatly between MUDs based on the existing electrical infrastructure [77]. Consequently, Williams and DeShazo (2015) found MUD BEV L2 charging to only be less expensive than gasoline CV fueling for some scenarios, which depended on installation costs and utilizations [79]. Williams and DeShazo (2015) used a range of installation costs and utilizations coupled with pricing scenarios to compute the net present value. Thus, Williams and DeShazo (2015) did not attempt to estimate the average LCOC at MUDs but rather demonstrated pricing structures that yield a positive net present value [79]. Alternatively, Peterson (2011) estimated the average LCOC at MUDs in California, and the results show the LCOC to be less expensive when shared by multiple users [77]. However, Williams and DeShazo (2015) and Peterson (2011) only considered installation costs and California electricity prices, neglecting key TEA inputs like operational costs and taxes [77,79].

Regardless, qualitative findings from Peterson (2011) indicate initial capital costs are the primary barrier for charger installations by prospective owners [77]. A review by LaMonica and Ryan (2022) found current charger owners to include utilities, property owners, private companies, and vehicle owners [80]. Hall and Lutsey (2017) note that utilities may be well suited to develop charging infrastructure in underserved areas such as MUDs but may be regulatory restricted in certain states [81]. While some studies have evaluated the LCOC at MUDs for resident-owned stations [77,79], these studies did not model community charging hubs or include real-world utilization data, utility and private company ownership models, or high-fidelity techno-economic analysis (TEA) modeling. To guide decision-makers (policymakers, BEV owners, MUD owners, investors) on how to economically deploy charging infrastructure at MUDs, the LCOC needs to be quantified using MUD specific inputs to determine the financial impact of who owns the hub, what types of chargers are deployed, and where the chargers are deployed.

Furthermore, the economic efficiency of reducing GHG emissions from the vehicle sector with MUD BEVs depends on not only the LCOC but also the BEV GHG emissions at the service location. Specifically, BEV emissions depend on the grid mix that supplies the electricity to the chargers [27]. Burnham et al. (2021) found U.S. state grid mixes to vary greatly, resulting in a wide range of BEV GHG emissions reductions (2020: 10% to 87%) [28]. Additionally, since grid mixes are not uniform and hence GHG emissions vary significantly throughout the day, Fernández (2018) deduced that BEV GHG emissions should correspond with when the BEV charges [29]. Thus, BEV GHG emissions results from Burnham et al. (2021) and other studies nonspecific to MUD BEV charging schedules do not accurately estimate MUD BEV GHG emissions. While many studies have investigated BEV GHG emissions, to the author's knowledge none have coupled the MUD charging profile with a temporal grid mix and evaluated the cost of GHG emissions reduction for MUDs.

This research chapter compares the economics and GHG emissions of BEVs at MUDs and gasoline CVs using both geospatial and temporal resolution. MUD specific parameters are leveraged to determine the LCOC for different community charging hub ownership models (resident, utility, private company), charger types (Level 1 (L1), L2, DCFC), and locations (50 states). This work uses data from thousands of real-world MUD charging sessions to characterize the charging schedule and utilization of chargers at MUDs. This work features a sensitivity analysis to identify high impact TEA and LCA inputs. Furthermore, the economic system boundary expands upon the LCOC to account for the TCO for BEVs and gasoline CVs. The difference between BEV's and gasoline CV's TCO and GHG emissions are then combined to calculate the cost of GHG emissions reductions, an indicator of the cost effectiveness of GHG reducing technologies. The contribution of this work is the quantification of MUD specific LCOCs for different scenarios, MUD specific GHG emissions, and the cost of GHG emissions reductions, all of which can be used by decision-makers to strategically deploy MUD charging infrastructure.

3.2 Methods

This work evaluated the sustainability of MUD community charging hubs with a coupled TEA (3.2.1) and LCA (3.2.2) for different ownership models, regions, charger types, and cases as shown in Figure 6. The TEA calculated the LCOC at MUDs and the LCA quantified the cradle to grave (C2G) GHG emissions from multi-unit dwellers' BEVs. The MUD charging hub was compared to the refueling costs and GHG emissions of an equivalent gasoline CV to assess sustainability metrics. The final stage of this analysis leveraged the results of the TEA and LCA to determine the cost of GHG emissions reduction (3.2.3). These analyses used the Charging Hub Economic and Costing Tool (CHECT) developed at Argonne National Laboratory [82].

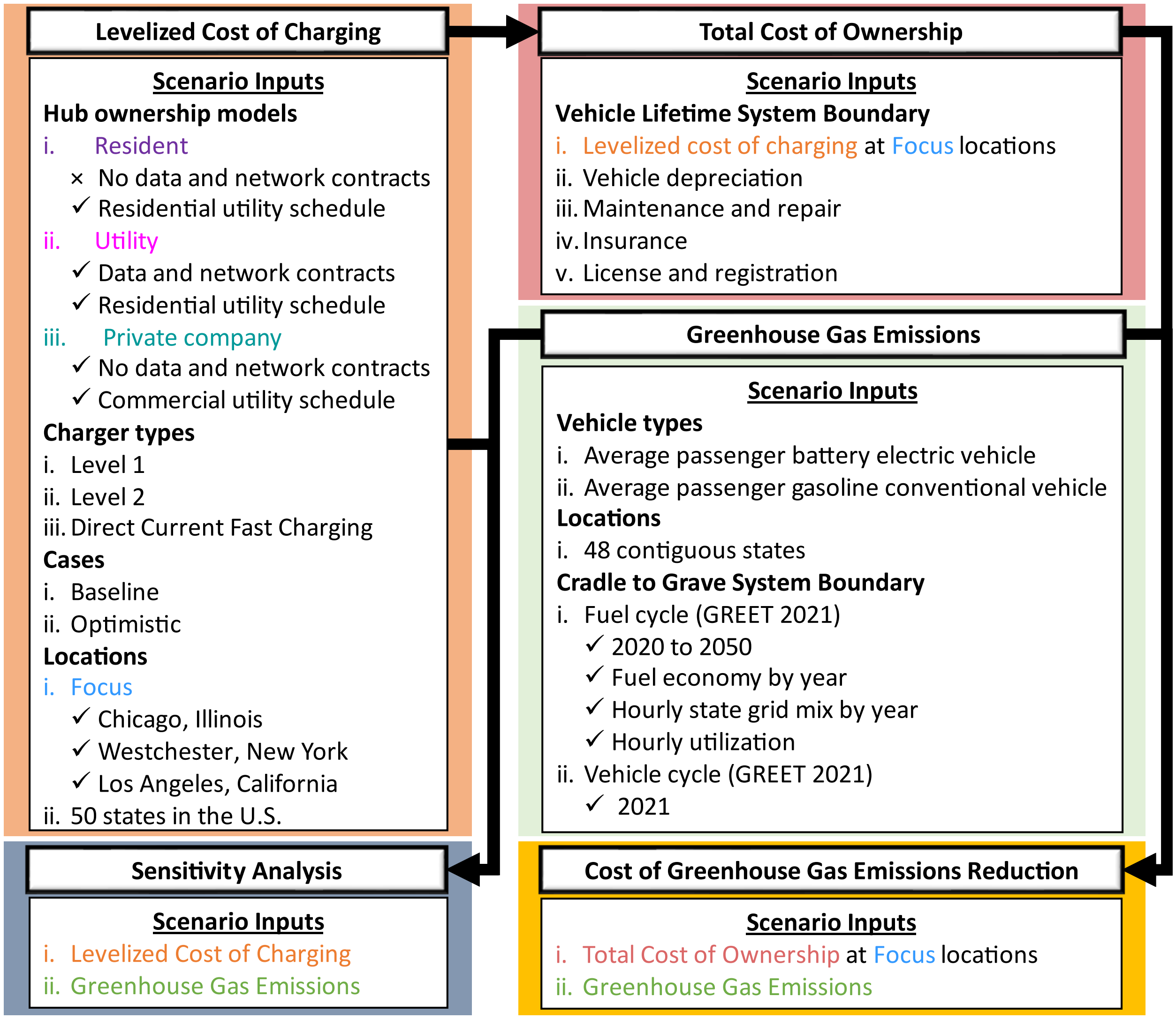

Figure 6. Flow diagram of the scenarios used to evaluate the levelized cost of charging (LCOC), total cost of ownership (TCO), cradle to grave (C2G) greenhouse gas (GHG) emissions, and cost of GHG emissions reduction for Multi-Unit Dwelling (MUD) battery electric vehicle (BEV) charging. The MUD BEV was compared to a gasoline conventional vehicle (CV) for each analysis. The sensitivity analysis was performed for the LCOC and GHG emissions.

3.2.1 Techno-economic Analysis

3.2.1.1 Techno-economic Analysis Scenarios

As shown in Figure 6, the TEA evaluated the economics for a community charging hub with 9 baseline and 9 optimistic scenarios (ownership model, charger type) at one service location in each U.S. state. The hub served 30 BEVs with one DCFC, three L2, and six L1 chargers located in community parking spaces at or nearby a MUD. The acquisition of the spaces was assumed to be facilitated by MUD management or the lot owner at no additional cost [77]. For each charger type, a baseline and optimistic case was formulated such that the baseline case was representative of current economics and the optimistic case was representative of future economics achieved. The baseline case assumed mean capital and operational costs (Table 3) along with real-world utilization data while the optimistic case assumed the minimum capital and operational costs (Table 3) combined with increased utilization in the future.

Table 3. Capital and operational costs of Level 1, Level 2, and DCFC chargers for baseline and optimistic cases.

Parameter	**Optimistic**	**Baseline**	**Units**
Capital Costs			
Level 1 Procurement	$0 [83]	$56 [83]	$/charger
Level 1 Installation	$0 [83]	$171 [83]	$/charger
Level 2 Procurement	$2,270 [15]	$2,500 [15]	$/charger
Level 2 Installation	$1,436 [16]	$4,266 [16]	$/charger
DCFC Procurement	$21,105 [15]	$29,442 [15]	$/charger
DCFC Extra Cable	$1,583 [15]	$2,638 [15]	$/extra-cable
DCFC Installation	$9,188 [84]	$25,578 [84]	$/charger
Credit Card Reader	$343 [15]	$700 [15]	$/charger
Operational Costs			
Network Contract	$198 [15]	$223 [15]	($/charger-year)
Data Contract	$83 [15]	$161 [15]	($/hub-year)
Level 2 Maintenance	$23 [26]	$125 [26,85]	($/charger-year)
DCFC Maintenance	$211 [26]	$1,472 [26,85]	($/charger-year)

The ownership model of the MUD charging hub dictated the applicability of each cost from Table 3, since the ownership model determined who paid for the charging infrastructure and how the hub was managed. In this study, three ownership models were formulated: resident, utility, and private company. Under a resident ownership model, it was assumed that either the residential property owner (condo, building) or homeowner association owned the charging hub [77], and therefore had a residential load. Based on our discussions with two utility companies (Commonwealth Edison and Baltimore Gas & Electric), the utility ownership model assumed that the utility owned the charging hub and billed the customers along with the existing residential building load. A private company that owned the charging hub, such as a charger vendor, automaker, or investor, would require a separate load from the MUD building and be classified as a commercial load.

3.2.1.2 Techno-economic Analysis Methodology

Capital costs, operational costs, electricity costs, and charger utilization at the MUD charging hub were inputs into the 31-year DCFROR, which is a consistent methodology with other TEA studies [86,87]**.** The DCFROR assumed capital debt financing of 50% with an annual 6% interest rate over a 10-year period; combined state and federal income tax of 26%; sales tax of 4.5%; and an IRR of 3% for resident, 6% for utility, and 10% for private company owners. The initial capital costs included procurement, installation, and credit card reader and were assumed to be incurred during the build period, the first year of the cashflow. The chargers were modeled to be replaced after 15-years [26] of operation, which required an additional procurement capital cost and debt financing in year 16. After the build period (year 1), the operational costs, electricity costs, and charger utilization were applied for 30-years or two charger lifetimes. The costs and utilization were set to be constant throughout the entire 31-year cashflow. The 31-year DCFROR calculated the LCOC by solving for the minimum energy selling price such that a net present value of zero was achieved (Eq. B1-B8). All costs were converted to 2021 values using producer price indexes [88–90].

3.2.1.3 Capital Costs

The capital costs from Table 3 were scaled by the number of chargers by type for the modeled MUD charging hub: six L1, three L2, and one DCFC station with one extra cable. The charging hub had three types of capital costs: 1) procurement (baseline: $40K; optimistic: $29K), the cost to acquire the chargers and extra DCFC cable; 2) installation (baseline: $39K; optimistic: $13K), the make-ready costs of the site and installation costs of the chargers; and 3) credit card reader (baseline: $7.0K; optimistic: $3.4K), the device that collected payment from users at each station.

3.2.1.4 Operational Costs

The three types of operational costs (Table 3) for the modeled charging hub (six L1, three L2, and one DCFC station) were 1) data contracts (baseline: 160 $/year [15]; optimistic: 83 $/year [15]), which provided internet capabilities to the charging hub; 2) network contracts (baseline: 2.2K $/year [15]; optimistic: 2.0K $/year [15]), which collected data and enabled smart charging; and 3) maintenance (baseline: 1.9K $/year [26,85]; optimistic 280 $/year [26]), estimated from literature (1% [26] to 10% [85]) for the baseline scenario to be 5% of each station's procurement cost annually. Based on our discussions with two utility companies (Commonwealth Edison and Baltimore Gas & Electric), data and network contracts were included for utility and private company ownership models but not for resident ownership models.

3.2.1.5 Charger Utilization

EV charging session data (Figures B1-B2) from Electric Vehicle Widescale Analysis for Tomorrow's Transportation Solutions (EV WATTS) were collected intermittently from October 2019 through October 2021 [91]. The charging data at MUD venues were processed (detailed in Appendix B) to determine MUD charger utilization behavior (Figure B3) for 6.6-kW L2 and 50-kW DCFC; L1 utilization was simulated from the L2 sessions. To determine the utilization at each station (Table 4), the mean *daily utilization* (sessions/day-charger), mean *session power* (kW), and mean *charge duration* (hours/session) were calculated for L2 and DCFC. The number of chargers at the hub was found to not clearly impact utilization (Figure B4) likely because the charger per vehicle ratio is far from reaching saturation. Therefore, more chargers are installed in the locations with high charging demand. The baseline case used outputs directly from EV WATTS data to compute the *total daily energy consumption* (kWh/day-charger) using Eq. 6.

$$Total\ Daily\ Energy\ Consumption = (Daily\ Utilization)\ (Session\ Power)\ (Charge\ Duration) \quad (6)$$

The optimistic case used an increased utilization that could be realized by a mature market [92]. The utilization demonstrated by Tesla Superchargers (>50-kW), which averaged 171 kWh/day-charger in July 2019, was used as the reference point to estimate an optimistic utilization rate of the future MUD charging hub [93]. To calculate the *total daily energy consumption* (Eq. 6), the optimistic case used the mean *session power* and mean *charge duration* from EV WATTS but increased the mean *daily utilization* (sessions/day-charger) such that the charger would be used 30% of the time [92], as shown in Eq. 7.

$$Daily\ Utilization = (30\%)\ (24)/\ (Charge\ Duration) \qquad (7)$$

Table 4. Charger utilization of Level 1, Level 2, and DCFC for cases (a) baseline [91] & (b) optimistic [92].

Charger Type	**Daily Utilization (sessions/day-charger)**	**Session Power (kW)**	**Charge Duration (hours/session)**	**Total Daily Energy Consumption (kWh/day-charger)**
Level 1	1.0[a], 1.3[b]	1.5	5.4	8.0[a], 11[b]
Level 2	1.6[a], 2.0[b]	5.2	3.6	30[a], 37[b]
DCFC	2.6[a], 11[b]	33	0.65	56[a], 240[b]

3.2.1.6 Electricity Costs

The MUD hub's electricity costs included an electricity rate ($/kWh), demand charge ($/month-kW), and fixed charge ($/month-hub). The charger utilization schedule (Figure B3) was coupled with an appropriate utility rate schedule based on each scenario's service location, ownership model, and 15-minute peak power demand (47-kW). The peak power demand was computed as the maximum summed product of the number of active chargers (Figure B3) and *session power* (Table 4). Utility rate schedules in each U.S. state (Tables B1-B2) were acquired from the Utility Rate Database [94] (except California [95,96]) for residential (resident, utility) and commercial loads (private company). The three focus locations (Chicago, Illinois; Westchester, New York; and Los Angeles, California) were chosen since they have a large MUD presence and different commercial electricity schedule characteristics (Appendix B).

3.2.1.7 Gasoline Equivalent Cost

The gasoline equivalent cost ($/kWh) of an average passenger vehicle at the focus locations was computed using Illinois, New York, and California fuel prices from January to November 2021. The gasoline equivalent cost (*Gas*) was computed using Eq. 8 with the following four inputs: 1) energy per gallon (gal) of gasoline (*EGG* = 33.7 kWh/gal), 2) location *(L)* gasoline price (P_L = 3.1-4.1 $/gal [97–99]), 3) powertrain efficiency ratio (*PER* = 4.5), which is the amount of tractive work relative to the fuel energy consumed for an average passenger BEV (155 miles per gallon gasoline equivalent (MPGGE)) and gasoline conventional vehicle (34 MPGGE) from 2020 to 2050 [100], and 4) BEV charging efficiency (*CE* = 0.85) [100].

$$Gas_L = (P_L)(PER)(CE)/(EGG) \qquad (8)$$

3.2.2 Life Cycle Assessment

The LCA utilized the Greenhouse gases, Regulated Emissions, and Energy use in Technologies (GREET) model from 2021 [100] to compare the C2G GHG emissions of an average U.S. passenger gasoline CV (34 MPGGE) to an average passenger BEV (155 MPGGE) at MUDs. The C2G system boundary was composed of two cycles from GREET 2021: 1) the fuel-cycle (3.2.2.1) and 2) the vehicle-cycle (3.2.2.2) [100]. The functional unit was grams (g) of Carbon Dioxide equivalent (CO_{2e}) per mile driven.

3.2.2.1 Fuel-cycle

The fuel-cycle emissions in GREET included the average (rather than marginal [101]) emissions from the feedstock, fuel, and vehicle operation [100]. The fuel-cycle emissions were determined with geographical (state) and temporal (hourly & yearly) resolution for BEVs and temporal (yearly) resolution for gasoline CVs. The GREET model included projections for improved vehicle fuel economies (kWh/mi) from 2020 to 2050. Accordingly, the GREET model was run from 2020 to 2050 with 5-year increments for both gasoline CVs and BEVs. All default inputs from GREET for a gasoline CV were used and most default inputs from GREET for a BEV were used except the grid mix [100]. Specifically, GREET's default grid mixes were replaced with grid mix projection data from Cambium 2020 (detailed in Appendix B) [27] to enhance the geographical (state & U.S. aggregate) and temporal (hourly) resolution of the BEV fuel-cycle GHG emissions.

3.2.2.2 Vehicle-cycle

The second cycle of the C2G system boundary was the vehicle-cycle, and the vehicles were assumed to use the default conventional materials [100]. For BEVs and gasoline CVs, the vehicle-cycle included emissions from components; assembly, disposal, and recycling (ADR); batteries; and fluids. The change to C2G GHG (*Δ C2G GHG*) emissions from *BEV*s relative to gasoline *CV*s was computed using Eq. 9 which combined the vehicle-cycle (*VEH*) GHG emissions with the fuel-cycle (*FUEL)* GHG emissions.

$$\Delta\, C2G\ GHG = (FUEL_{BEV} + VEH_{BEV} - FUEL_{CV} - VEH_{CV})/\ (FUEL_{CV} + VEH_{CV}) \qquad (9)$$

3.2.3 Cost of Greenhouse Gas Emissions Reduction

In culmination, the cost of GHG emissions reduction was evaluated at the focus locations to determine the cost effectiveness of reducing GHG emissions from deploying BEVs rather than gasoline CVs. The cost of GHG emissions reductions was evaluated by combining the respective TEA and LCA results for BEVs and gasoline CVs. The system boundary of the TEA was expanded to determine the TCO ($/mi) to match the LCA's C2G system boundary. The TCO was computed using the Alternative Fuel Life-Cycle Environmental and Economic Transportation (AFLEET) [25,102] modeling framework and inputs from 2020 (assumptions in Appendix B). The TCO includes vehicle depreciation, maintenance and repair, insurance (state dependent), license and registration (state dependent), and LCOC (scenario dependent). Custom inputs were entered into AFLEET to update vehicle prices [103] and be consistent with this study's TEA (LCOC) and LCA (fuel economy & vehicle lifetime) assumptions. The TCO was calculated for the 54 BEV LCOC scenarios and 3 gasoline CVs (gas CV) refueling scenarios from 3.2.1. The *cost of GHG* emissions reduction was calculated using Eq. 10 with the following numerator and denominator: the numerator was the *BEV TCO* scenario *(n)* minus the corresponding gasoline equivalent

(*CV*) *TCO* at the location *L* and the denominator was the average (2020-2050) *BEV*'s *C2G* GHG emissions at the location *L* minus the average (2020-2050) gasoline *CV*'s *C2G* GHG emissions.

$$Cost\ of\ GHG_n = (TCO_{CV,L} - TCO_{BEV,n}) / \ (C2G_{BEV,L} - C2G_{CV}) \qquad (10)$$

3.2.4 Sensitivity Analysis

A sensitivity analysis was performed to identify sensitive TEA and LCA inputs. All TEA (46) and major LCA (8) inputs were independently adjusted by ±50%. The sensitivity analysis of the TEA was performed for 9 baseline LCOC scenarios (charger types, ownership models) at each focus location (Illinois, New York, California). The sensitivity analysis of the LCA was performed for the U.S. aggregate mix scenario in 2020 and 2050.

3.3 Results and Discussion

The results from this work are presented in three sections: Techno-economic Analysis, Life Cycle Assessment, and Cost of Greenhouse Gas Emissions Reductions. The TEA section presents the LCOC at MUDs, the LCA section presents the GHG emissions reductions from MUD BEVs relative to gasoline conventional vehicles, and the cost of GHG emissions reduction section combines the results from the LCA and TEA to evaluate the cost of GHG emissions reduction based on the LCOC scenarios.

3.3.1 Techno-economic Analysis

This section consists of three parts: the LCOC in 3 focus locations with all charger levels considered, the LCOC in 50 states focusing on L2, and a sensitivity analysis. Capital, operational, and electricity costs combined with utilization estimates are used to determine the costs associated with multiple charger options (L1, L2, DCFC) and charging hub ownership models (resident (Res.), utility (Util.), private company (PrC.)) to evaluate 9 baseline and 9 optimistic charging scenarios at each hub location. The LCOC is shown to vary substantially between charger types, charging locations, ownership models, and cases.

3.3.1.1 Focus Locations

The MUD charging LCOC results for the focus locations (Illinois, New York, California) are presented by major cost component, with a direct comparison to a traditional gasoline fueled vehicle in the same three locations based on 2021 gasoline fuel prices (Figure 2). The gasoline equivalent cost is presented in terms of the charging cost on per kWh supplied basis. Results show the economically optimal charger is either a L1 or L2 depending on ownership type and location. DCFC has the highest improvement potential to be cheaper than the gasoline equivalent with higher utilization.

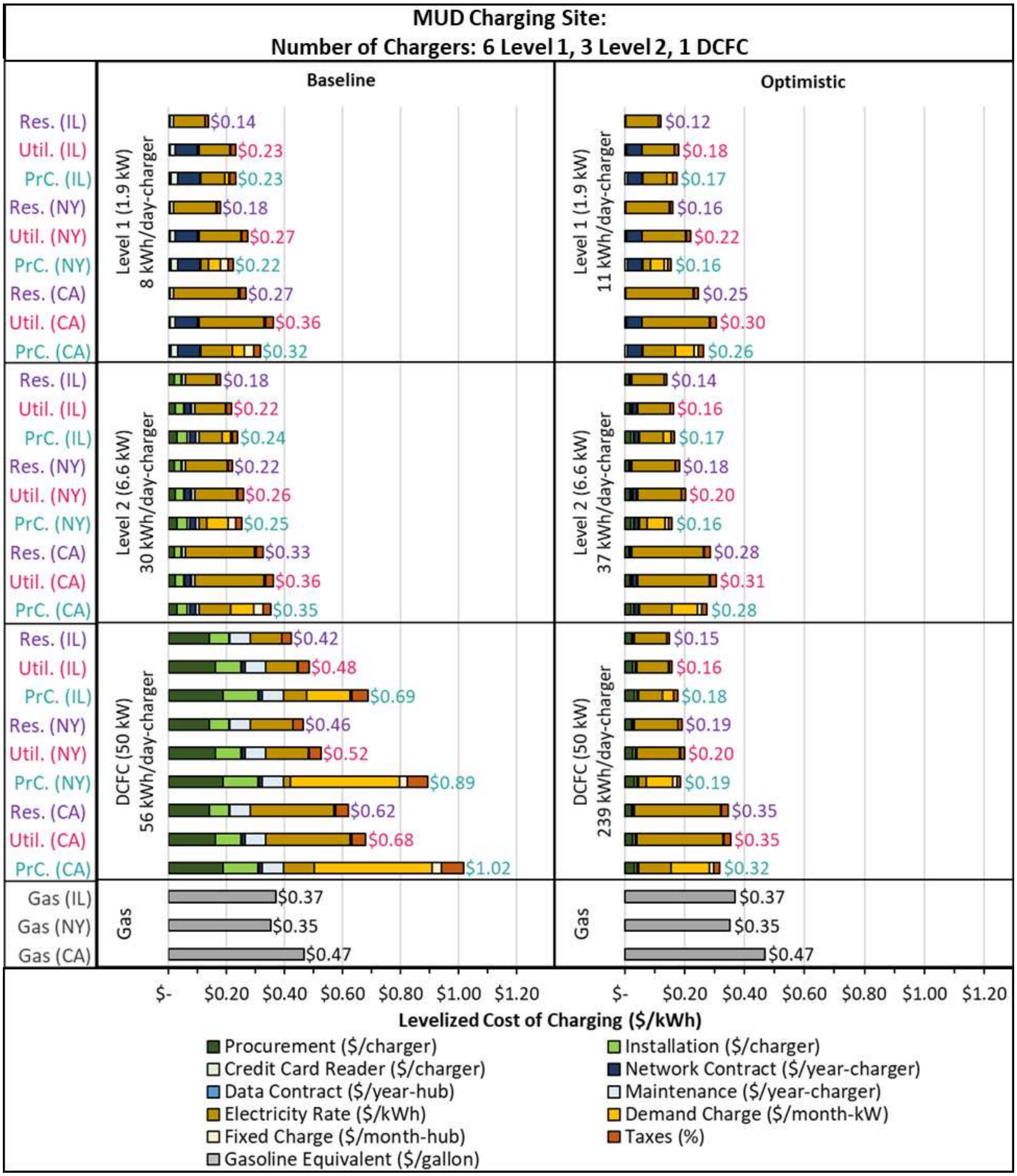

Figure 7. Breakdown of the baseline and optimistic levelized cost of charging (LCOC) for a Level 1 (L1), Level 2 (L2), and Direct Current Fast Charging (DCFC) station at a Multi-Unit Dwelling (MUD) in Illinois (IL), New York (NY), and California (CA) for resident (Res.), utility (Util.), and private company (PrC.) ownership models. The levelized cost of charging is compared to the gasoline equivalent cost (Gas) in the same three locations in 2021 [97–99].

Two key metrics are considered to determine the best charger type for BEV owners: BEV owner savings from the LCOC (0.12-1.02 $/kWh) relative to the gasoline equivalent cost (0.35-0.47 $/kWh); and the performance, assessed here as the charging duration (L1: 5.4 hours; L2: 3.6 hours; DCFC: 0.65 hours) needed for the BEV to reach the desired state of charge. DCFC is considered to have the best performance since it has the shortest charging duration (Table 4). However, the baseline LCOC scenario for DCFC (0.42-1.02 $/kWh) is shown to be economically disadvantageous relative to the gasoline equivalent for every ownership model and location. Alternatively, the baseline LCOC scenarios for L1 (0.14-0.36 $/kWh) and L2 (0.18-0.36 $/kWh) are shown to be economically favorable to the gasoline equivalent. Therefore, under the baseline case, which represents current market conditions and utilization, L1 and L2 are the suggested charger types due to their economical LCOCs with L2 chargers demonstrating a better performance. However, if the future economics encompassed by the optimistic case are achieved (higher utilization, reduced costs), then there will be significant cost savings for DCFC (44-79%) and only minor cost savings for L1 (7.3-30%) and L2 (13-37%) compared to the baseline. Resultantly, the optimistic LCOC scenario for DCFC (0.15-0.35 $/kWh) is economically advantageous relative to the gasoline equivalent and has a similar LCOC as L1 (0.12-0.30 $/kWh) and L2 (0.14-0.31 $/kWh). Thus, DCFC has a competitive LCOC and the best performance making it the most appealing charger type for BEV owners under the optimistic case.

The ownership model, in addition to the charger type, has a substantial impact on the LCOC especially for the baseline case. The ownership model may be determined by a combination of the preferences of the property manager or residents and the desires or allowances of the local utility or a private company to fulfill the MUD's charging needs. The ownership model determines the following: 1) the type of utility schedule (residential, commercial), which impacts the electricity rate, demand charge, and fixed charge; 2) the applicability of data and network contracts; and 3) the IRR (Res: 3%; Util: 6%; PrC: 10%) of the DCFROR, which impacts the capital costs (procurement, installation, credit card reader).

For the baseline DCFC scenarios, the ownership model makes a larger change to the LCOC than for L1 and L2 by contributing a total difference of 10-93% primarily due to the electricity schedule (0-0.30 $/kWh) and IRR (0.04-0.10 $/kWh). Specifically, the resident and utility ownership models benefit from not having a demand charge in their residential schedule, whereas the private company uses a commercial schedule that has an expensive demand charge (0.15-0.40 $/kWh) due to DCFC's high power rate (50-kW) coupled with the baseline case's low utilization (Table 4). Thus, under the baseline case, DCFC is much less expensive for resident or utility ownership models than private company ownership models.

Moreover, the resident ownership model is the least expensive ownership model for most scenarios (Figure 7). This ownership type uses a residential electricity schedule, avoids data and network contract costs, and has the lowest IRR of 3%. Under utility and private company ownership models, the combined cost from data (0.01 $/kWh) and network (0.08 $/kWh) contracts are expensive for the baseline L1 scenario due to their low utilization (Table 4), suggesting the utility and private company ownership models may not be suitable for L1 chargers considering their 19-64% higher LCOC than a resident ownership model. The data and network contract costs for baseline L2 (0-0.02 $/kWh) and DCFC (0-0.01 $/kWh), however, are minor. In total, the ownership model for baseline L2, which also impacts the electricity schedule (0-0.03 $/kWh) and IRR (0.01-0.03 $/kWh), is shown to be of lower importance to the LCOC (9.1-33%) than for baseline L1 and DCFC. Likewise, the optimistic case shows the ownership model to have a minimal impact on the LCOC for each charger type, 0.06 $/kWh for L1, 0.04 $/kWh for L2, and 0.03 $/kWh for DCFC. The optimistic case's higher utilization and reduced costs decrease several LCOC components that are affected by the ownership model including the electricity schedule (demand charge and fixed charge), data and network contracts, and IRR (procurement, installation, credit card reader).

Although the optimistic case reduced many LCOC components, the electricity rate ($/kWh) remained unchanged between the baseline and optimistic case (and between charger types) and accounted for different portions of each location's LCOC: 12-89% in Illinois; 3-90% in New York; and 11-91% in California. When the capital and operational costs are minimal and the utilization is high, as shown by the optimistic L1 charger with a resident ownership model (Figure 7), the lowest achievable LCOC is limited by the electricity rate at the service location. In this instance, the electricity rate contributes 89-91% to the total cost (IL: 0.11 $/kWh; NY: 0.14 $/kWh; CA: 0.22 $/kWh), demonstrating that the LCOC is largely dependent on the electricity costs at the service location.

Utilization has the highest or second highest impact on LCOC. Specifically, it impacts all cost components but the electricity rate in Figure 7. The optimistic case assumes a higher utilization such that the chargers deliver energy 30% [92] of the time, based on the Tesla chargers' utilization [93]. In comparison, under the baseline case, which represents current market conditions (Figure B5), the chargers deliver energy 22% of the time for L1, 24% of the time for L2, and 7% of the time for DCFC [91]. Due to the differences between the observed utilization and the expected utilization, the real-world cost of charging may be between this study's baseline and optimistic LCOC estimates. The median MUD charging cost of L2 (0.23 $/kWh) and DCFC (0.25 $/kWh) derived from EV WATTS [91] is shown to be similar to the LCOC estimated in this analysis. The lower charging cost from the EV WATTS data could be due to the stations receiving subsidies or enduring a loss until higher utilization is achieved [80].

EV WATTS also shows the L2 charging cost at MUDs is more expensive than at every other venue (0.09-0.20 $/kWh) except retail (0.23 $/kWh) [91]. Moreover, the data show L2 charging at MUDs (0.23 $/kWh) is 64% more expensive than at single-family homes (0.14 $/kWh). When harmonizing the assumptions of this study with single-family home charging (assumptions in SI, Figure B6), the equivalent home charging scenarios show the single-family home LCOC is 0.16 $/kWh in Illinois (MUD: 0.18 $/kWh), 0.19 $/kWh in New York (MUD: 0.22 $/kWh), and 0.29 $/kWh in California (MUD: 0.33 $/kWh). Thus, based on the DCFROR, the MUD LCOC with resident ownership is more expensive than the single-family home LCOC at every location modeled (IL: 13%; NY: 16%; CA: 14%). Uniquely, MUD charging hubs can also be owned by a utility or private company, in addition to a resident, which could make home charging at MUDs even more expensive (IL: 38-50%; NY: 32-37%; CA: 21-24%) than at single-family homes. Therefore, the authors deduce that charging at MUDs will be financially inequitable relative to single-family homes but by a lesser amount (<64%) than the median EV WATTS charging costs suggest.

3.3.1.2 All States

The LCOC results at the focus locations (Figure 7) are expanded to all 50 states considering the different electricity rates.

Figure 8 shows the results for L2 while Figures B7-B8 show results for L1 and DCFC. Among states, the baseline LCOC varies from 0.09 to 0.43 $/kWh for L1, 0.13 to 0.44 $/kWh for L2, and 0.36 to 1.02 $/kWh for DCFC. In comparison, gasoline equivalent costs (on September 2, 2022) vary from 0.38 to 0.60 $/kWh (Figure B9). Gasoline price is from AAA (2022) [104].

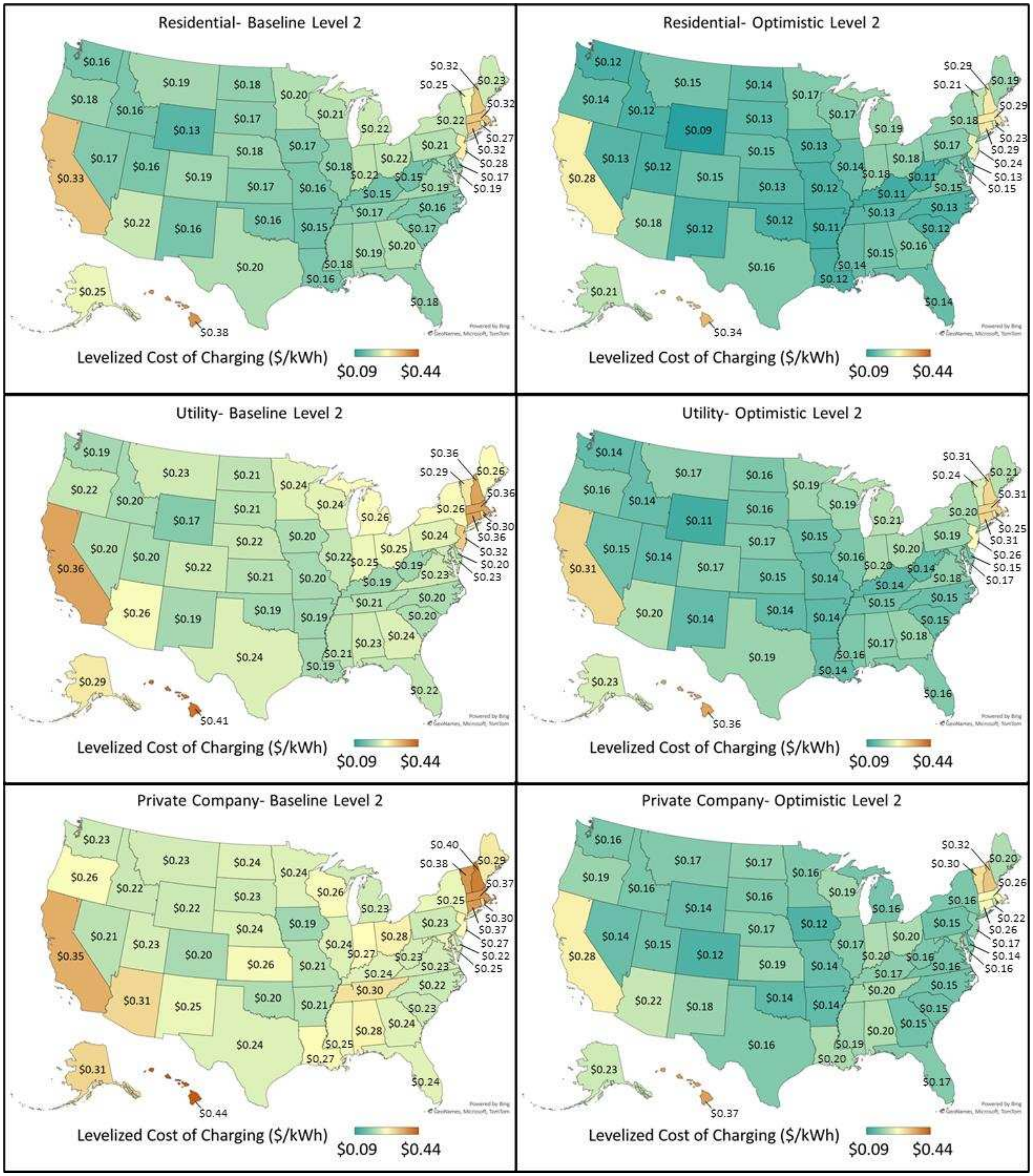

Figure 8. Baseline and optimistic levelized cost of charging (LCOC) for Level 2 (L2) stations in 50 U.S. states at Multi-Unit Dwellings under residential (Res.), utility (Util.), and private company (PrC.) ownership models. The gasoline equivalent cost ranges from $0.38 to $0.60 per kWh (Figure B9).

As displayed in Figure 8, the least cost ownership model for each state varies by case and charger type. The largest difference in baseline LCOC between ownership models for each state ranges from 0.09 to 0.16 $/kWh for L1, 0.03 to 0.12 $/kWh for L2, and 0.06 to 0.44 $/kWh for DCFC. Thus, the ownership model's importance depends on the state. Nevertheless, the resident ownership model has the lowest LCOC under the baseline case in nearly all 50 states and in most states under the optimistic case for L1 (45) and L2 (38). Contrarily, the private company ownership model has the lowest optimistic LCOC for DCFC in 19 states. Therefore, when demand charges are spread across a higher utilization in the optimistic case, the total electricity cost of commercial electricity schedules (private company) can be less expensive than residential schedules (resident, utility) in certain states.

3.3.1.3 Sensitivity Analysis

Sensitivity analysis is performed for every baseline case by ownership model at focus locations. Results for the 10 most sensitive inputs are presented in Figure 9 for California. Similar trends are found for Illinois (Figure B10) and New York (Figure B11).

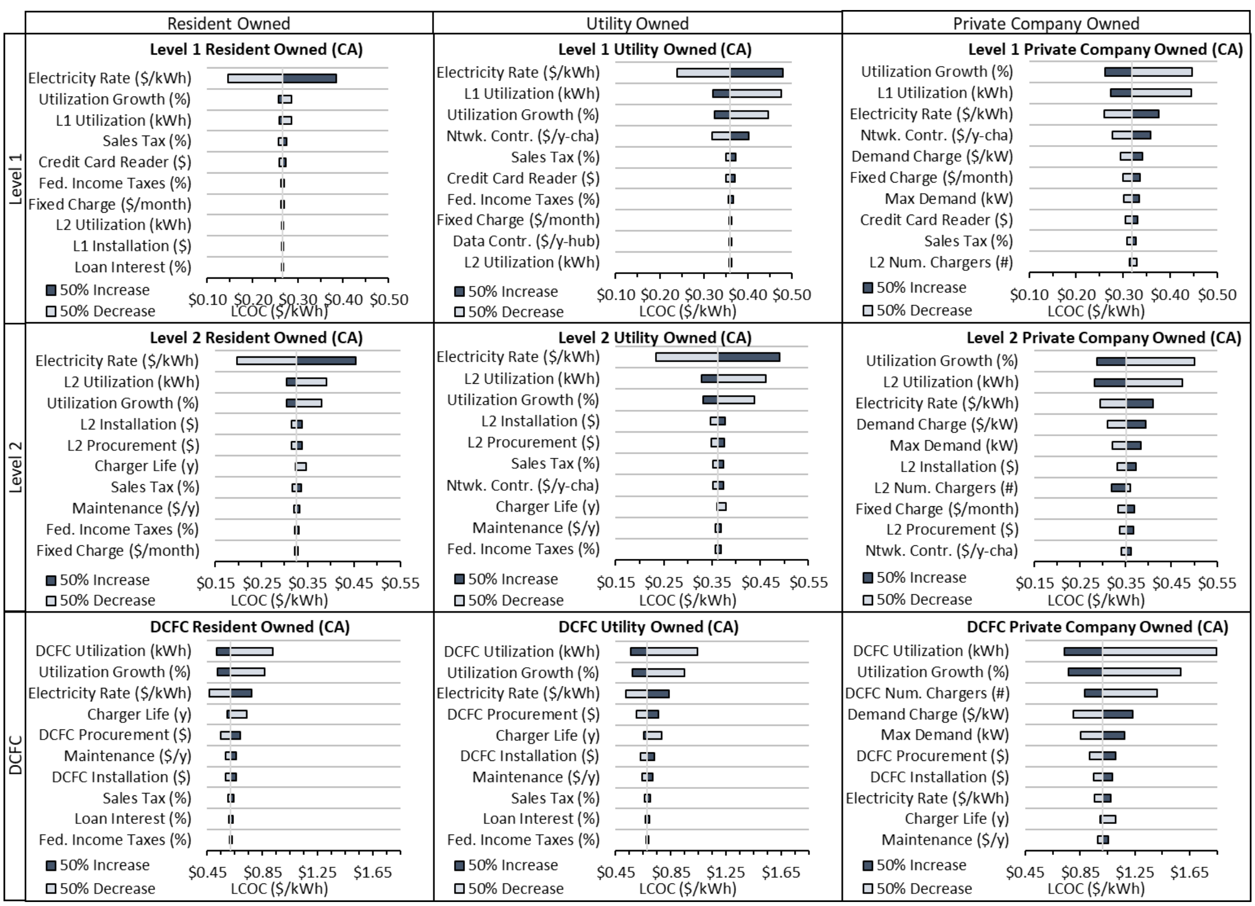

Figure 9. Sensitivity of techno-economic analysis (TEA) model inputs for a Multi-Unit Dwelling (MUD) charging hub in California (CA) with baseline scenarios: Level 1 (L1), Level 2 (L2), and Direct Current Fast Charging (DCFC) stations; and resident, utility, and private company ownership models. Abbreviations: year (y), federal (Fed.), network (Ntwk.), contract (Contr.), charger (cha.), number (num.).

As illustrated in Figure 9, utilization (Table 4) is sensitive in every scenario since it affects most costs (except electricity rate). EV WATTS charging data [91] represent current charger utilization. The daily utilization keeps evolving and hence has a high uncertainty due to factors such as tenant status and BEV adoption [77,92]. Additionally, the electricity rate is sensitive especially for L1 and L2. Moreover, the electricity rate can substantially vary by service location and rate type. Credit card readers for L1 may or may not be needed at the hub depending on the location's regulations [105]. In addition, sales tax in California for L1 is shown to be sensitive under the resident ownership. Furthermore, network contracts are sensitive for L1 under utility and private company ownership primarily due to L1 having a lower utilization than L2 and DCFC (Table 4). Demand charges in California and New York are sensitive for L2 stations under private company ownership. Further, the maximum demand of L2 stations under private company ownership is sensitive in New York. Lastly, the LCOC is sensitive to the number of DCFC stations in California and New York under private company ownership.

3.3.2 Life Cycle Assessment

The LCA results include the C2G GHG emissions from the fuel-cycle and vehicle-cycle (BEV: 63 gCO_{2e}/mi; Gas CV: 35 gCO_{2e}/mi [100]). The fuel-cycle shows the impact of an evolving grid mix for charging and vehicle fuel efficiency (detailed in Appendix B, Figure B12). Figure 10 shows the C2G GHG reduction from switching from a gasoline CV to a BEV charging at the MUD in each contiguous state. Results show the BEVs reduce C2G GHG emissions relative to gasoline CVs (U.S. average) for all 48 contiguous states' grid mixes in 2020 and 2050, but some states' grid mixes have lower BEV GHG emissions than others. These results are consistent with previous studies [27,28].

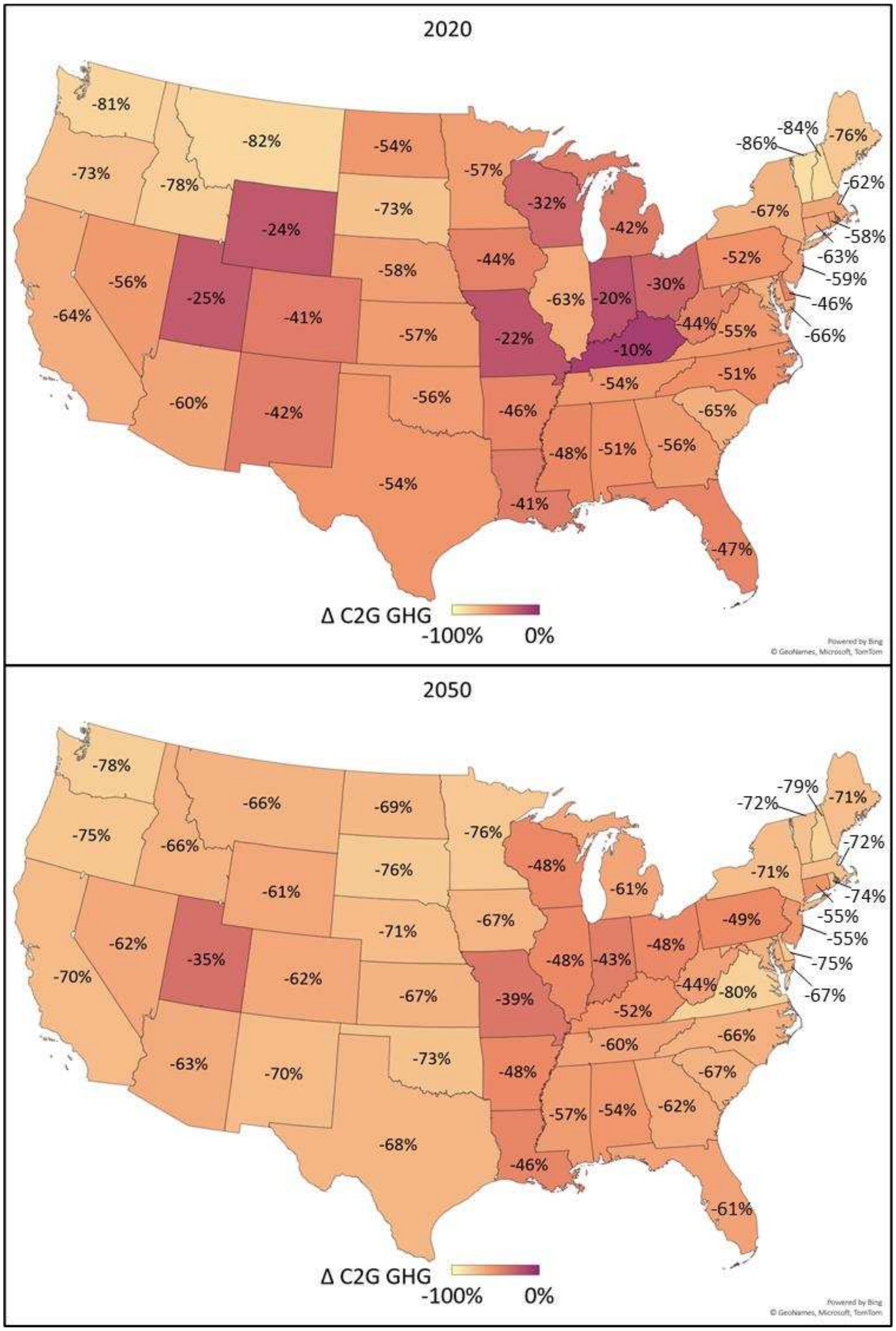

Figure 10. Change (Δ) in cradle to grave (C2G) greenhouse gas (GHG) emissions for the 48 contiguous states in 2020 and 2050 by using an average passenger Battery Electric Vehicle (BEV) rather than an average passenger gasoline conventional vehicle (CV).

As shown in Figure 10, BEVs can substantially reduce C2G GHG emissions in states with low GHG emitting grid mixes like Washington (2020: -81%; 2050: -78%). However, states with high GHG emitting grid mixes like Kentucky (2020: -10%; 2050: -52%) can have a much lower reduction to GHG emissions as low emitting states. The total impact of BEV adoption for each state also depends on the number of vehicles in the state. For this reason, the states with a high population of MUD vehicles and low GHG emitting grids can benefit from MUD vehicle electrification.

3.3.2.1 Sensitivity Analysis

Sensitivity analysis is performed for the U.S. aggregate emissions reduction from 2020 to 2050. Results are presented in Figure 11.

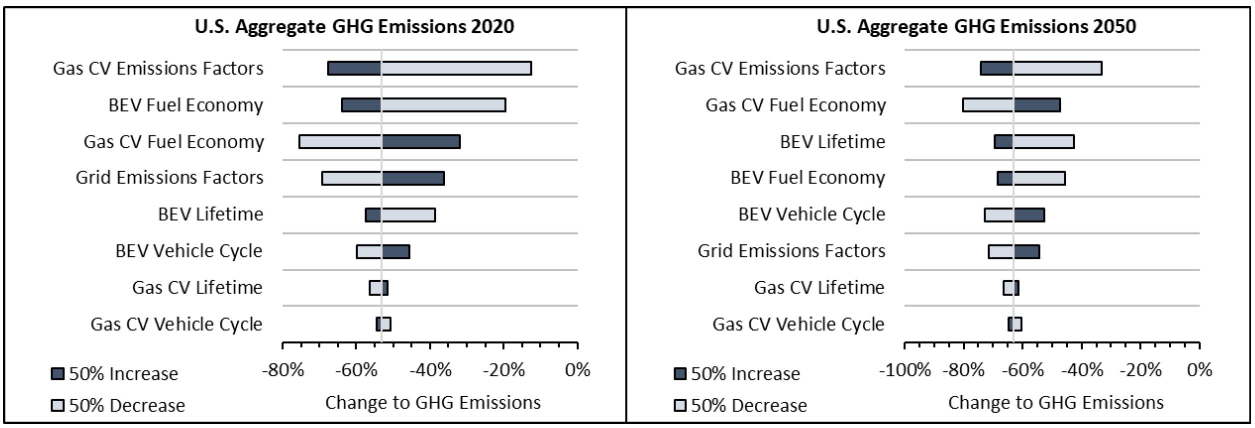

Figure 11. Sensitivity of Life Cycle Assessment (LCA) inputs for the change in cradle to grave (C2G) greenhouse gas (GHG) emissions for the U.S. aggregate grid mix in 2020 and 2050 by using an average passenger battery electric vehicle (BEV) rather than an average passenger gasoline (Gas) conventional vehicle (CV).

As shown in Figure 11, results are sensitive to gasoline CV emissions factors and vehicle fuel economies. Additionally, grid emissions factors are more sensitive in 2020 while BEV lifetime and BEV vehicle-cycle are more sensitive in 2050. This is due to the BEV vehicle-cycle contributing more to total BEV emissions when the grid emissions reduce in 2050. Moreover, vehicle-cycle emissions per mile driven are reduced with a longer BEV lifetime.

3.3.3 Cost of Greenhouse Gas Emissions Reduction

The cost of GHG emissions reduction quantifies the economic efficiency of a GHG reducing technology, such as BEVs, which enables strategic cost-effective investments from policymakers. This analysis includes the costs and emissions over the entire life of each vehicle type. The TCO of BEVs (0.45-0.72 $/mi) and gasoline CVs (0.53-0.60 $/mi), shown in Figure B13, includes the LCOC for every scenario determined in 3.3.1 plus all other major cost components (vehicle depreciation, maintenance and repair, insurance, and license and registration). Section 3.2 (Figure 10) shows that a BEV has lower C2G GHG emissions than an equivalent gasoline CV in Illinois (-60%), New York (-72%), and California (-69%) on average from 2020 to 2050 (5-year increments). Results presented in Figure 12 illustrate the costs or cost savings in terms of GHG emissions. Specifically, since BEV has lower emissions, a positive cost per tonne of CO_{2e} (tCO_{2e}) shows a BEV to be more expensive and a negative cost per tCO_{2e} shows a BEV to be less expensive relative to a gasoline CV.

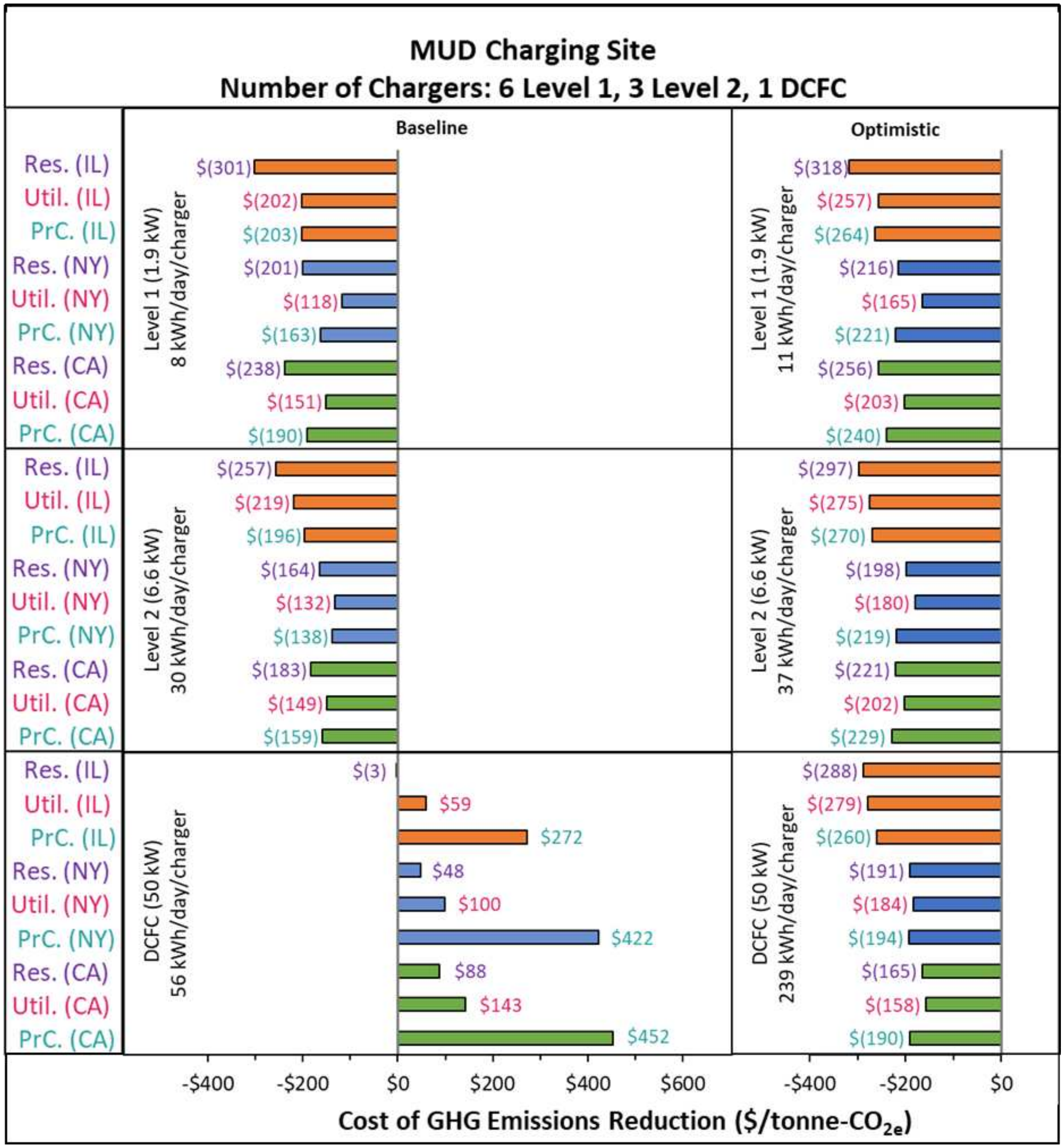

Figure 12. Cost of greenhouse gas (GHG) emissions reduction from battery electric vehicles (BEVs) that charge at a Multi-Unit Dwelling (MUD) instead of gasoline conventional vehicles from 2020 to 2050. Results are based on cradle to grave GHG emissions and the total cost of ownership which includes the levelized cost of charging (LCOC) for Level 1, Level 2, and Direct Current Fast Charging (DCFC) in Illinois (IL), New York (NY), and California (CA) under resident (Res.), utility (Util.), and private company (PrC.) ownership models. A negative cost means that the MUD charging scenario for BEVs would be less expensive and reduce GHG emissions relative to a gasoline conventional vehicle. A positive cost means that the MUD charging scenario for BEVs would be more expensive and reduce GHG emissions relative to a gasoline conventional vehicle.

As shown in Figure 12, under certain scenarios, MUD BEVs can have a lower TCO and lower C2G GHG emissions than a gasoline CV resulting in a negative cost of GHG emissions reduction. However, under baseline parameters for DCFC, the cost of GHG emissions reduction is positive for all (48 to 452 $/tCO_{2e}$) but one scenario meaning MUD BEVs may need a subsidy to be competitive with gasoline CVs. In relation to other technologies and policies that reduce GHG emissions, MUD BEVs are shown to potentially be a cost-effective (-\$318 to \$452 $/tCO_{2e}$) way to reduce GHG emissions. Gillingham and Stock (2018) found vehicle related policies to have positive costs, including Gasoline Tax (18-47 $/tCO_{2e}$), CAFE Standards (48-310 $/tCO_{2e}$), Renewable Fuel Subsidies (100 $/tCO_{2e}$), Biodiesel (150-420 $/tCO_{2e}$), Cash for Clunkers (270-420 $/tCO_{2e}$), and Dedicated Battery Electric Vehicle Subsidy (350-640 $/tCO_{2e}$) [106]. An alternative to vehicle related policies is direct air capture (134-342 $/tCO_{2e}$) which also has positive costs [107]. In conclusion, this study demonstrates that MUD BEVs can reduce both costs (without subsidies) and GHG emissions for the vehicle owners, making MUD charging infrastructure a cost-effective investment that can reduce U.S. GHG emissions to help meet the U.S.'s climate goals [108].

3.4 Conclusion

The LCOC and C2G GHG emissions for BEVs at MUDs was evaluated and determined to yield both driver savings (except baseline DCFC) and GHG emissions reductions (10-86%) across the U.S. relative to gasoline CVs. Thus, MUD BEV charging infrastructure can be a cost-effective endeavor to reduce GHG emissions. However, regulatory restrictions for utilities and private companies to own and operate MUD charging hubs need to be lifted to facilitate greater charger deployment. Currently, property owners and homeowner associations may be hesitant to bear the financial and logistical burden of owning chargers. The results from this study demonstrate that utility and private company ownership models result in a large LCOC premium for L1 chargers and a moderate LCOC premium for L2 chargers relative to the resident ownership model. Furthermore, DCFC chargers were shown to be expensive for the baseline scenarios but economical for the optimistic scenarios especially under private company ownership. Until the optimistic scenario's parameters are achieved for DCFC, this study recommends the following two sets of combinations of MUD charger deployment scenarios: 1) L1 for resident ownership which has long charging durations but large cost savings; and 2) L2 for resident, utility, or private company ownership which have moderate charging durations and moderate cost savings. Moreover, the LCOC is sensitive to charger utilization so adequate usage is needed to be cost comparable with the gasoline equivalent. Future work will consider different mixes of L1, L2, and DCFC chargers to analyze the trade-off between charging time and cost.

CHAPTER 4: COMPARISON OF THE COST AND ENVIRONMENTAL IMPACT OF ELECTRIC VEHICLE CHARGING SYSTEMS IN THE UNITED STATES[3]

4.1 Main

The U.S. is currently undertaking an ambitious initiative to deploy public charging infrastructure to facilitate the widespread adoption of EVs necessary for achieving climate targets [1]. As EVs continue to gain popularity in all vehicle classes, ensuring uninterrupted transportation has become a critical objective for policymakers and stakeholders [1,13]. While initial efforts have focused on deploying L2 and DCFC infrastructure [109], a significant challenge lies in the charging time required to replenish EV batteries [13]. Long charging times pose potential inconveniences for EV drivers, particularly those embarking on long journeys or requiring urgent charging [13]. Addressing this issue necessitates the implementation of charging systems capable of addressing consumer needs [13,110]. With the electrification of medium-duty vehicles (MDVs) and heavy-duty vehicles (HDVs) [110], the infrastructure needs to accommodate a broader range of vehicles beyond passenger cars and light-duty trucks (LDTs) [111]. Consequently, it is imperative to transition towards technologies that minimize dwell times for all vehicle types, such as 350-kW DCFC, BSS, or DWPT [111].

Each of these technologies presents a distinct set of benefits and challenges. DCFC operates similarly to traditional liquid refueling and allows for scalability by increasing the number of stations

[3] This chapter was submitted for publication as a peer-reviewed journal article: Horesh N, Trinko D, Quinn J.C. (Manuscript in review). Comparing Costs and Climate Impacts of Electric Vehicle Charging Systems in the United States.

according to demand. However, the intermittent high-power loads of DCFC present challenges to the electrical grid and costs to the consumer [112]. In contrast, BSS optimizes loads by charging batteries before they are swapped, but it relies on battery standardization to cater to different vehicle brands [111]. Moreover, the implementation of BSSs requires two different sizes: a small size for cars and LDTs and a large size for MDVs and HDVs [113]. Alternatively, DWPT inductively charges vehicles while they are in motion using embedded electronics in the roadway, effectively reducing the required battery size and eliminating the need for vehicles to stop between destinations [24]. DWPT, however, may cause traffic disruptions during roadway replacements, has limited deployment experience, and is capital intensive [114,115]. Despite the well-understood performance of these technologies, there remains a meaningful gap in understanding the economic and environmental implications that would arise from their widescale deployment.

This research chapter addresses this gap by simulating the nationwide deployment of DCFC, BSS, and DWPT and assessing the global warming potential (GWP) and TCO of EVs utilizing these systems. By leveraging geospatial charging demand, emissions, and cost data, this study determines precise location-specific sustainability outcomes. Deployment scenarios for the charging systems, spanning from 2031 to 2050, are formulated based on the geospatial demand derived from traffic data forecasts [116] and three EV adoption scenarios (Figures C1-C2): optimistic, baseline, and conservative [110,117]. DCFC and BSS charging infrastructure is strategically placed at existing DCFC sites, gas stations, and surface parking lots near grid interconnections. At each charging site, the number of charging stations for DCFC and number of batteries for each vehicle category using the BSS is adjusted to accommodate the charging demand up to the charging site's limited power, spatial, and time capacities (Eqs. 11-12) [13]. In contrast, DWPT infrastructure is deployed along major roadways to ensure that EVs can maintain their state of charge, consequently requiring a fixed amount of infrastructure (Eqs. 13-14) [114]. Specifically, in optimistic and baseline EV adoption scenarios, DWPT is deployed on interstates, freeways, and principal arterial roads, thereby reducing the required EV battery sizes to a range of 56-kilometers (35-miles) (Tables C1-C2, Figure C3) [24]. However, with fewer EVs, the conservative EV adoption scenario assumes that only interstates are electrified, necessitating the use of full-size batteries for EVs. Simulation results are used to determine the levelized cost of charging (Eqs. 15-23) and GWP for each DCFC site, BSS site, and DWPT roadway, accounting for each location's design, utilization, electricity costs, and electricity mix. The levelized cost of charging is used to determine the TCO for EVs, which is then compared to internal combustion engine vehicles (ICEVs) and hybrid electric vehicles (HEVs) over a 10-year period per vehicle-kilometer travelled (VKT) [25]. The TCO encompasses location-specific charging/fuel costs, license and registration fees, insurance expenses, as well as average depreciation and maintenance costs in the U.S. (Tables C2-C7). Additionally, the GWP of EVs is compared to ICEVs and HEVs over their full vehicle lifetime per VKT [100]. The GWP encompasses all attributional emissions, including local and time-specific charging emissions, local embodied charging infrastructure emissions, and the U.S. average embodied vehicle emissions for EVs, as well as fuel and embodied vehicle emissions for ICEVs and HEVs (Figures C4-C5, Tables C8-C13, Eq. 24). Finally, to account for the adaptability of variables that highly influence TCO and GWP, optimistic, baseline, and conservative scenarios are modeled for electricity mixes, capital costs, electricity prices, and fuel prices (Figures C6-C7). These scenarios result in a total of 81 TCO and 9 GWP comparisons for each charging system with results presented as interactive figures.

4.1.1 Cost Savings from EV Adoption

The change in combined TCO when switching from ICEVs to EVs (Eqs. 25-26) is illustrated on a county level in interactive Figure 13 (Data C1), which displays the results specific to the chosen scenarios for EV adoption, capital costs, electricity prices, and fuel prices. The findings suggest that the economic impacts of vehicle electrification in the U.S. are location-dependent and subject to variable changes, emphasizing the necessity of a dynamic figure. The change in TCO is weighted by EV adoption from 2031 to 2050 and presented for baseline scenarios as a percentage in Figure 13**A-C** and in billions (B) of 2022 U.S. Dollars (USD) in Figure 13**D-F**.

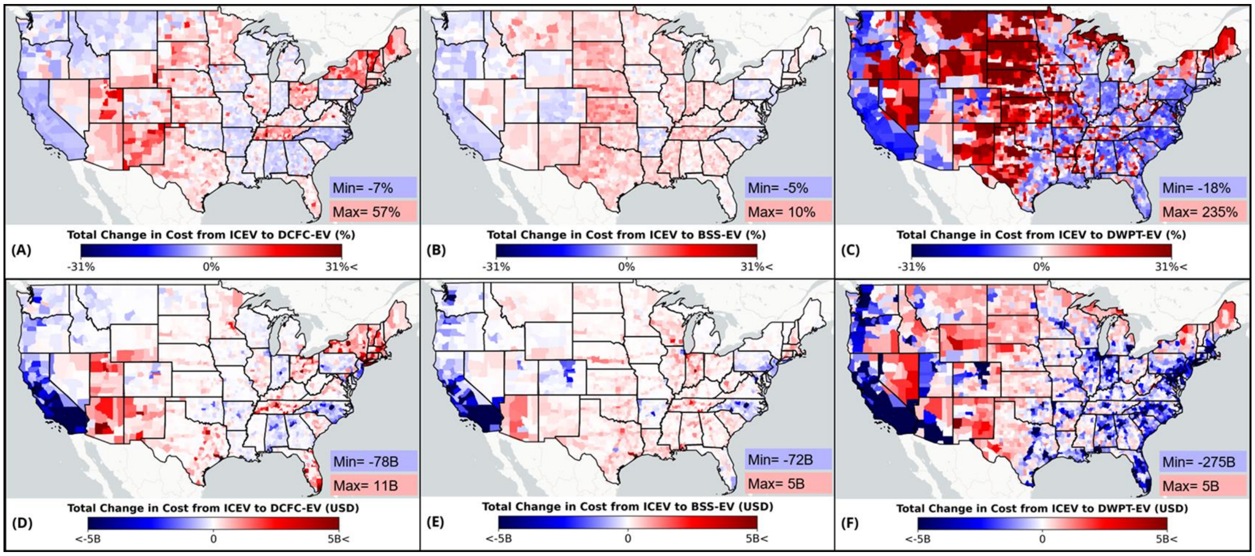

*Figure 13. Total change in cost due to electric vehicle (EV) adoption. County level results are presented for the change in total cost of ownership due to the transition from internal combustion engine vehicles (ICEVs) to EVs (**A-C**) as a percentage and (**D-F**) in billions (B) of 2022 United States Dollars (USD). Each map corresponds to EVs charged via (**A, D**) Direct Current Fast Charging (DCFC), (**B, E**) Battery Swapping (BSS), and (**C, F**) Dynamic Wireless Power Transfer (DWPT). The baseline scenarios are shown in this static figure with all scenarios shown in the interactive Figure 13 or Data C1. Instructions for the interactive figure are in Appendix C.*

Depending on the assumptions for each technology, the TCO of EVs can vary from being more favorable than ICEVs to less favorable, as demonstrated in interactive Figure 13 when combining conservative fuel prices with optimistic EV adoption, capital costs, and electricity prices, or vice versa. Moreover, the change to the TCO by switching from ICEVs to EVs varies depending on the location, with local fuel prices, electricity prices, and traffic volumes playing a considerable role in the change. In highly trafficked areas, substantial reductions in TCO are typically observed both as a percentage and in USD. Conversely, low traffic areas typically show a relative increase in TCO, although the national impact in terms of USD remains limited due to fewer VKT. For instance, DWPT demonstrates the largest range of TCO change (-31% to +429%) and charging costs (interactive Figure C8), primarily due to the heavy dependence on infrastructure utilization for upfront capital cost recovery. Thus, the capital cost allocation for using DWPT roadways may need to be based on a national average to ensure price equity. The charging cost for DCFC is heavily influenced by local demand charges (USD/kW per month), allocated based on site utilization (interactive Figure C9). In contrast, BSS exhibits minimal price variability within a state by optimizing charging times to minimize electricity costs (interactive Figure C9).

Although the charging cost for BSS has limited geographical variability, it is highly dependent on the assumptions around capital cost and EV adoption. Specifically, BSS has large capital costs, which can be reduced on a per kWh dispensed basis through lower battery prices (90-150 USD/kWh [118]) and greater utilization. Moreover, DWPT exhibits a wide range of capital costs (0.94M-5.4M USD/lane-kilometer [24,114,119]) across different scenarios due to the technology being in the R&D phase. Consequently, DWPT can have the highest or the lowest capital cost per kWh dispensed (interactive Figure C9). This highlights the opportunity for cost reduction in DWPT, driven by the potential to decrease infrastructure capital expenses and its high utilization capacity. In contrast, DCFC incurs the highest electricity costs, mainly due to demand charges that are challenging to reduce given the requirement of supplying electricity at high power levels simultaneously with urgent charging. Further, projected electricity price scenarios exhibit minimal variations (Figure C6). Conversely, the energy or fuel price scenarios for ICEVs are highly variable (Figure C7) and impact whether EVs are economically favorable. The EV adoption scenarios, however, pose ambiguity as charging costs typically decrease with greater EV adoption, yet the combined change to the TCO from all vehicle categories can increase due to a higher portion of EVs in a vehicle category where EVs are more expensive than ICEVs.

The TCO of EVs can be lower than that of ICEVs for cars and LDTs but are in general higher for MDVs and HDVs, as illustrated in interactive Figure 14 (Data C1) with results reactive to the selected scenarios. Figure 14 presents the aggregated TCO at the national level for ICEVs, HEVs, DCFC-EVs, BSS-

EVs, and DWPT-EVs under baseline scenarios. The variation of TCO among vehicle categories is due to the distinct contributions of each cost component to the overall TCO of the vehicles.

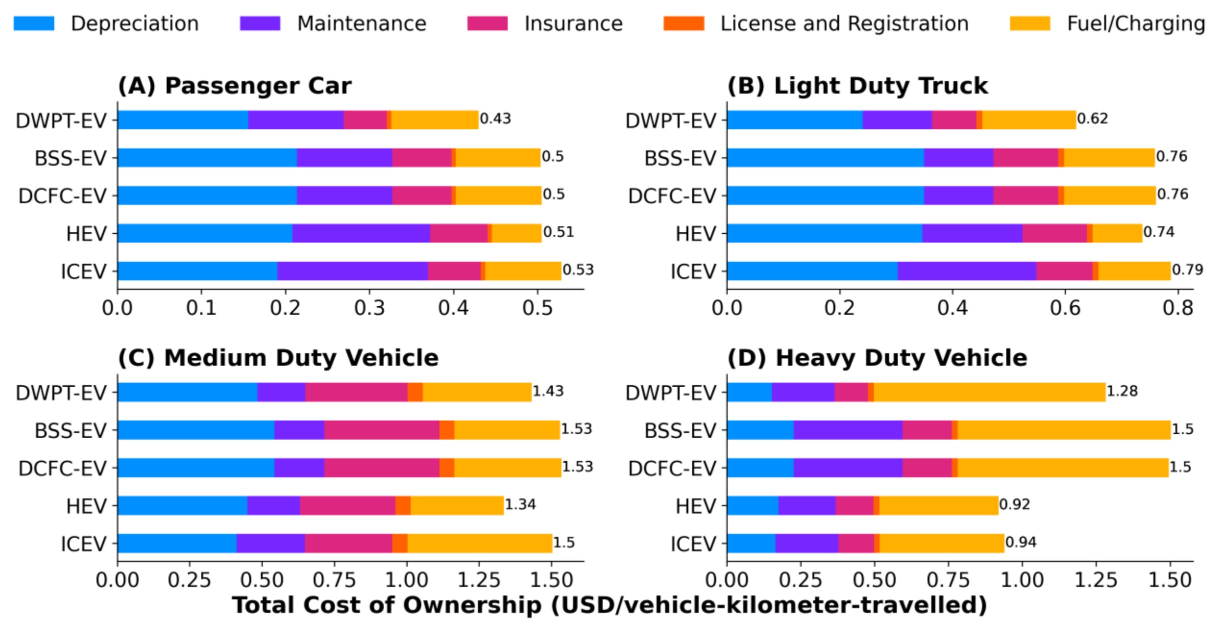

*Figure 14. Breakdown of the 10-year total cost of ownership. Results are presented for an average (**A**) passenger car, (**B**) light-duty truck, (**C**) medium duty vehicle, and (**D**) heavy duty vehicle in the contiguous United States. The vehicle types include electric vehicles charged via Direct Current Fast Charging (DCFC-EV), Battery Swapping (BSS-EV), and Dynamic Wireless Power Transfer (DWPT-EV). The EVs are compared to an average internal combustion engine vehicle (ICEV) and hybrid electric vehicle (HEV) from each vehicle category. The baseline scenarios are shown in this static figure with all scenarios shown in the interactive figure or Data C1. Instructions for the interactive figure are in Appendix C.*

The breakdown of the TCO in Figure 14 reveals several noteworthy findings. Depreciation emerges as a major cost contributor for cars, LDTs, and MDVs across all technologies. When comparing HEVs to ICEVs, there is a trade-off between higher depreciation costs and reduced maintenance and fuel costs for HEVs. Similarly, there are lower maintenance costs and higher depreciation costs for EVs in the car and LDT categories. In contrast, EV maintenance costs are more expensive for HDVs due to expensive battery replacements within the initial 10-year lifespan, resulting from the combined factors of higher annual VKT and limited battery cycle life (Table C2). As a result, the DWPT-EV, with a reduced battery size that effectively lowers depreciation and maintenance costs, is the only electric HDV to demonstrate a cost advantage over an ICEV and HEV. Moreover, electric MDVs charged through DCFC or

BSS exhibit cost advantages over ICEVs and HEVs solely in scenarios with high fuel prices, whereas MDVs charged via DWPT can achieve lower costs across all fuel price scenarios.

4.1.2 Reduction to Global Warming Potential from EV Adoption

The change in GWP resulting from EV adoption (Eqs. 27-28) is examined at the county level in interactive Figure 15 (Data C1), and the results reflect the optimistic, baseline, or conservative scenarios selected for EV adoption and electricity mixes. The findings highlight the influence of the grid mix and infrastructure utilization on GWP changes from 2031 to 2050, presented both as percentages (Figure 15**A-C**) and in kilograms of Carbon Dioxide equivalent (CO_{2e}) (Figure 15**D-F**) for the baseline scenarios.

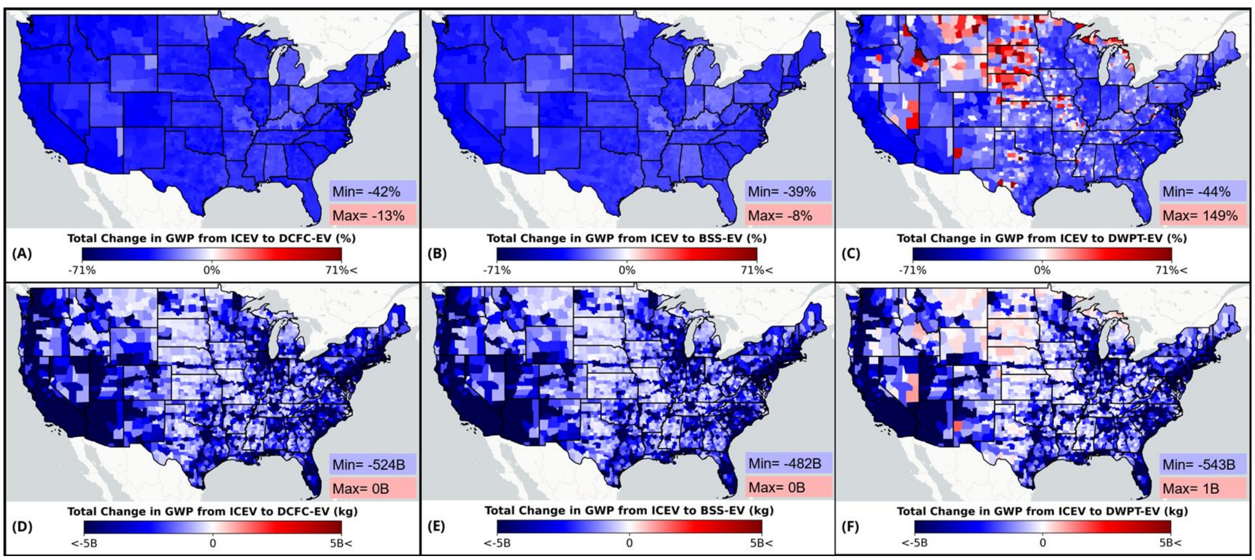

*Figure 15. Total change to global warming potential (GWP) from electric vehicle (EV) adoption. The maps are for the change in GWP of on-road vehicle transportation in United States counties by switching from internal combustion engine vehicles (ICEVs) to EVs charged via (**A, D**) Direct Current Fast Charging (DCFC), (**B, E**) Battery Swapping (BSS), and (**C, F**) Dynamic Wireless Power Transfer (DWPT). The results are presented as (**A-C**) a percentage and (**D-F**) in billions (B) of kilograms (kg) of Carbon Dioxide equivalent. The baseline scenarios are shown in this static figure with all scenarios shown in the interactive figure or Data C1. Instructions for the interactive figure are in Appendix C.*

The percent change in GWP is predominantly influenced by the local electricity mix for DCFC-EVs and BSS-EVs, while for DWPT-EVs, it is dependent on infrastructure utilization, as depicted in Figure 15. In numerous locations, the scenarios for electricity mix and EV adoption change whether EVs increase or reduce transportation GWP. Deploying DWPT in areas with lower utilization may increase the county

GWP by up to 167% but these areas have a limited national impact in terms of kilograms of CO_{2e} due to fewer VKT. Similarly, certain areas may experience an increase in vehicle GWP due to an electricity mix with a high carbon intensity, which depends on the scenario. Conversely, when infrastructure utilization is high and charging emissions are small due to a clean grid, the reduction in county-level GWP emissions can reach up to 71%.

Overall, EVs have a lower GWP nationally than ICEVs and HEVs across all scenarios and vehicle categories, as demonstrated in [interactive Figure 16](#) (Data C1) and summarized in Figure 16 for baseline scenarios. The breakdown of GWP reveals that the contribution of time-of-day (Figures C4-C5) charging emissions is similar for all EV charging systems, while vehicle and infrastructure emissions differ.

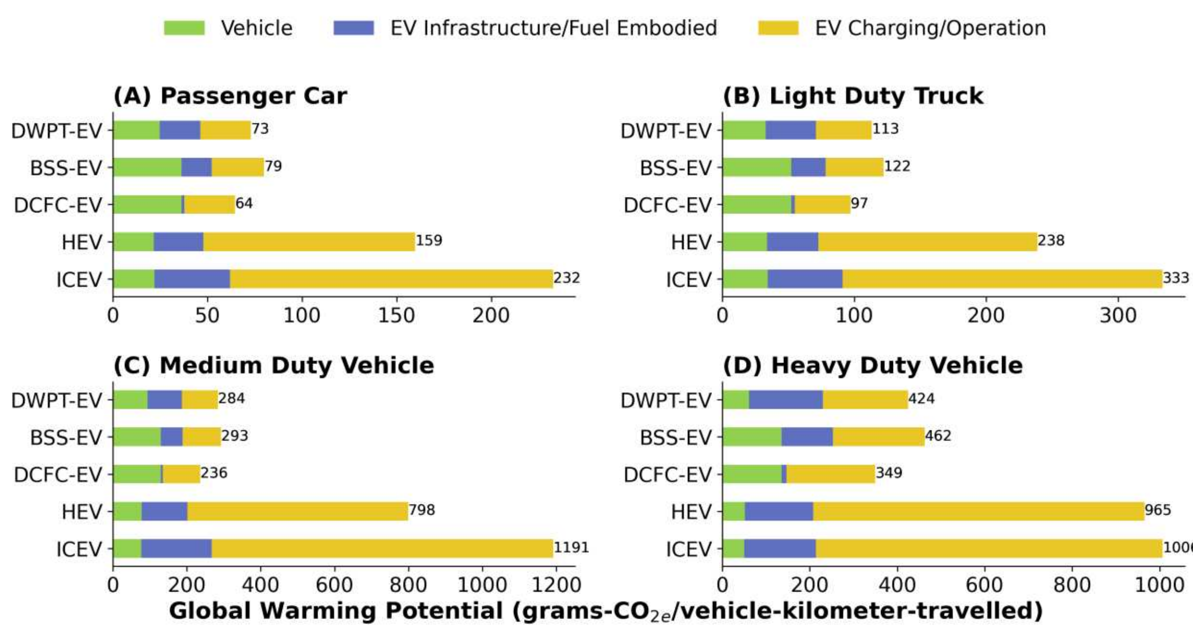

*Figure 16. Breakdown of the lifetime global warming potential. Results are for an average (**A**) passenger car, (**B**) light-duty truck, (**C**) medium duty vehicle, and (**D**) heavy duty vehicle in the contiguous United States. The vehicle scenarios include electric vehicles (EVs) charged via Direct Current Fast Charging (DCFC-EV), Battery Swapping (BSS-EV), and Dynamic Wireless Power Transfer (DWPT-EV). Results are compared to an internal combustion engine vehicle (ICEV) and hybrid electric vehicle (HEV) from each vehicle category. The baseline scenarios are shown in this static figure with all scenarios shown in the interactive figure or Data C1. Instructions for the interactive figure are in Appendix C.*

The breakdown presented in Figure 16 reveals that infrastructure emissions have a minimal contribution for DCFC-EVs, whereas they become substantial for BSS-EVs and DWPT-EVs, primarily due to the embodied emissions associated with high battery and concrete usage, respectively. Notably, the vehicle emissions reduction achieved through a reduced battery size in DWPT-EVs does not fully offset the infrastructure emissions when compared to DCFC-EVs. Additionally, HEVs exhibit considerable emissions reductions compared to ICEVs, although their emissions are still much higher than those of EVs, even in scenarios with conservative EV adoption and electricity mix. This highlights the critical importance of EVs in decarbonizing the transportation sector. Moreover, the magnitude of this impact depends on both the decarbonization of the electricity mix and the level of EV adoption, as illustrated in interactive Figure 16.

4.1.3 Charging System Implications

The transition from ICEVs to EVs could lead to remarkable changes to transportation TCO and GWP, electricity grid infrastructure, and automotive manufacturing. The results of this study show that from 2031 to 2050, on-road transportation costs can change by -22% to +11% and GWP can change by -53% to -19% depending on various adoption and technology scenarios. During this period, the annual average electricity generation would increase by 16% to 38% relative to 2022 levels [120], potentially requiring utilities to upgrade distribution and generation capacities. Controlling the charging loads from BSS and DWPT could reduce the need for distribution and generation capacity upgrades, in contrast to DCFC [113,121]. Furthermore, the total (2031-2050) anticipated battery production needed for full-size EV batteries ranges from 13 to 31 terawatt-hours, highlighting the necessity for major expansions to production capacity compared to the global production of 700 gigawatt-hours in 2022 [122]. However, by using a smaller battery size, DWPT could reduce the battery production needed by 79%. This reduction could alleviate the global resource and manufacturing constraints associated with battery production [8].

DWPT, however, requires an order of magnitude higher capital investment at 134B to 1.7 trillion USD, as compared to 41B to 115B USD for BSS and 23B to 52B USD for DCFC. Notably, DWPT provides a much larger share of charging for EVs at 35-61% for cars, 32-61% for LDTs, 29-56% for MDVs, and 67-83% for HDVs. In comparison, DCFC and BSS are estimated to supply 5% of charging for cars and LDTs, 0.6% for MDVs, and 14% for HDVs. Therefore, DCFC and BSS deployment assumes EVs will primarily use home, workplace, or fleet charging [26,123].

Given that both DCFC and BSS charging infrastructure can be implemented simultaneously, their deployment can be optimized in areas where they offer the most cost-effective solution [124]. For instance, BSS is more advantageous in regions with high demand charges or time-of-use rates, whereas BSS may be less favorable in low-traffic areas due to expensive upfront capital costs. Moreover, each size of the BSS caters to different vehicle categories, with a small size for cars and LDTs and a large size for MDVs and HDVs. Thus, the deployment of BSS could be focused exclusively on MDVs and HDVs, which is especially advantageous due to their pressing charging requirements coupled with longer dwell times when utilizing DCFC to charge their larger battery capacities and the ability for fleets to overcome social challenges with BSS. DWPT eliminates dwell times, but has been shown to be most cost effective when utilized by all vehicle categories [114]. Further, if the deployment of DWPT is restricted to specific corridors, then it may necessitate EVs to utilize full-size batteries and multiple charging systems. Ultimately, the most suitable charging system will differ depending on the location and stakeholders involved, considering the geographical variations in TCO, GWP, and performance across different charging systems.

4.2 Methods

An integrated TEA and LCA was developed to comprehensively compare the widescale deployment of DCFC, BSS, and DWPT charging infrastructure in the contiguous U.S. In this analysis, the three charging systems were deployed independently to facilitate comparison. The analysis focused on four vehicle categories: passenger car, LDT, MDV, and HDV For each of the vehicle categories, the TCO and C2G GWP were evaluated for each of the EV charging systems and compared to a representative

HEV and ICEV with a functional unit of one VKT. The analysis assumed the charging infrastructure was implemented in 2030 and online from 2031 to 2050, a 20-year lifetime [114].

4.2.1 Charging System Energy Usage

To assess the portion of each vehicle's overall energy consumption contributed from different charging systems, the usage of public charging was evaluated for DCFC, BSS, and DWPT. The DWPT system was assumed to maintain the vehicle's state of charge while driving on the electrified roadway, whereas the DCFC and BSS systems were modeled to provide energy only during daytime trips. The vehicle energy efficiencies per VKT were 0.19-kWh for cars, 0.30-kWh for LDTs, 0.68-kWh for MDVs, 1.34-kWh for HDVs, and 1.35-kWh for buses [100]. The usage of these systems was categorized into stationary charging usage (DCFC and BSS) and electrified roadway usage (DWPT). Cars, LDTs, MDVs, and HDVs were assumed to utilize the stationary charging systems and electrified roads. Buses were included in the usage of the electrified roadway; however, their TCO and GWP were not explicitly modeled in the analysis.

4.2.1.1 Stationary Charging System Usage

For each vehicle category, the usage of stationary charging systems was modeled separately. Cars and LDTs were assumed to have the same usage since they are both considered light-duty vehicles. Among light-duty vehicles, only BEVs were assumed to utilize the infrastructure, as plug-in hybrid electric vehicles are typically incompatible with the high-power rates of DCFC and the standardized battery sizes required for BSS. Hence, it was estimated that 82% of electric cars and LDTs would use the infrastructure [125]. Observational data indicated that public charging usage for light-duty vehicles is around 6%, resulting in a 5% usage of public charging for electric cars and LDTs [126].

However, due to the lack of available data for electric MDVs and HDVs, the usage of public charging was simulated for multiple vehicle operating ranges [127] and corresponding battery sizes.

MDVs and HDVs were assumed to undergo overnight charging and start each day with a fully charged battery [123]. The battery sizes were divided into 90-kWh battery modules [128], and the number of modules onboard the EV was determined to minimize battery expenses while ensuring that the vehicle required no more than one public charging event per day during the operator's required driving break [129]. The simulated driving break was modeled such that the vehicle's state of charge would be above 20% before the charging event to maintain battery health and below 80% at the end of the charging event to optimize charging time [130]. The vehicle was assumed to only charge the minimum amount to complete its trip. The battery size, portion of VKT in the vehicle category, and portion of public charging usage were presented in Table C1 for each operating range. The average portion of energy supplied from public charging, weighted by VKT in each operating range, was found to be 0.6% for MDVs and 14% for HDVs.

4.2.1.2 Electrified Roadway Usage

The electrified roadway was assumed to provide continuous power, maintain the vehicle's state of charge, and be used by cars, LDTs, MDVs, HDVs, and buses. The minimum portion (*R*) of each roadway segment (*i*) that needed to be electrified for each vehicle category was calculated in Eq. 14 based on the segment's speed limit (*S*), receiving pad power rating (*P*) of 50-kW, number of receiving pads (*N*) on the vehicle (*v)*, vehicle energy efficiencies per VKT (*EE*), charging efficiency (*CE*) of 85%, and amount failed (*F*). The amount failed was calculated in Eq. 13 based on the *VKT* by each vehicle type over the life of the roadway segment, number of receiving pads on the vehicle, failure rate (*FR*) of 2.87 pads per million hours [131], number of roadway pads (*RP*) per segment (200 per kilometer (km)), and speed limit.

$$\mathrm{F_i} = \sum\nolimits_{\mathrm{v}} \mathrm{FR} * \mathrm{VKT_{i,v}} * \mathrm{N_v}/(\mathrm{RP_i} * \mathrm{S_i}) \qquad (13)$$

$$\mathrm{R_{v,i}} = \mathrm{S_i} * \mathrm{EE_v}/(\mathrm{P} * \mathrm{N_v} * \mathrm{CE} * \mathrm{F_i}) \qquad (14)$$

The electrified portion of roadway was modeled based on the vehicle category that needed the highest portion electrified. The number of receiving pads for each vehicle category depended on their charging requirements and wheelbase allowances, with cars having one pad, LDTs having two pads, MDVs having four pads, and HDVs and buses having five pads [114].

4.2.2 Time of Day Usage

Time-of-day resolution was added to the EV energy demand using arrival and departure time data for cars, LDTs, MDVs, and HDVs. The charging schedule for DWPT and BSS was aligned with the vehicles' in-route periods since these systems have minimal charging times (Figure C4). In contrast, the DCFC schedule corresponded to the vehicles' dwell periods due to the slower charging rate of DCFC (Figure C5).

The arrival and departure time data for cars and LDTs were extracted from the 2017 National Household Survey, which provides trip data for various vehicles [132]. Specifically, the schedule for cars was derived from 280K automobile trips, while the LDT schedule was based on 289K van, sport utility vehicle, pickup truck, other truck, and recreational vehicle trips. The energy consumed during each trip was assumed to represent the amount of energy replenished through charging. For in-route charging, the trip energy was evenly distributed throughout the trip, calculated based on the trip distance and vehicle energy efficiency. For charging during car and LDT dwell periods, the energy was replenished up to the amount consumed during the trip. The charging schedules for cars and LDTs can be seen in Figure C4.

The charging schedule for MDVs and HDVs was determined using the National Renewable Energy Laboratory's Fleet DNA database, which contains operating data for commercial fleet vehicles [133]. The MDV schedule was developed from 1,471 trips made by class 3 to 7 delivery trucks and vans, while the HDV schedule was based on 969 trips made by class 8 tractors. The trip data was categorized into each vehicle operating range and weighted by VKT from Table C1; trip data for over 322 VKT (200 vehicle miles travelled) was used for all operating ranges above 322-km. It was assumed that the VKT for each trip was evenly distributed between the arrival and departure times, resulting in a distribution of the in-route charging profile throughout the day. The weighted average charging schedules for MDVs and HDVs were illustrated in Figure C5.

4.2.3 Deployment of Infrastructure

Deployment scenarios were developed for DCFC, BSS, and DWPT to assess the charging cost and GWP of individual charging locations across the U.S. The estimated usage of each charging system was scaled using yearly traffic data and EV adoption projections. Vehicle traffic data from the Freight Analysis Framework Version 4 (FAF4) provided VKT estimates for 2012 and 2045 on 663K individual roadways for freight trucks (MDV and HDV) and all vehicles [116]. These estimates were interpolated and extrapolated linearly up to 2050.

To break down the FAF4 data by vehicle category, multiple datasets from the Federal Highway Administration (FHWA) were utilized, incorporating the 2019 FHWA VKT data and their projected increase in 2049 [134]. The FHWA VKT data included breakdowns for cars, light trucks (LDTs), single-unit trucks (MDVs), combination trucks (HDVs), motorcycles, and buses [135,136]. The FHWA VKT data were used to calculate the portion of vehicles in the FAF4 data that fell into the categories of cars, LDTs, MDVs, and HDVs based on the percentage of FHWA VKT from each vehicle category on state roadways, including interstates (FAF4 interstates), other arterials (FAF4 freeways, principal arterials, and minor arterials), and other road types (FAF4 major collector and minor collector) [136]. It is worth noting that the FAF4 data did not include VKT on local roads. As a result, the FAF4 VKT data for stationary charging systems (DCFC and BSS) were scaled to match the total VKT of the FHWA data for each vehicle category in 2019 and 2049. In contrast, the FAF4 data for DWPT were not scaled to match the FHWA VKT total, as the VKT on individual roads was directly used in the analysis.

The VKT data, categorized by vehicle type on each roadway segment, were combined with EV adoption forecasts, a charging efficiency of 85% for each system [100], and vehicle energy efficiencies to estimate the charging demand from EVs. To account for uncertainty, three EV adoption scenarios were considered: optimistic, baseline, and conservative. The optimistic adoption curves for MDVs and HDVs were derived from Konstantinou and Gkritza (2023) [110], while the conservative and optimistic scenarios for cars, LDTs, and buses, as well as the conservative and baseline scenarios for MDVs and HDVs, were obtained from Mai et al. (2018) [117]. The baseline scenario for cars, LDTs, and buses represented the average of the conservative and optimistic EV adoption rates. The EV adoption forecasts for cars, LDTs, MDVs, and HDVs from 2030 to 2050 can be seen in Figure C1, with the adoption forecast for buses shown in Figure C2.

In summary, the energy demand for public EV charging was computed on major roadways in the contiguous U.S. from 2031 to 2050. The energy demand included hourly and yearly resolution for cars, LDTs, MDVs, and HDVs.

4.2.3.1 Stationary Charging

The yearly energy demand on the roadways from each EV adoption scenario was used to allocate EV charging to suitable charging sites. A total of 122K potential charging site locations were identified, including 85K gas stations [137], 30K public surface parking lots [137], and 7K existing DCFC sites [109]. The suitability of the sites for high-power charging stations was evaluated based on their proximity to grid interconnections and minimum EV charging utilization. Since load growth from widescale EV adoption was expected to require new substations, the location of grid interconnections was modeled as transmission lines with voltages under 200-kV [138] rather than existing substations. Site locations within 6-km of grid interconnections [139], based on the 95th percentile of existing DCFC sites, were deemed to be within the maximum proximity to grid interconnections. Further, sites within

1.5-km were not restricted on their maximum power due to the allowances of line extension policy [140]. Sites with power limitations were restricted to a maximum power of 2.5-megawatts [141].

DCFC sites without power limitations were restricted to a maximum daily energy dispensed of 30% of the time [92] for 32 stations with space constraints, as observed. The DCFC stations were set to use either 150-kW or 350-kW chargers as observed from major charging networks [15]. In contrast, BSS energy dispensation was constrained by a 3-minute swap time [142], limiting the maximum number of swaps during peak demand hours to prevent queuing. Each BSS site was designed to have two sizes of swapping stations: a small size for cars and LDTs, and a large size for MDVs and HDVs.

The maximum capacity (*m1*) of each site (*i*) was used in a gravity model [143] (Eq. 12) to allocate the yearly demand for EV charging on each roadway segment to the nearest 30 sites. The allocation of EV charging (*F*) to each site was also based on the amount of charging demand on the roadways (*m2*), the distance between the charging site and roadway (*d*), and a scalar (*g*). The scalar *g* was computed in Eq. 11 to ensure that the sum of *F* was equal to *m2* for each roadway segment.

$$\mathrm{g} = \left[\sum_{1}^{30} \mathrm{m1_i}/\mathrm{d_i}^2\right]^{-1} \qquad (11)$$

$$F_i = g * m1_i * m2/{d_i}^2 \qquad (12)$$

The allocation of EV charging to each site was then corrected to ensure that the maximum capacity of the site was not exceeded, and sites with very low usage were removed to avoid poor economics. The minimum allowed energy allocated to a DCFC site was set such that one 150-kW charger would dispense energy at least 5% of the time based on today's conditions [15], which represented the minimum usage threshold for the highest demand year. Similarly, each BSS site was designed to have a total energy demand of at least 4 swaps per day for both sizes of swapping stations during the highest demand year. Eqs. 11 and 12 were then used to allocate the energy for the remaining viable locations.

The required amount of charging equipment at each site was then determined based on its expected usage. For DCFC sites, the number of chargers needed was calculated separately for the first (2031-2040) and second (2041-2050) 10-year life of the equipment. DCFC sites with low expected usage were equipped with 150-kW chargers, whereas those with high expected usage were equipped with 350-kW chargers. Specifically, 150-kW chargers were only deployed at sites where the highest usage was below the maximum capacity of a single 350-kW charger during the initial 10-year period, and also below the maximum combined spatial capacity of 32 150-kW chargers over the full 20-year period. Alternatively, for BSS sites, the number of batteries and support equipment needed was determined annually, with a minimum usage of 4 batteries per site. Figure C3 shows the coverage of DCFC and BSS infrastructure within 80-km (50 miles [1]) for each EV adoption scenario.

4.2.3.2 Dynamic Wireless Power Transfer

DWPT infrastructure was deployed on major roadways in the contiguous U.S. to maintain every vehicle's state of charge. The energy dispensed from the electrified roadway was set to match the vehicle energy consumption on each roadway. If over half of vehicle traffic saturates the electrified lane, a second lane is assumed to be electrified in each direction, reducing the utilization by half for the analyzed lane. In the optimistic and baseline scenarios, one electrified lane was deployed in each direction on interstates, freeways, and principal arterial roadways. This allowed every vehicle's battery to be reduced to a 56-km (35-mile) range (Table C2) as illustrated in Figure C3 [24]. For the conservative EV adoption scenario, where EV adoption was lower, electrified lanes were only deployed on interstates, and vehicles required the same full-size batteries as with DCFC and BSS. The FAF4 dataset contained data for 75K of 76K km of interstates, 25K of 30K km of freeways, and 240K of 251K km of principal arterial roads in the contiguous U.S. [144]. Notably, the FAF4 data accounted for the combined VKT from both directions of traffic, and the length of the roadway segment represented the distance for one direction only. As a result, the electrified distance for one lane in both directions encompassed twice the length of the roadway segment.

4.2.4 Techno-economic Analysis

The TEA conducted an evaluation of the charging cost and TCO for EVs using DCFC, BSS, and DWPT charging systems. In this study, only public charging costs from these systems were considered for the TCO comparison, although the actual TCO would include a mix of charging costs from home, workplace, and public locations. To capture the full range of values, optimistic, baseline, and conservative scenarios were developed for capital costs (Table C2), electricity prices (Figure C6), and EV adoption (Figures C1 and C2), resulting in 27 charging cost and TCO scenarios for EVs. Additionally, optimistic, baseline, and conservative scenarios were developed for traditional fuel prices (Figure C6) to evaluate refueling costs for ICEVs and HEVs.

4.2.5 Levelized Cost of Charging

The charging cost for each DCFC site, BSS site, and DWPT roadway segment was evaluated individually using a DCFROR. The DCFROR considered capital costs, operational costs, electricity costs, and utilization. The DCFROR assumed a 5% internal rate of return, capital debt financing of 50% with 6% interest and 10-year loan term, state and average local sales tax (Table C7) [145], federal (21%) and state income tax (Table C7) [146], and a modified accelerated cost recovery system (MACRS) depreciation schedule. The cashflow spanned 21-years, including a 1-year build period and a 20-year operating life (2031 to 2050). The charging cost was calculated such that a net present value of zero was achieved. All costs were converted to 2022 U.S. Dollars (USD) using consumer price indexes [147,148] and producer price indexes [149–152].

4.2.5.1 Capital Costs

The capital costs for DCFC, BSS, and DWPT were evaluated individually and listed in Table C2. For every system, it was assumed that utilities would cover the cost of substations and line-extensions up to a certain distance [140], with expenses being recouped through electricity sales. As noted in Nelder and Rogers (2019), however, certain utilities might have imposed line-extension fees [15]. Further, this study assumed that the land of each site was owned already and did not depreciate. Therefore, capital costs were limited to the installation and procurement of all necessary components of the charging system.

The capital costs for DCFC were calculated by scaling the costs (Table C2) with the number of chargers at the site. These costs included a procurement component that was scaled linearly and an installation component that decreased on a per charger basis as the number increased. The procurement cost was incurred in 2030 and 2040, corresponding to the number of chargers deployed during each respective 10-year period. The installation costs, on the other hand, were incurred upfront in 2030 to future-proof the charging system for both sets of charger lifespans.

In contrast, the capital costs for BSS (Table C2) included fixed costs for the small (19 square meters) and large (46 square meters) sizes of BSSs, which covered the automated storage and retrieval system required for battery swapping and the building housing the BSS. The number of cabinets, comprising containers, thermal management systems, and fire suppression systems, were determined based on the number of batteries needed to meet the annual demand. Furthermore, the number of chargers for each BSS was calculated based on the maximum charging load from 2031 to 2040 and from 2041 to 2050, utilizing 7.7-kW chargers for the small BSS and 50-kW chargers for the large BSS. Similar to DCFC, the procurement costs for the chargers were incurred in 2030 and 2040 for the first and second set of chargers required, respectively. The installation, automated storage and retrieval system, and building costs were incurred in 2030, while the battery and cabinet costs were incurred in the respective years when they were added to the BSS.

For DWPT, the capital cost (Table C2) was scaled according to the electrified distance of each roadway. Separate estimates were utilized for urban and rural roads, taking into account the substantial difference in civil costs between the two [153]. The electronics cost was assumed to be the same for both urban and rural roads. For the optimistic scenarios, the low estimate from Limb et al. (2019) was used for rural roads, while the high estimate was used for urban roads [24]. As for the baseline and conservative scenarios, the electronics cost of 1.6M USD per km (adjusted to 2022 USD [149]), as reported by Haddad et al. (2022), was employed [119]. The conservative civil cost for urban roads was derived from the 1st-of-a-kind case in Trinko et al. (2022), with a lower contingency cost of 10% compared to the original 30% [114]. The baseline urban civil cost was also adapted from Trinko et al. (2022), incorporating a combination of the 1st-of-kind and nth-of-a-kind cases, which is further detailed in Table C3 [114]. Regarding the civil costs for rural roads, the nth-of-kind case from Trinko et al. (2022) was utilized for the baseline scenario, while the estimate from Haddad et al. (2022) was adapted (without substation) for the conservative scenario [119].

4.2.5.2 Operational Costs

The DCFC sites were modeled to have data contracts, network contracts, and maintenance costs annually (Table C2). BSS sites were modeled to only have maintenance costs (Table C2) on the chargers. The replacement of BSS batteries was assumed to be the responsibility of the vehicle owner. The operational costs for DWPT consisted of replacing failed roadside inverters (Table C2) with a mean time to failure of 101 years [154]. Since the failed DWPT roadway pads were modeled to have excess capacity in the design (Eq. 12), they were not replaced. The maintenance costs of the roadway were assumed to be out of scope since they are typically paid for by taxes, which are not part of the DCFC and BSS analysis.

4.2.5.3 Electricity Costs

Commercial electricity schedules from the U.S. Utility Rate Database [94] were collected [82] for the largest utility company in each state to determine electricity costs for each DCFC site, BSS site, and DWPT roadway segment on an annual basis. The electricity schedules were categorized into demand charges (USD/kW-month), electricity rates (USD/kWh), and fixed charges (USD/month), with applicable demand charges and electricity rates determined by the time-of-day charging profiles (Figure C4 for DWPT and Figure C5 for DCFC). The fixed charges were assessed to each BSS and DCFC site as well as to each DWPT roadway segment per 16 lane-km of electrified road. The most affordable schedule was selected based on the service location and power range for each load, with BSS charging profiles optimized to minimize electricity costs.

The BSS charging profile was optimized to ensure that each battery could be fully charged prior to the swap, with a one-hour buffer period. The charging time (t) required to charge the battery of each vehicle (v) was calculated using Eq. 24, which accounts for the charger rating (p) (7.7-kW for small BSS and 50-kW for large BSS), average power rate (a) (95%), charging efficiency (e) (85%), starting state of charge (soc_s) (20%), final state of charge (soc_f) (80%), and battery size (b) (Table C2).

$$t_v = \left(soc_f - soc_s\right) * b_v/(a * p_v * e) \qquad (24)$$

The minimum number of batteries needed was determined by considering the required charging time and the swap schedule of batteries within the BSS (Figure C4). These constraints were integrated into the charging load optimization algorithm, which aimed to minimize electricity costs while ensuring that each battery was charged within the designated window and that the daily charging volume met the demand from EVs.

Once the electricity costs were calculated for each charging system, the electricity costs were adjusted using the 2022 and 2031 to 2050 price projections for generation (electricity rate) and distribution (demand charge) from the Annual Energy Outlook (AEO) (2023) [155]. Three scenarios were considered (Figure C6) to account for future changes in electricity prices: optimistic, using the AEO low macro and low renewable technology cost case; baseline, using the AEO reference case; and conservative, using the AEO high macro and high renewable technology cost case.

4.2.5.4 Solving for Charging Cost

For each DCFC site, BSS site, and DWPT roadway, the charging cost was iteratively calculated to achieve a net present value of zero in the discounted cashflow analysis [156]. This was done using Eqs. 15-23. The yearly (*y*) discount factor (*df*) (Eq. 15) was computed using the internal rate of return (*irr*).

$$\mathrm{df_y} = (1 + \mathrm{irr})^{-\mathrm{y}} \qquad (15)$$

The loan payment for the initial capital debt financing in 2030 was computed using Eq. 16. The loan payment was based on the capital cost, investor equity (*ey*), loan interest rate (*IntRate*), and loan term (*term*).

$$\mathrm{loan_y} = \mathrm{cpx_0} * (1 - \mathrm{ey}) * \mathrm{IntRate}/(1 - (1 + \mathrm{IntRate})^{-\mathrm{term}}) \qquad (16)$$

The loan interest payment, which is tax deductible, was computed in Eq. 17. The loan interest payment was determined by subtracting the loan principal from the loan payment.

$$\mathrm{int_y} = \mathrm{loan_y} - (\mathrm{cpx_0} * (1 - \mathrm{ey})/\mathrm{term}) \qquad (17)$$

The depreciation (*dep*) of the initial capital was computed using Eq. 18 based on a *MACRS* rate, salvage value (*SalvageValue*), and capital cost [157]. Specifically, a 10% salvage value and 5-year MACRS rate were used for all DCFC and BSS capital costs except installation. DCFC and BSS installation used a salvage value of 0% and 10-year MACRS rate. Further, DWPT used a 0% salvage value and 15-year MACRS rate for all capital costs.

$$\mathrm{dep_y} = \mathrm{MACRS_Y} * (1 - \mathrm{SalvageValue}) * \mathrm{cpx_0} \quad (18)$$

The annual revenue (*rev*) of each DCFC site, BSS site, and DWPT roadway was calculated in Eq. 19 using the charging cost (*ChargingCost*) and annual utilization (*use*). The additional revenue from the capital salvage value was assumed to cancel out with the disposal cost of the infrastructure.

$$\mathrm{rev_y} = \mathrm{ChargingCost} * \mathrm{use_y} \qquad (19)$$

The annual taxable income (*TaxInc*) was determined using Eq. 20 based on the revenue, depreciation, electricity costs (*ele*), operational costs (*opx*), loan interest, and negative taxable income from the previous year (*NegTaxInc*). The taxable income from the previous year was only carried over if it was negative.

$$\mathrm{TaxInc_y} = \mathrm{rev_y} - \mathrm{dep_y} - \mathrm{ele_y} - \mathrm{opx_y} - \mathrm{int_y} + \mathrm{NegTaxInc_{y-1}} \; (20)$$

The income tax (*IncTax*) was computed in Eq. 21 based on the taxable income and income tax rate. The income tax rate was a combination of federal income tax (*FedTax*) and the state income tax (*StateTax*) specific to the charging location (Table C7).

$$\mathrm{IncTax_y} = \mathrm{TaxInc_y} * \big(\mathrm{StateTax} + \mathrm{FedTax} * (1 - \mathrm{StateTax})\big) \quad (21)$$

The total annual expenses (*exp*) were computed (Eq. 22) by combining the income tax, capital costs, investor equity, loan payments, electricity costs, operational costs, and sales tax (*sTax*). The sales tax represented the average combination of state and local sales taxes paid by the vehicle operator.

$$\mathrm{exp_y} = \big(\mathrm{IncTax_y} + \mathrm{ey} * \mathrm{cpx_0} + \mathrm{cpx_{y>0}} + \mathrm{L_y} + \mathrm{ele_y} + \mathrm{opx_y}\big) * (1 + \mathrm{sTax}) \qquad (22)$$

Finally, the net present value (*npv*) was solved for in Eq. 23. Eqs. 19-23 were iteratively computed by adjusting the charging cost until the net present value was within 0.01 USD of zero.

$$\mathrm{npv} = \left[\textstyle\sum_1^{20} \mathrm{rev_y} * \mathrm{df_y}\right] - \left[\textstyle\sum_0^{20} \mathrm{exp_y} * \mathrm{df_y}\right] \qquad (23)$$

4.2.6 Total Cost of Ownership

The TCO analysis utilized the charging cost results for DCFC, BSS, and DWPT to estimate the charging cost for EVs per VKT. The TCO of each modeled EV was compared to that of a HEV and an ICEV.

The fuel prices for HEVs and ICEVs were broken out by state and adjusted to 2031 through 2050 values (Figure C7) for optimistic (AEO low oil price case), baseline (AEO reference case), and conservative (AEO high oil price case) scenarios [155].

The TCO was computed over the first 10 years of the vehicle's life and included the charging (Figure C8) or fueling cost (Table C4), depreciation (Table C2), maintenance (Table C2) [102], license and registration (Table C5), and insurance (Table C6) expenses. The analysis of ICEVs and HEVs considered gasoline fuel for cars and LDTs, and diesel fuel for MDVs and HDVs. Cars and LDTs were assumed to have a discount factor of 1.2% for yearly expenses, while MDVs and HDVs had a discount factor of 3% [25].

The purchase price (Table C2) for each vehicle category was determined based on an average vehicle. For EVs, the purchase price included the cost of the EV without the battery and the marked-up cost of the EV battery (Table C2). The price of an EV without the battery was obtained from Burnham et al. (2021) for a 2025 model year midsize sedan (car), pickup truck (LDT), class 6 pickup/delivery truck (MDV), and sleeper tractor (HDV) [25]. The battery size for electric LDTs was adjusted to match the range of an electric car by considering vehicle efficiencies [158]. Reduced battery sizes were determined for a 56-km operating range with a maximum depth of discharge of 80%.

The depreciation cost was calculated annually based on the purchase price. Cars and LDTs lost 29% of their original value in the first year and 11% of their remaining value in each consecutive year [25]. For MDVs and HDVs, 9% of their remaining value was lost every year [25]. Insurance costs were assessed based on the remaining value of the vehicle each year and the location of the charging system. License and registration costs were fixed annually and varied by state. Maintenance costs were based on the U.S. average fixed rate per VKT plus any battery replacement costs. Battery life was assumed to be 1000 full cycles for full size batteries [159], while reduced battery sizes charged via DWPT were assumed to have the same life in years due to optimal operating characteristics, such as a smaller depth of discharge and a state of charge that can be maintained around 50% [160–162]. Based on these assumptions, only electric HDVs needed battery replacements in the first 10-year period due to their high annual VKT [163]. The sum of the vehicle costs was discounted along with their yearly utilization to obtain the TCO on a per VKT basis.

The impact of switching from ICEVs to EVs charged with DCFC, BSS, or DWPT systems (*cs*) was calculated using Eq. 25 for the percentage change (*ΔTCO%*) and Eq. 26 for the change in USD (*ΔTCO$*). These equations used the TCO of an ICEV (TCO_{ICEV}) and an EV (TCO_{EV}) for each vehicle category (*v*), as well as the VKT of EVs (VKT_{EV}) and the VKT of all vehicle powertrains (VKT_{All}).

$$\Delta \mathrm{TCO\%}_{\mathrm{CS}} = 1 + \left(\left[\sum_{\mathrm{v}} \mathrm{VKT}_{\mathrm{EV,v}} * \left(\mathrm{TCO}_{\mathrm{EV,cs,v}} - \mathrm{TCO}_{\mathrm{ICEV,v}}\right)\right] / \left[\sum_{\mathrm{v}} \mathrm{VKT}_{\mathrm{All,v}} * \mathrm{TCO}_{\mathrm{ICEV,v}}\right]\right) \quad (25)$$

$$\Delta \mathrm{TCO\$}_{\mathrm{CS}} = \sum_{\mathrm{v}} \mathrm{VKT}_{\mathrm{EV,v}} * \left(\mathrm{TCO}_{\mathrm{EV,cs,v}} - \mathrm{TCO}_{\mathrm{ICEV,v}}\right) \quad (26)$$

4.2.7 Life Cycle Assessment

An attributional LCA was conducted to compare the GWP of EVs charged with DCFC, BSS, and DWPT, as well as ICEVs and HEVs. Specifically, the impact assessment used an economic allocation method and the 100-year GWP from the Intergovernmental Panel on Climate Change's (IPCC) 6th impact assessment report [164]. The study used a C2G system boundary with a functional unit of one VKT. For EVs, the emissions were divided into charging emissions, embodied charging infrastructure emissions, and embodied vehicle emissions for different vehicle categories: cars, LDTs, MDVs, and HDVs. Charging and infrastructure emissions were allocated on a per unit of energy dispensed basis (kWh). The study used Ecoinvent 3.8 and openLCA 3.10 to collect the life cycle inventory data for charging infrastructure and charging emissions [165]. The GREET (2022) model [100] was used to determine embodied vehicle emissions, as well as the HEV and ICEV feedstock, fuel, and vehicle operation emissions (Table C8). The feedstock and fuel emissions were combined as the equivalent infrastructure emissions for HEVs and ICEVs.

4.2.7.1 Charging Infrastructure

The DCFC infrastructure emissions were calculated based on the charger pedestal, power cabinet, implementation, and construction (Table C9) [166]. The pedestal inventory data were taken from Ecoinvent 3.8 and scaled to a weight of 250-kilograms (kg) for 150-kW and 350-kW chargers [165,167]. Emissions from the power cabinet were broken out by material (Table C10) using primary data for a weight of 1340-kg per 150-kW charger and 2680-kg per 350-kW charger [167]. Implementation emissions for DCFC were adapted from Lucas et al. (2012) [168].

The BSS infrastructure emissions included the charger pedestal, battery, battery cabinet, automated storage and retrieval system, building, and construction (Table C11). The emissions of each BSS site were scaled based on the amount of equipment used.

The DWPT infrastructure emissions were based on the electronics, pavement, and construction (Table C12). DWPT infrastructure components were based on Marmiroli et al. (2019), however, the emissions factors were adjusted to use concrete rather than asphalt and use the IPCC 6th impact assessment [169]. The emissions for DWPT were scaled based on the electrified distance.

4.2.7.2 Charging Emissions

The emissions from EV charging were calculated using the forecasted hourly electricity mix in 134 Cambium (2022) zones from 2031 through 2050 [170]. Three electricity mix scenarios were examined: optimistic, based on the Cambium (2022) mid-case with 100% decarbonization by 2035; baseline, based on the Cambium (2022) mid-case; and conservative, based on the Cambium (2022) high renewable energy cost. The charging emissions were calculated using the average electricity consumption mix from each zone, rather than the marginal mix [101].

The consumption mix was determined by tracking the net energy imports and exports from each zone within the Western, Eastern, and Texas U.S. interconnections. Furthermore, the electricity mix used for charging energy storage resources was accounted for and assigned to the mix at the time of EV charging. Emissions factors for various grid resources in North American Reliability Corporation regions were obtained from Ecoinvent 3.8, encompassing both operating and embodied emissions (Table C13) [165]. Notably, carbon capture associated with the electricity grid was not attributed to EV charging as it was beyond the system boundary.

The charging emissions (*ChgGWP*) were computed on a per unit of energy basis (kWh) using Eq. 27. The calculation was based on each grid resource's (*r*) emissions factor (*EF*) and fraction of the consumption mix (*M*) at the time-of-day (*h*), year (*y*), and location (*z*) of charging.

$$\mathrm{ChgGWP}_{\mathrm{h,y,z}} = \sum\nolimits_{\mathrm{r}} \mathrm{EF}_{\mathrm{z}} * \mathrm{M}_{\mathrm{r,h,y,z}} \qquad (27)$$

The charging emissions were then scaled (Eq. 28) by the hourly and yearly charging load (*load*) from each DCFC site, BSS site, and DWPT road segment to get the average charging emissions per unit of energy (kWh) over the life of each system.

$$\mathrm{ChgGWP}_{\mathrm{z}} = \left[\sum\nolimits_{\mathrm{y=1}}^{20} \sum\nolimits_{\mathrm{h=1}}^{24} \mathrm{ChgGWP}_{\mathrm{h,y,z}} * \mathrm{load}_{\mathrm{h,y,z}}\right] / \left[\sum\nolimits_{\mathrm{y=1}}^{20} \sum\nolimits_{\mathrm{h=1}}^{24} \mathrm{load}_{\mathrm{h,y,z}}\right] \qquad (28)$$

4.2.7.3 Embodied Vehicle Emissions

Embodied vehicle emissions for each vehicle type were calculated using a representative 2025 vehicle with conventional materials from GREET (2022) [100]. Specifically, the vehicle modeled for each vehicle category from GREET (2022) were a passenger car, pickup truck (LDT), class 6 pickup-and-delivery truck (MDV), and class 8 sleeper-cab truck (HDV).

The vehicle emissions were divided into components; assembly, disposal, and recycling (ADR); batteries; and fluids. EV battery sizes (Table C2) were input into GREET (2022) for the corresponding charging system and EV-adoption scenario [100]. The batteries for both EVs and HEVs were assumed to be manufactured in China and use a Li-ion chemistry. One replacement of the hybrid electric HDV battery was assumed to occur over the vehicle's lifetime. Further, electric MDVs and HDVs were calculated to average 1.7 and 2.9 battery replacements in their lifetime, while cars and LDTs had none.

The modeled vehicle emissions are summarized in Table C8.

CHAPTER 5: CONCLUSIONS AND RECOMMENDATIONS

5.1 Overall Conclusions

The findings and recommendations derived from this research can guide policymakers, industry stakeholders, and researchers in making informed decisions to accelerate the adoption and deployment of EV technologies, contributing to the broader goals of reducing costs, mitigating GHG emissions, and creating a sustainable transportation sector. The detailed modeling and analysis conducted in this study have provided a comprehensive understanding of the cumulative costs and emissions associated with EVs, illuminating key factors that drive the economics and environmental impacts of these technologies. The research emphasizes that the economic viability of EV technologies is highly influenced by capital utilization, highlighting the need for efficient resource allocation and utilization to maximize economic benefits. Simultaneously, the study underscores the crucial role of transitioning to cleaner energy sources in order to leverage the full environmental benefits of EVs, as the emissions from EVs are strongly influenced by the local electricity mixes. The findings demonstrate the economic feasibility of integrating 2nd EV batteries into grid ESS to provide grid services, offering a promising sustainable solution for meeting future energy demands. Moreover, the research demonstrates that careful consideration of charger levels and hub ownership models enables the economical deployment of charging infrastructure at MUDs. This allows for widespread EV adoption, thereby reducing GHG emissions. Furthermore, the study highlights the varying degrees of economic and environmental advantages associated with different types of public charging systems, dependent on specific levels of EV adoption, traffic volumes, capital costs, and electricity prices. By tailoring the selection and deployment of charging systems, stakeholders can optimize the outcomes in terms of both economics and environmental sustainability.

5.2 Future Research on Second Life Batteries

The TEA model built to assess the economic viability of reconditioning 2nd life batteries was able to determine the minimum required resale price of the batteries while in the R&D phase. Future work should focus on updating the TEA model to incorporate updated cost and performance estimates as the reconditioning technology for 2nd life batteries progresses towards commercialization. The modeled usage of the 2nd life batteries in a grid ESS remains limited due to a lack of experimental data on the cycle life of the batteries. The model should be improved by integrating battery aging to analyze dynamic battery performance and improve accuracy in quantifying battery usage in grid ESSs performing specific grid services.

Additionally, conducting a LCA is necessary to determine the environmental impacts of different refurbishing methods. The GHG emissions associated with the reconditioning process should also be compared to new Li-ion batteries to assess emissions savings achieved through battery reuse.

5.3 Future Research on Multi-Unit Dwelling Charging Hubs

The TEA and LCA models for MUD charging hubs were evaluated to determine the consumer savings and GHG emissions reductions associated with deploying MUD charging infrastructure. Future work could enhance the TEA by incorporating specific costing data for a range of MUD characteristics, including installation costs for both new and existing buildings to identify potential cost advantages from future-proofing new MUD constructions. Additionally, the fixed utilization level per charger in the TEA model should be changed such that the charging costs are evaluated by varying the number of chargers while maintaining a fixed total utilization from the charging hub. By incorporating variable charger utilization and comparing the charging costs with waiting time, charging hub owners can determine the optimal number of chargers that provides a balance between cost and waiting times. Furthermore, a comparison between the charging costs of individually owned chargers at MUDs and MUD charging hubs should be conducted to quantify the potential savings associated with shared charging infrastructure.

5.4 Future Research on Public Charging Infrastructure

An integrated TEA and LCA was conducted for the deployment of DCFC, BSS, and DWPT to assess the TCO and GWP of EVs using these charging systems. However, the study was limited and can be expanded to understand additional factors that influence the overall advantages of each charging system. A more comprehensive understanding of the performance characteristics of each charging system can be achieved by quantifying the value of time savings associated with charging for both personal and commercial vehicles. Considering that charging time is known to impact EV adoption, future work should incorporate varying levels of EV adoption based on consumer preferences. Additionally, assessing the infrastructure upgrades required to support each charging system can be accomplished by evaluating the capacity of existing substations and feeders at each charging location.

Improvements to the LCA should incorporate the assessment Particulate Matter 2.5 impacts on human health. The geospatial and temporal EV charging demand and generation electricity mixes modeled in this work should be leveraged to quantify these emissions. The human health impacts should be assessed on a local level to determine the net change in Particulate Matter 2.5 due to varying levels of EV adoption.

To optimize the deployment of charging infrastructure, the TEA and LCA should include various charging venues (home, fleet, workplace) and explore combinations of public charging systems. This would provide a holistic evaluation encompassing TCO, GWP, performance, and human health for a comprehensive understanding of vehicle electrification.

REFERENCES

[1] FACT SHEET: The Biden-Harris Electric Vehicle Charging Action Plan. The White House 2021. https://www.whitehouse.gov/briefing-room/statements-releases/2021/12/13/fact-sheet-the-biden-harris-electric-vehicle-charging-action-plan/ (accessed March 23, 2022).

[2] US EPA. Fast Facts on Transportation Greenhouse Gas Emissions 2019. https://www.epa.gov/greenvehicles/fast-facts-transportation-greenhouse-gas-emissions (accessed March 23, 2022).

[3] Capasso C, Veneri O. Experimental analysis on the performance of lithium based batteries for road full electric and hybrid vehicles. Applied Energy 2014;136:921–30. https://doi.org/10.1016/j.apenergy.2014.04.013.

[4] Zablocki A. Fact Sheet | Energy Storage (2019). Environmental and Energy Study Institute 2019. https://www.eesi.org/papers/view/energy-storage-2019 (accessed May 12, 2022).

[5] Gallagher KG, Goebel S, Greszler T, Mathias M, Oelerich W, Eroglu D, et al. Quantifying the promise of lithium–air batteries for electric vehicles. Energy Environ Sci 2014;7:1555–63. https://doi.org/10.1039/C3EE43870H.

[6] Fotouhi A, Auger DJ, Propp K, Longo S, Wild M. A review on electric vehicle battery modelling: From Lithium-ion toward Lithium–Sulphur. Renewable and Sustainable Energy Reviews 2016;56:1008–21. https://doi.org/10.1016/j.rser.2015.12.009.

[7] Berckmans G, Messagie M, Smekens J, Omar N, Vanhaverbeke L, Mierlo JV. Cost Projection of State of the Art Lithium-Ion Batteries for Electric Vehicles Up to 2030. Energies 2017;10:1314. https://doi.org/10.3390/en10091314.

[8] Wadia C, Albertus P, Srinivasan V. Resource constraints on the battery energy storage potential for grid and transportation applications. Journal of Power Sources 2011;196:1593–8. https://doi.org/10.1016/j.jpowsour.2010.08.056.

[9] Olsson L, Fallahi S, Schnurr M, Diener D, Van Loon P. Circular Business Models for Extended EV Battery Life. Batteries 2018;4:57. https://doi.org/10.3390/batteries4040057.

[10] Canepa K, Hardman S, Tal G. An early look at plug-in electric vehicle adoption in disadvantaged communities in California. Transport Policy 2019;78:19–30. https://doi.org/10.1016/j.tranpol.2019.03.009.

[11] FOTW #1200, August 23, 2021: Sales of New Electric Vehicles in the U.S. Were Up for 2020 While Conventional New Light-Duty Vehicle Sales Were Down. EnergyGov 2021. https://www.energy.gov/eere/vehicles/articles/fotw-1200-august-23-2021-sales-new-electric-vehicles-us-were-2020-while (accessed March 23, 2022).

[12] Lee JH, Chakraborty D, Hardman SJ, Tal G. Exploring electric vehicle charging patterns: Mixed usage of charging infrastructure. Transportation Research Part D: Transport and Environment 2020;79:102249. https://doi.org/10.1016/j.trd.2020.102249.

[13] Metais MO, Jouini O, Perez Y, Berrada J, Suomalainen E. Too much or not enough? Planning electric vehicle charging infrastructure: A review of modeling options. Renewable and Sustainable Energy Reviews 2022;153:111719. https://doi.org/10.1016/j.rser.2021.111719.

[14] Baldwin S, Myers A, O'Boyle M. INCREASING ELECTRIC VEHICLE CHARGING ACCESS AT MULTI-UNIT DWELLINGS: WORKSHOP SUMMARY REPORT. Energy Innovation Policy & Technology LLC; 2020.

[15] Nelder C, Rogers E. Reducing EV Charging Infrastructure Costs. Rocky Mountain Institute; 2019.

[16] Alexander M. Electric Vehicle Supply Equipment Installed Cost Analysis. Electric Power Research Institute; 2013.
[17] 15 states and the District of Columbia join forces to accelerate bus and truck electrification | California Air Resources Board n.d. https://ww2.arb.ca.gov/news/15-states-and-district-columbia-join-forces-accelerate-bus-and-truck-electrification (accessed June 19, 2021).
[18] Duran A, Ragatz A, Prohaska R, Kelly K, Walkowicz K. Characterization of in-use medium duty electric vehicle driving and charging behavior. 2014 IEEE International Electric Vehicle Conference (IEVC), Florence: IEEE; 2014, p. 1–8. https://doi.org/10.1109/IEVC.2014.7056213.
[19] Sripad S, Viswanathan V. Performance Metrics Required of Next-Generation Batteries to Make a Practical Electric Semi Truck. ACS Energy Lett 2017;2:1669–73. https://doi.org/10.1021/acsenergylett.7b00432.
[20] Nedelea A. Take A Closer Look At A Nio EV Battery Swapping Station In China. InsideEVs 2022. https://insideevs.com/news/570403/nio-battery-swap-station-china/ (accessed April 25, 2022).
[21] Trinko D, Horesh N, Zane R, Song Z, Kamineni A, Konstantinou T, et al. Economic feasibility of in-motion wireless power transfer in a high-density traffic corridor. ETransportation 2022;11:100154. https://doi.org/10.1016/j.etran.2021.100154.
[22] Bi Z, Song L, De Kleine R, Mi CC, Keoleian GA. Plug-in vs. wireless charging: Life cycle energy and greenhouse gas emissions for an electric bus system. Applied Energy 2015;146:11–9. https://doi.org/10.1016/j.apenergy.2015.02.031.
[23] Yang L, Hao C, Chai Y. Life Cycle Assessment of Commercial Delivery Trucks: Diesel, Plug-In Electric, and Battery-Swap Electric. Sustainability 2018;10:4547. https://doi.org/10.3390/su10124547.
[24] Limb BJ, Asher ZD, Bradley TH, Sproul E, Trinko DA, Crabb B, et al. Economic Viability and Environmental Impact of In-Motion Wireless Power Transfer. IEEE Transactions on Transportation Electrification 2019;5:135–46. https://doi.org/10.1109/TTE.2018.2876067.
[25] Burnham A, Gohlke D, Rush L, Stephens T, Zhou Y, Delucchi M, et al. Comprehensive Total Cost of Ownership Quantification for Vehicles with Different Size Classes and Powertrains. 2021. https://doi.org/10.2172/1780970.
[26] Borlaug B, Salisbury S, Gerdes M, Muratori M. Levelized Cost of Charging Electric Vehicles in the United States. Joule 2020;4:1470–85. https://doi.org/10.1016/j.joule.2020.05.013.
[27] Gagnon P, Frazier AW, Hale E, Cole W. Cambium data for 2020 Standard Scenarios. National Renewable Energy Laboratory 2020. https://cambium.nrel.gov/ (accessed March 23, 2022).
[28] Burnham A, Lu Z, Wang M, Elgowainy A. Regional Emissions Analysis of Light-Duty Battery Electric Vehicles. Atmosphere 2021;12:1482. https://doi.org/10.3390/atmos12111482.
[29] Álvarez Fernández R. A more realistic approach to electric vehicle contribution to greenhouse gas emissions in the city. Journal of Cleaner Production 2018;172:949–59. https://doi.org/10.1016/j.jclepro.2017.10.158.
[30] Mosquet X, Arora A, Xie A, Renner M. Who Will Drive Electric Cars to the Tipping Point? | BCG. Boston Consulting Group 2020. https://www.bcg.com/publications/2020/drive-electric-cars-to-the-tipping-point.aspx (accessed May 25, 2020).
[31] Mathews I, Xu B, He W, Barreto V, Buonassisi T, Peters IM. Technoeconomic model of second-life batteries for utility-scale solar considering calendar and cycle aging. Applied Energy 2020;269:115127. https://doi.org/10.1016/j.apenergy.2020.115127.
[32] Neubauer J, Pesaran A. The ability of battery second use strategies to impact plug-in electric vehicle prices and serve utility energy storage applications. Journal of Power Sources 2011;196:10351–8. https://doi.org/10.1016/j.jpowsour.2011.06.053.
[33] Song Z, Feng S, Zhang L, Hu Z, Hu X, Yao R. Economy analysis of second-life battery in wind power systems considering battery degradation in dynamic processes: Real case scenarios. Applied Energy 2019;251:113411. https://doi.org/10.1016/j.apenergy.2019.113411.

[34] Assunção A, Moura PS, de Almeida AT. Technical and economic assessment of the secondary use of repurposed electric vehicle batteries in the residential sector to support solar energy. Applied Energy 2016;181:120–31. https://doi.org/10.1016/j.apenergy.2016.08.056.

[35] Saez-de-Ibarra A, Martinez-Laserna E, Koch-Ciobotaru C, Rodriguez P, Stroe D-I, Swierczynski M. Second life battery energy storage system for residential demand response service. 2015 IEEE International Conference on Industrial Technology (ICIT), 2015, p. 2941–8. https://doi.org/10.1109/ICIT.2015.7125532.

[36] Heymans C, Walker SB, Young SB, Fowler M. Economic analysis of second use electric vehicle batteries for residential energy storage and load-levelling. Energy Policy 2014;71:22–30. https://doi.org/10.1016/j.enpol.2014.04.016.

[37] Cready E, Lippert J, Pihl J, Weinstock I, Symons P. Technical and Economic Feasibility of Applying Used EV Batteries in Stationary Applications. 2003. https://doi.org/10.2172/809607.

[38] Neubauer J, Smith K, Wood E, Pesaran A. Identifying and Overcoming Critical Barriers to Widespread Second Use of PEV Batteries. 2015. https://doi.org/10.2172/1171780.

[39] Sun Y, Wachche SV, Mills A, Ma O. 2018 Renewable Energy Grid Integration Data Book. National Renewable Energy Lab. (NREL), Golden, CO (United States); 2020.

[40] Consumer Choice | Alliance of Automobile Manufacturers 2018. https://autoalliance.org/economy/consumer-choice/electric-vehicles/ (accessed May 25, 2020).

[41] Electric Schedule A-10 Medium General Demand-Metered Service 2020.

[42] Electric Schedule E-20 Service to Customers With Maximum Demands of 1000 Kilowatts or More 2020.

[43] OASIS - OASIS Prod - PUBLIC - 0. California ISO 2019. http://oasis.caiso.com/mrioasis/logon.do (accessed June 24, 2020).

[44] Rehman MMU, Zhang F, Evzelman M, Zane R, Smith K, Maksimovic D. Advanced cell-level control for extending electric vehicle battery pack lifetime. 2016 IEEE Energy Conversion Congress and Exposition (ECCE), 2016, p. 1–8. https://doi.org/10.1109/ECCE.2016.7854827.

[45] National Institute of Building Sciences. Light Industrial | WBDG - Whole Building Design Guide. Whole Building Design Guide 2019. https://www.wbdg.org/space-types/light-industrial (accessed May 28, 2020).

[46] National Institute of Building Sciences. Parking: Surface | WBDG - Whole Building Design Guide. Whole Building Design Guide 2020. https://www.wbdg.org/space-types/parking-surface#spcatt (accessed May 28, 2020).

[47] Plotner S. Building Construction Cost Data. 74th ed. Rockland, MA: RSMeans; 2016.

[48] PPI industry data for New industrial building construction, not seasonally adjusted. US Bureau of Labor Statistics 2020. https://data.bls.gov/timeseries/PCU236211236211 (accessed November 2, 2020).

[49] Fu R, Remo TW, Margolis RM. 2018 U.S. Utility-Scale Photovoltaics-Plus-Energy Storage System Costs Benchmark. National Renewable Energy Lab. (NREL), Golden, CO (United States); 2018. https://doi.org/10.2172/1484345.

[50] PPI industry data for Electric bulk power transmission and control, not seasonally adjusted. US Bureau of Labor Statistics n.d. https://data.bls.gov/timeseries/PCU221121221121 (accessed October 9, 2020).

[51] New & Used Semi Trucks For Sale. Kenworth Sales Company 2020. https://www.kenworthsalesco.com/semi-trucks-for-sale/ (accessed May 28, 2020).

[52] Used Semi-Trailers For Sale | Arrow Truck Sales. Used Semi-Trailers for Sale 2020. https://www.arrowtruck.com/docs/used-semi-trailers.aspx (accessed May 28, 2020).

[53] Forklift Pricing 101: What You Should Know. Toyota Forklifts n.d. https://www.toyotaforklift.com/resource-library/material-handling-solutions/finance/forklift-pricing-101-what-you-should-know (accessed May 28, 2020).
[54] Huo H, Xing Y, Pecht M, Züger BJ, Khare N, Vezzini A. Safety Requirements for Transportation of Lithium Batteries. Energies 2017;10:793. https://doi.org/10.3390/en10060793.
[55] Foxx A. Compilation of Existing State Truck Size and Weight Limit Laws - FHWA Freight Management and Operations. US Department of Transportation Federal Highway Administration Freight Management and Operations 2015. https://ops.fhwa.dot.gov/freight/policy/rpt_congress/truck_sw_laws/index.htm (accessed May 28, 2020).
[56] Material Moving Machine Operators : Occupational Outlook Handbook: : U.S. Bureau of Labor Statistics. US Bureau of Labor Statistics 2019. https://www.bls.gov/ooh/transportation-and-material-moving/material-moving-machine-operators.htm (accessed May 28, 2020).
[57] Inspectors, Testers, Sorters, Samplers, and Weighers. US Bureau of Labor Statistics 2020. https://www.bls.gov/oes/current/oes519061.htm (accessed May 28, 2020).
[58] General Office Clerks : Occupational Outlook Handbook: : U.S. Bureau of Labor Statistics. US Bureau of Labor Statistics 2020. https://www.bls.gov/ooh/office-and-administrative-support/general-office-clerks.htm (accessed May 28, 2020).
[59] Industrial Production Managers : Occupational Outlook Handbook: : U.S. Bureau of Labor Statistics. US Bureau of Labor Statistics 2020. https://www.bls.gov/ooh/management/industrial-production-managers.htm (accessed May 28, 2020).
[60] Sales Engineers : Occupational Outlook Handbook: : U.S. Bureau of Labor Statistics. US Bureau of Labor Statistics 2020. https://www.bls.gov/ooh/sales/sales-engineers.htm (accessed May 28, 2020).
[61] First-Line Supervisors of Production and Operating Workers. US Bureau of Labor Statistics 2019. https://www.bls.gov/oes/2018/may/oes511011.htm (accessed June 1, 2020).
[62] Cole WJ, Frazier A. Cost Projections for Utility-Scale Battery Storage. 2019. https://doi.org/10.2172/1529218.
[63] Mongird K, Viswanathan VV, Balducci PJ, Alam MJE, Fotedar V, Koritarov VS, et al. Energy Storage Technology and Cost Characterization Report. 2019. https://doi.org/10.2172/1573487.
[64] Oudalov A, Chartouni D, Ohler C, Linhofer G. Value Analysis of Battery Energy Storage Applications in Power Systems. 2006 IEEE PES Power Systems Conference and Exposition, 2006, p. 2206–11. https://doi.org/10.1109/PSCE.2006.296284.
[65] Eyer JM, Corey GP. Energy storage for the electricity grid : benefits and market potential assessment guide : a study for the DOE Energy Storage Systems Program. 2010. https://doi.org/10.2172/1031895.
[66] Casals LC, Amante García B, Canal C. Second life batteries lifespan: Rest of useful life and environmental analysis. Journal of Environmental Management 2019;232:354–63. https://doi.org/10.1016/j.jenvman.2018.11.046.
[67] Balducci PJ, Alam MJE, Hardy TD, Wu D. Assigning value to energy storage systems at multiple points in an electrical grid. Energy Environ Sci 2018;11:1926–44. https://doi.org/10.1039/C8EE00569A.
[68] Vejdan S, Grijalva S. Analysis of multiple revenue streams for privately-owned energy storage systems. 2018 IEEE Power and Energy Conference at Illinois (PECI), 2018, p. 1–5. https://doi.org/10.1109/PECI.2018.8334979.
[69] Van/Box Trucks in Vehicle Mileage:Less than 100,000 miles. EBay 2020. https://www.ebay.com/b/Van-Box-

Trucks/80761?Vehicle%2520Mileage=Less%2520than%2520100%252C000%2520miles (accessed June 4, 2020).
[70] AAA Gas Prices. AAA Gas Prices 2020. https://gasprices.aaa.com/ (accessed June 4, 2020).
[71] Gas Mileage of 2014 Vans, Cargo Type. Environmental Protection Agency n.d. https://www.fueleconomy.gov/feg/byclass/Vans__Cargo_Type2014.shtml (accessed May 29, 2020).
[72] Ramoni MO, Zhang H-C. End-of-life (EOL) issues and options for electric vehicle batteries. Clean Techn Environ Policy 2013;15:881–91. https://doi.org/10.1007/s10098-013-0588-4.
[73] Martinez-Laserna E, Gandiaga I, Sarasketa-Zabala E, Badeda J, Stroe D-I, Swierczynski M, et al. Battery second life: Hype, hope or reality? A critical review of the state of the art. Renewable and Sustainable Energy Reviews 2018;93:701–18. https://doi.org/10.1016/j.rser.2018.04.035.
[74] White C, Thompson B, Swan LG. Comparative performance study of electric vehicle batteries repurposed for electricity grid energy arbitrage. Applied Energy 2021;288:116637. https://doi.org/10.1016/j.apenergy.2021.116637.
[75] Gohlke D, Zhou Y. Assessment of Light-Duty Plug-in Electric Vehicles in the United States, 2010 – 2019. Argonne National Lab. (ANL), Argonne, IL (United States); 2020. https://doi.org/10.2172/1642114.
[76] Martin C. Used Electric Car Batteries Get Second Life as Home Storage. BloombergCom 2016.
[77] Peterson D. Addressing Challenges to Electric Vehicle Charging in Multifamily Residential Buildings. UCLA Luskin School of Public Affairs; 2011.
[78] STATE System Multiunit Housing Fact Sheet. Center for Disease Control 2022. https://www.cdc.gov/statesystem/factsheets/multiunithousing/MultiUnitHousing.html (accessed March 23, 2022).
[79] Williams B, DeShazo JR. Pricing Plug-in Electric Vehicle Recharging in Multi-unit Dwellings: Financial Viability and Fueling Costs. In: Beeton D, Meyer G, editors. Electric Vehicle Business Models: Global Perspectives, Cham: Springer International Publishing; 2015, p. 89–107. https://doi.org/10.1007/978-3-319-12244-1_6.
[80] LaMonaca S, Ryan L. The state of play in electric vehicle charging services – A review of infrastructure provision, players, and policies. Renewable and Sustainable Energy Reviews 2022;154:111733. https://doi.org/10.1016/j.rser.2021.111733.
[81] Hall D, Lutsey N. Literature review on power utility best practices regarding electric vehicles. icct 2017:52.
[82] CHECT Download. Argonne National Laboratory 2023. https://www.anl.gov/esia/chect-download (accessed May 9, 2023).
[83] Melaina M, Bush B, Eichman J, Wood E, Stright D, Krishnan V, et al. National Economic Value Assessment of Plug-in Electric Vehicles: Volume I. NREL; 2016. https://doi.org/10.2172/1338175.
[84] What were the Cost Drivers for the Direct Current Fast Charging Installations? Idaho National Laboratory; 2015.
[85] Snyder J. Financial Viability Of Non-Residential Electric Vehicle Charging Stations. UCLA Luskin School of Public Affairs; 2012.
[86] Horesh N, Quinn C, Wang H, Zane R, Ferry M, Tong S, et al. Driving to the future of energy storage: Techno-economic analysis of a novel method to recondition second life electric vehicle batteries. Applied Energy 2021;295:117007. https://doi.org/10.1016/j.apenergy.2021.117007.
[87] Kobashi T, Say K, Wang J, Yarime M, Wang D, Yoshida T, et al. Techno-economic assessment of photovoltaics plus electric vehicles towards household-sector decarbonization in Kyoto and Shenzhen by the year 2030. Journal of Cleaner Production 2020;253:119933. https://doi.org/10.1016/j.jclepro.2019.119933.

[88] PPI industry data for Electrical equipment mfg, not seasonally adjusted. BLS Data Viewer 2021. https://beta.bls.gov/dataViewer/view/timeseries/PCU33531-33531- (accessed September 17, 2021).
[89] PPI Commodity data for Telecommunication, cable, and internet user services-Cellular phone and other wireless telecommunication services, seasonally adjusted. BLS Data Viewer 2021. https://beta.bls.gov/dataViewer/view/timeseries/WPS3721 (accessed September 17, 2021).
[90] PPI industry data for Electric power distribution, not seasonally adjusted. BLS Data Viewer 2021. https://data.bls.gov/pdq/SurveyOutputServlet (accessed September 17, 2021).
[91] EV WATTS Charging Station Dashboard Q4-21. Energetics 2021. https://www.energetics.com/evwatts (accessed February 21, 2022).
[92] Fitzgerald G, Nelder C. DCFC Rate Design Study. Rocky Mountain Institute; 2019.
[93] Kane M. In July Tesla Superchargers Dispensed 72 GWh Of Electricity. InsideEVs 2019. https://insideevs.com/news/367053/july-tesla-superchargers-dispensed-72-gwh/ (accessed December 27, 2021).
[94] U.S. Utility Rate Database. OpenEI US Utility Rate Database 2022. https://apps.openei.org/USURDB/ (accessed September 1, 2022).
[95] Southern California Edison. Schedule TOU-EV-1 DOMESTIC TIME-OF-USE ELECTRIC VEHICLE CHARGING 2021.
[96] Southern California Edison. Schedule TOU-GS-2 Time-of-Use General Service - Demand Metered 2021.
[97] Average Energy Prices, Chicago-Naperville-Elgin — November 2021. U.S. Bureau of Labor Statistics; 2021.
[98] Average Energy Prices, New York-Newark-Jersey City – November 2021. US Bureau of Labor Statistics 2021. https://www.bls.gov/regions/new-york-new-jersey/news-release/averageenergyprices_newyorkarea.htm (accessed December 28, 2021).
[99] Average Energy Prices, Los Angeles-Long Beach-Anaheim – November 2021. US Bureau of Labor Statistics 2021. https://www.bls.gov/regions/west/news-release/averageenergyprices_losangeles.htm (accessed December 28, 2021).
[100] The Greenhouse gases, Regulated Emissions, and Energy use in Technologies Model 2022.
[101] Lin Z. Mostly positive implications of long-haul truck electrification. Joule 2021;5:2548–50. https://doi.org/10.1016/j.joule.2021.10.009.
[102] Alternative Fuel Life-Cycle Environmental and Economic Transportation (AFLEET) Tool 2021.
[103] Electric Cars to Reach Price Parity by 2025. BloombergNEF 2017. https://about.bnef.com/blog/electric-cars-reach-price-parity-2025/ (accessed March 27, 2022).
[104] AAA Gas Prices. AAA 2022. https://gasprices.aaa.com/state-gas-price-averages/ (accessed March 10, 2022).
[105] Electric Vehicle Supply Equipment (EVSE) Standards. California Air Resources Board 2022. https://ww2.arb.ca.gov/our-work/programs/electric-vehicle-supply-equipment-evse-standards/about (accessed March 27, 2022).
[106] Gillingham K, Stock JH. The Cost of Reducing Greenhouse Gas Emissions. Journal of Economic Perspectives 2018;32:53–72. https://doi.org/10.1257/jep.32.4.53.
[107] Baylin-Stern A, Berghout N. Is carbon capture too expensive? – Analysis. IEA 2021. https://www.iea.org/commentaries/is-carbon-capture-too-expensive (accessed April 20, 2022).
[108] FACT SHEET: President Biden Sets 2030 Greenhouse Gas Pollution Reduction Target Aimed at Creating Good-Paying Union Jobs and Securing U.S. Leadership on Clean Energy Technologies. The White House 2021. https://www.whitehouse.gov/briefing-room/statements-releases/2021/04/22/fact-sheet-president-biden-sets-2030-greenhouse-gas-pollution-reduction-

target-aimed-at-creating-good-paying-union-jobs-and-securing-u-s-leadership-on-clean-energy-technologies/ (accessed May 26, 2021).
[109] Alternative Fueling Station Locator. Alternative Fuels Data Center 2022. https://afdc.energy.gov/stations/ (accessed December 22, 2022).
[110] Konstantinou T, Gkritza K. Are we getting close to truck electrification? U.S. truck fleet managers' stated intentions to electrify their fleets. Transportation Research Part A: Policy and Practice 2023;173:103697. https://doi.org/10.1016/j.tra.2023.103697.
[111] Al-Hanahi B, Ahmad I, Habibi D, Masoum MAS. Charging Infrastructure for Commercial Electric Vehicles: Challenges and Future Works. IEEE Access 2021;9:121476–92. https://doi.org/10.1109/ACCESS.2021.3108817.
[112] Burnham A, Dufek EJ, Stephens T, Francfort J, Michelbacher C, Carlson RB, et al. Enabling fast charging – Infrastructure and economic considerations. Journal of Power Sources 2017;367:237–49. https://doi.org/10.1016/j.jpowsour.2017.06.079.
[113] Chen X, Xing K, Ni F, Wu Y, Xia Y. An Electric Vehicle Battery-Swapping System: Concept, Architectures, and Implementations. IEEE Intelligent Transportation Systems Magazine 2022;14:175–94. https://doi.org/10.1109/MITS.2021.3119935.
[114] Trinko D, Horesh N, Zane R, Song Z, Kamineni A, Konstantinou T, et al. Economic feasibility of in-motion wireless power transfer in a high-density traffic corridor. ETransportation 2022;11:100154. https://doi.org/10.1016/j.etran.2021.100154.
[115] Jensen M. ASPIRE Partners with Central Florida Expressway and Evolgy for Electrified Roadway Pilot. Utah State Today 2022. https://www.usu.edu/today/story/aspire-partners-with-central-florida-expressway-and-evolgy-for-electrified-roadway-pilot (accessed May 25, 2023).
[116] FAF4 Network Database and Flow Assignment: 2012 and 2045 - FHWA Freight Management and Operations. Freight Management and Operations 2020. https://ops.fhwa.dot.gov/freight/freight_analysis/faf/faf4/netwkdbflow/index.htm (accessed January 5, 2021).
[117] Mai TT, Jadun P, Logan JS, McMillan CA, Muratori M, Steinberg DC, et al. Electrification Futures Study: Scenarios of Electric Technology Adoption and Power Consumption for the United States. 2018. https://doi.org/10.2172/1459351.
[118] Mulholland E. Cost of electric commercial vans and pickup trucks in the United States through 2040. ICCT; 2022.
[119] Haddad D, Konstantinou T, Aliprantis D, Gkritza K, Pekarek S, Haddock J. Analysis of the financial viability of high-powered electric roadways: A case study for the state of Indiana. Energy Policy 2022;171:113275. https://doi.org/10.1016/j.enpol.2022.113275.
[120] Use of electricity. US Energy Information Administration 2023. https://www.eia.gov/energyexplained/electricity/use-of-electricity.php (accessed May 23, 2023).
[121] ElGhanam E, Sharf H, Odeh Y, Hassan MS, Osman AH. On the Coordination of Charging Demand of Electric Vehicles in a Network of Dynamic Wireless Charging Systems. IEEE Access 2022;10:62879–92. https://doi.org/10.1109/ACCESS.2022.3182700.
[122] Fleischmann J, Hanicke M, Horetsky E, Ibrahim D, Jautelat S, Linder M, et al. Battery 2030: Resilient, sustainable, and circular. McKinsey & Company; 2023.
[123] Borlaug B, Muratori M, Gilleran M, Woody D, Muston W, Canada T, et al. Heavy-duty truck electrification and the impacts of depot charging on electricity distribution systems. Nat Energy 2021;6:673–82. https://doi.org/10.1038/s41560-021-00855-0.
[124] Liu J. Electric vehicle charging infrastructure assignment and power grid impacts assessment in Beijing. Energy Policy 2012;51:544–57. https://doi.org/10.1016/j.enpol.2012.08.074.

[125] Trends in electric light-duty vehicles – Global EV Outlook 2022 – Analysis. IEA n.d. https://www.iea.org/reports/global-ev-outlook-2022/trends-in-electric-light-duty-vehicles (accessed December 13, 2022).
[126] Lee JH, Chakraborty D, Hardman SJ, Tal G. Exploring electric vehicle charging patterns: Mixed usage of charging infrastructure. Transportation Research Part D: Transport and Environment 2020;79:102249. https://doi.org/10.1016/j.trd.2020.102249.
[127] 2002 Economic Census: Vehicle Inventory and Use Survey. U.S. Census Bureau: U.S. Department of Commerce; 2004.
[128] Battery packs for heavy-duty electric vehicles. Volvo n.d. https://www.volvogroup.com/en/news-and-media/news/2022/may/battery-packs-for-electric-vehicles.html (accessed January 13, 2023).
[129] Summary of Hours of Service Regulations. Federal Motor Carrier Safety Administration 2022. https://www.fmcsa.dot.gov/regulations/hours-service/summary-hours-service-regulations (accessed January 13, 2023).
[130] Kostopoulos ED, Spyropoulos GC, Kaldellis JK. Real-world study for the optimal charging of electric vehicles. Energy Reports 2020;6:418–26. https://doi.org/10.1016/j.egyr.2019.12.008.
[131] Ghavami M, Essakiappan S, Singh C. A framework for reliability evaluation of electric vehicle charging stations. 2016 IEEE Power and Energy Society General Meeting (PESGM), 2016, p. 1–5. https://doi.org/10.1109/PESGM.2016.7741872.
[132] National Household Travel Survey. Federal Highway Administration 2017. https://nhts.ornl.gov/ (accessed September 26, 2022).
[133] Fleet DNA Project Data. National Renewable Energy Laboratory 2022. https://www.nrel.gov/fleetdna (accessed September 27, 2022).
[134] 2022 FHWA Forecasts of Vehicle Miles Traveled (VMT). Federal Highway Administration 2022. https://www.fhwa.dot.gov/policyinformation/tables/vmt/vmt_forecast_sum.cfm#ftn3 (accessed September 19, 2022).
[135] Table VM-2 - Highway Statistics 2019 - Policy | Federal Highway Administration. US Department of Transportation Federal Highway Administration 2020. https://www.fhwa.dot.gov/policyinformation/statistics/2019/vm2.cfm (accessed September 27, 2022).
[136] Table VM-4 - Highway Statistics 2019 - Policy | Federal Highway Administration. US Department of Transportation Federal Highway Administration 2020. https://www.fhwa.dot.gov/policyinformation/statistics/2019/vm4.cfm (accessed September 27, 2022).
[137] OpenStreetMap contributors. Planet dump retrieved from https://planet.osm.org 2022. https://www.openstreetmap.org (accessed December 22, 2022).
[138] ASPEN Environmental Group. Electric Transmission 2021.
[139] All Energy Infrastructure and Resources. US Energy Information Administration n.d. https://atlas.eia.gov/apps/all-energy-infrastructure-and-resources/explore (accessed November 15, 2022).
[140] Commonwealth Edison Company. Petition to Approve, Revisions to its Rider DE – Distribution System Extensions 2017.
[141] Nicholas M. Estimating electric vehicle charginginfrastructure costs across major U.S. metropolitan areas. ICCT 2019:11.
[142] NIO Power. NIO 2023. https://www.nio.com/nio-power (accessed May 27, 2023).
[143] Kulcsár M, Földes D, Nagy S. Determining the number of collection points for autonomous vehicle-based service using gravity model. 2021 Smart City Symposium Prague (SCSP), 2021, p. 1–6. https://doi.org/10.1109/SCSP52043.2021.9447388.

[144] Table HM-20 - Highway Statistics 2020 - Policy. Federal Highway Administration 2021. https://www.fhwa.dot.gov/policyinformation/statistics/2020/hm20.cfm (accessed September 27, 2022).
[145] State Sales Tax Rates. Sales Tax Institute n.d. https://www.salestaxinstitute.com/resources/rates (accessed February 13, 2023).
[146] Fritts J. State Corporate Income Tax Rates and Brackets. Tax Foundation 2023. https://taxfoundation.org/publications/state-corporate-income-tax-rates-and-brackets/ (accessed February 1, 2023).
[147] Motor vehicle insurance in U.S. city average, all urban consumers, not seasonally adjusted. Bureau of Labor Statistics 2023. https://data.bls.gov/timeseries/CUUR0000SETE?output_view=data (accessed April 14, 2023).
[148] New vehicles in U.S. city average, all urban consumers, not seasonally adjusted. Bureau of Labor Statistics 2023. https://data.bls.gov/timeseries/CUUR0000SETA01?output_view=data (accessed April 14, 2023).
[149] PPI industry data for Electrical equipment mfg, not seasonally adjusted. Bureau of Labor Statistics 2023. https://beta.bls.gov/dataViewer/view/timeseries/PCU33531-33531- (accessed April 14, 2023).
[150] PPI industry data for Electric power distribution, not seasonally adjusted. Bureau of Labor Statistics 2023. https://data.bls.gov/timeseries/PCU221122221122 (accessed April 14, 2023).
[151] PPI industry data for New industrial building construction, not seasonally adjusted. Bureau of Labor Statistics 2023. https://data.bls.gov/timeseries/PCU236211236211 (accessed April 14, 2023).
[152] PPI Commodity data for Telecommunication, cable, and internet user services-Cellular phone and other wireless telecommunication services, seasonally adjusted. Bureau of Labor Statistics 2023. https://beta.bls.gov/dataViewer/view/timeseries/WPS3721 (accessed April 14, 2023).
[153] Cost Per Mile Models for Long Range Estimating. FDOT 2021. https://www.fdot.gov/programmanagement/estimates/documents/costpermilemodels (accessed September 28, 2022).
[154] Nagarajan A, Thiagarajan R, Repins IL, Hacke PL. Photovoltaic Inverter Reliability Assessment. National Renewable Energy Laboratory; 2019. https://doi.org/10.2172/1573462.
[155] Annual Energy Outlook. US Energy Information Administration 2023. https://www.eia.gov/outlooks/aeo/data/browser/ (accessed April 28, 2023).
[156] Horesh N, Zhou Y, Quinn J. Home charging for all: Techno-economic and life cycle assessment of multi-unit dwelling electric vehicle charging hubs. Journal of Cleaner Production 2023;383:135551. https://doi.org/10.1016/j.jclepro.2022.135551.
[157] Publication 946 (2021), How To Depreciate Property. Internal Revenue Service 2021. https://www.irs.gov/publications/p946 (accessed September 4, 2022).
[158] EV Database. Useable battery capacity of full electric vehicles cheatsheet. Electric Vehicle Database 2023. https://ev-database.org/cheatsheet/useable-battery-capacity-electric-car (accessed January 13, 2023).
[159] Severson KA, Attia PM, Jin N, Perkins N, Jiang B, Yang Z, et al. Data-driven prediction of battery cycle life before capacity degradation. Nat Energy 2019;4:383–91. https://doi.org/10.1038/s41560-019-0356-8.
[160] Park S-J, Song Y-W, Kang B-S, Kim W-J, Choi Y-J, Kim C, et al. Depth of discharge characteristics and control strategy to optimize electric vehicle battery life. Journal of Energy Storage 2023;59:106477. https://doi.org/10.1016/j.est.2022.106477.

[161] Xie S, Hu X, Qi S, Tang X, Lang K, Xin Z, et al. Model predictive energy management for plug-in hybrid electric vehicles considering optimal battery depth of discharge. Energy 2019;173:667–78. https://doi.org/10.1016/j.energy.2019.02.074.
[162] Laporte S, Coquery G, Deniau V, De Bernardinis A, Hautière N. Dynamic Wireless Power Transfer Charging Infrastructure for Future EVs: From Experimental Track to Real Circulated Roads Demonstrations. World Electric Vehicle Journal 2019;10:84. https://doi.org/10.3390/wevj10040084.
[163] Davis SC, Boundy RG. Transportation Energy Data Book: Edition 40. Oak Ridge National Laboratory; 2022.
[164] IPCC 2021. Climate Change 2021: Impacts, Adaptation and Vulnerability. Cambridge University Press: 2021.
[165] Wernet G, Bauer C, Steubing B, Reinhard J, Moreno-Ruiz E, Weidema B. The ecoinvent database version 3 (part I): overview and methodology. Int J Life Cycle Assess 2016;21:1218–30. https://doi.org/10.1007/s11367-016-1087-8.
[166] Mulrow J, Grubert E. Greenhouse gas emissions embodied in electric vehicle charging infrastructure: a method and case study of Georgia, US 2021–2050. Environ Res: Infrastruct Sustain 2023;3:015013. https://doi.org/10.1088/2634-4505/acc548.
[167] Terra HP GEN 3 CE & UL Markets - Leaflet. ABB 2023. https://search.abb.com/library/Download.aspx?DocumentID=9AKK107991A9632&LanguageCode=en&DocumentPartId=&Action=Launch (accessed February 8, 2023).
[168] Lucas A, Alexandra Silva C, Costa Neto R. Life cycle analysis of energy supply infrastructure for conventional and electric vehicles. Energy Policy 2012;41:537–47. https://doi.org/10.1016/j.enpol.2011.11.015.
[169] Marmiroli B, Dotelli G, Spessa E. Life Cycle Assessment of an On-Road Dynamic Charging Infrastructure. Applied Sciences 2019;9:3117. https://doi.org/10.3390/app9153117.
[170] Gagnon P, Cowiestoll B, Schwarz M. Cambium 2022 Data. National Renewable Energy Laboratory 2023. https://scenarioviewer.nrel.gov/ (accessed February 14, 2023).
[171] NFPA 855: Standard for the Installation of Stationary Energy Storage Systems. National Fire Protection Association 2020. https://www.nfpa.org/codes-and-standards/all-codes-and-standards/list-of-codes-and-standards/detail?code=855 (accessed May 25, 2020).
[172] UL - 1974 Standard for Evaluation for Repurposing Batteries | Standards Catalog n.d. https://standardscatalog.ul.com/standards/en/standard_1974 (accessed May 28, 2020).
[173] Khani H, Zadeh MRD. Online Adaptive Real-Time Optimal Dispatch of Privately Owned Energy Storage Systems Using Public-Domain Electricity Market Prices. IEEE Transactions on Power Systems 2015;30:930–8. https://doi.org/10.1109/TPWRS.2014.2336753.
[174] Commonwealth Edison Co BES-Small Load Delivery Class (Secondary). OpenEI US Utility Rate Database 2021. https://apps.openei.org/USURDB/rate/view/60e771195457a3fc068b4568#1__Basic_Information (accessed January 7, 2022).
[175] Consolidated Edison Co-NY Inc SC-9 - General Large Low Tension Service [Westchester]. OpenEI US Utility Rate Database 2019. https://openei.org/apps/USURDB/rate/view/5cd1fc7e5457a3a52a54e9d8#1__Basic_Information (accessed September 27, 2021).
[176] Ramasamy V, Zuboy J, O'Shaughnessy E, Feldman D, Desai J, Woodhouse M, et al. U.S. Solar Photovoltaic System and Energy Storage Cost Benchmarks, With Minimum Sustainable Price Analysis: Q1 2022. 2022. https://doi.org/10.2172/1891204.
[177] Dube C. The Cost of Automated Storage & Retrieval Systems: ASRS Prices & Contributing Factors. Kardex 2023. https://us.blog.kardex-remstar.com/asrs-cost-factors (accessed March 21, 2023).

[178] Automotive Service Station - Commercial Construction Costs Per Square Foot. RSMeans 2019. https://www.rsmeans.com/model-pages/automotive-service-station (accessed March 21, 2023).
[179] blink. Level 2 AC EV IQ 200 Charging Stations Specifications 2020.
[180] blink. DCFC 50kW Fast Charger n.d.
[181] Ellingsen LA-W, Majeau-Bettez G, Singh B, Srivastava AK, Valøen LO, Strømman AH. Life Cycle Assessment of a Lithium-Ion Battery Vehicle Pack. Journal of Industrial Ecology 2014;18:113–24. https://doi.org/10.1111/jiec.12072.
[182] Gagnon P, Cowiestoll B, Schwarz M. Cambium 2022 Scenario Descriptions and Documentation. 2023. https://doi.org/10.2172/1915250.

APPENDIX A

Table A1. Target resale scenario input changes

Input	Grid Services	Energy Shuffle	Repurpose	Units
Reconditioning Cycles [a]	200	200	-	cycles
Acquisition Cost [b]	21.50	21.50	21.50	$/kWh-nameplate
DC-DC Converter/BMS [a]	250	250	-	$/kW
Adapter Tub [a]	50	50	-	$/kWh-nameplate
Testing Equipment [a]	-	-	1,718,750	$
Trip Distance [c]	100	100	100	miles
Labor Task Time [a]	-25%	-25%	-25%	% reduction
Warranty [a]	1%	1%	1%	% of resale price

a. Target reductions from learning
b. Reduction in acquisition price assumed to be 18% [38] of new electric vehicle battery price. New electric vehicle battery price is assumed to be $120/kWh in 2025 [7].
c. Reduced trip distance is assumed for a widespread adoption of second life batteries.

Table A2. Area breakdown for recondition with grid services, recondition through energy shuffle, and repurpose. Estimates were guided by wbdg.org

Area Name	Grid Services	Energy Shuffle	Repurpose
Transport	683 m^2	683 m^2	444 m^2
Park Forklifts	9 m^2	9 m^2	9 m^2
Process Batteries	619 m^2	619 m^2	619 m^2
Recondition or Repurpose	743 m^2	743 m^2	139 m^2
Store Batteries	121 m^2	121 m^2	121 m^2
Shipping and Receiving	98 m^2	98 m^2	98 m^2
Offices	42 m^2	42 m^2	42 m^2
Bathrooms	74 m^2	74 m^2	74 m^2
Break Room	74 m^2	74 m^2	74 m^2
Parking Lot	604 m^2	604 m^2	604 m^2
Total Facility Size	2,463 m^2	2,463 m^2	1,620 m^2
Total Land	3,067 m^2	3,067 m^2	2,224 m^2

Facility Building

The facility building costs were scaled based on the total facility size. The facility building costs included the land, enclosure, foundation, lights, furnishings, HVAC (heating, ventilation, and air conditioning), plumbing, electrical, roof, fire safety, flooring, walls, doors, parking lot, permits and inspections, engineering, construction management, and contingency. The fire safety costs accounted for the NFPA 855 standard that stated water was the preferred agent to suppress Li-ion battery fires [171]. Therefore, a sprinkler, a heat and smoke detection system, and an alarm system were included in the facility cost estimates to comply with this standard.

Table A3: Facility building cost breakdown

Cost Name	Grid Services	Energy Shuffle	Repurpose
Land [a]	$303,043	$303,043	$219,806
Enclosure [b]	$188,230	$188,230	$123,852
Foundation [c]	$165,056	$165,056	$119,720
Lights [d]	$27,503	$27,503	$18,364
Furnish Secondary Rooms [e]	$79,892	$79,892	$79,892
HVAC [f]	$132,556	$132,556	$87,220
Plumbing [g]	$148,463	$148,463	$97,686
Electrical [h]	$55,674	$55,674	$36,632
Roof [i]	$184,518	$184,518	$121,410
Fire Safety [j]	$95,021	$95,021	$73,568
Flooring [k]	$231,980	$231,980	$152,639
Walls and Doors [l]	$57,435	$57,435	$48,383
Parking Lot [m]	$20,990	$20,990	$20,990
Permits and Inspections [n]	$41,131	$41,131	$33,778
Engineering [o]	$121,204	$121,204	$86,376
Construction Management [p]	$86,575	$86,575	$49,358
Contingency [q]	$173,149	$173,149	$123,394
Producer Price Index [r]	+11%	+11%	+11%
Total	$2,353,636	$2,353,636	$1,663,562

a. Assumes $400,000 per acre based on a review of land costs by sacbee.com
b. Assumes a cost of $7.1/ft^2 for a steel building based on costs from buildingsguide.com
c. Facility and parking lot foundation assumed to cost $5/ft^2 based on costs from buildingsguide.com
d. Assumes inside facility with 70 lumens/ft^2, 10000 lumens/light, $44/light-installation from RSMeans 2016 Building Construction Cost Data, and $100/light. Loading dock lights $780 from RSMeans 2016 Building Construction Cost Data
e. Assumes $14,000 per bathroom, office area $70/ft^2, and breakroom $20,000
f. Assumes $5/ft^2
g. Assumes $5.5/ft^2
h. Assumes $2.1/ft^2
i. Assumes $5.5/ft^2 for commercial roofing from westroofingsystems.com. Assumes $1.46/ft^2 from RSMeans 2016 Building Construction Cost Data

j. Assumes sprinkler system costs \$2/ft^2 from costowl.com. From RSMeans 2016 Building Construction Cost Data the alarms cost \$4600, heat & smoke detectors cost \$0.37/ft^2, and 4 carbon dioxide extinguishers cost \$6924 each.
k. Assumes concrete costs 113/ft^3 from NRMCA.org and a depth of 16 inches. From RSMeans 2016 Building Construction Cost Data finishing costs \$2.15/ft^2 for hardener, \$0.50/ft^2 for dustproof, and \$0.52/ft^2 for epoxy.
l. Assumes 20 ft walls with costs of \$1.15/ft^2 for drywall and \$2.53/ft^2 for insulation based on RSMeans 2016 Building Construction Cost Data. Assumes dock door costs \$3000, 5 steel doors cost \$1200 each, and 5 wood doors cost \$100 each based on RSMeans 2016 Building Construction Cost Data.
m. From RSMeans 2016 Building Construction Cost Data assumes asphaltic concrete paving costs \$3.16/ft^2 and marking costs \$22.5 per stall for 20 stalls.
n. From RSMeans 2016 Building Construction Cost Data assumes \$10,250 to inspect steel building, \$4,426 to inspect concrete flooring, \$600 parking lot inspection, and 1.5% of all building costs for permits.
o. Assumed to be 7% of building costs based on RSMeans 2016 Building Construction Cost Data
p. Assumed to be 5% of building costs based on RSMeans 2016 Building Construction Cost Data
q. Assumed to be 10% of building costs based on RSMeans 2016 Building Construction Cost Data
r. Producer price index for new industrial buildings was 119.1 in January 2016 and 132.7 in January 2019 [48].

Table A4. Grid equipment cost breakdown. Approximated from Fu et al. (2018) [49]

Area Name	**Grid Services**	**Energy Shuffle**
Transformer [a]	\$134,400	\$13,440
Inverter [b]	\$840,000	\$84,000
Grid Electronics Installation [c]	\$864,000	\$86,400
Interconnection [d]	\$360,000	\$36,000
Subtotal	*\$2,198,400*	*\$219,840*
Grid Permitting [e]	\$295,000	\$295,000
EPC Overhead Labor [f]	\$259,200	\$25,920
EPC Overhead Equipment [g]	\$115,692	\$11,569
EPC Contingency [h]	\$65,952	\$6,595
Developer Overhead [i]	\$65,952	\$6,595
EPC/Developer Net Profit [j]	\$109,920	\$10,992
Producer Price Index [k]	-0.4%	-0.4%
Total	\$3,098,909	\$574,434

a. \$11.2/kW
b. \$70/kW
c. For 0.5 C-rate system costs \$36/kWh
d. \$30/kW
e. \$295,000 per system
f. 30% of labor costs
g. 8.67% of equipment costs
h. 3% of subtotal
i. 3% of subtotal
j. 5% of subtotal

k. Producer Price Index for electric transmission and control was 166.5 in January 2018 and 165.9 in January 2019 [50].

Facility Equipment

The facility equipment costs for RGS and RES included the loading dock, freight trucks, forklifts, DC-DC converter, and adapter tub. The DC-DC converter functioned as the battery management system (BMS) and controlled the flow of energy into the modules undergoing reconditioning. The DC-DC converters were assumed to have a lifetime of 15,000 cycles. The adapter tubs enabled hot-swapping of the battery modules to provide a plug-n-play connection between the battery modules and DC-DC converter which provided the cell-level balancing. The adapter tubs were assumed to be replaced every 10 years to account for new battery designs. All other equipment was assumed to last for 20 years; the lifetime of the facility.

The repurposing method required different facility equipment than RGS and RES. The repurposing facility equipment consisted of the loading dock, freight truck, forklifts, and testing equipment. The testing equipment was assumed to be replaced every 10 years.

Table A5. Facility equipment cost breakdown.

Cost Name	Grid Services	Energy Shuffle	Repurpose
Loading Dock [a]	\$8,500	\$8,500	\$8,500
Freight Truck(s) [b]	\$190,000	\$190,000	\$190,000
Forklift [c]	\$20,000	\$40,000	\$40,000
Testing Equipment [d]	-	-	\$3,437,500
DC-DC Converter/BMS [e]	\$6,000,000	\$6,000,000	-
Adapter Tub [f]	\$3,000,000	\$3,000,000	-
Total	\$9,218,500	\$9,238,500	\$3,934,503

a. \$8,500 for from RSMeans 2016 Building Construction Cost Data.
b. Estimated to be approximately \$150,000 for a new class 8 semi-truck based on listings from kenworthsalesco.com. Trailer estimated to cost \$40,000 based on listings from arrowtruck.com
c. Estimated to cost \$20,000 per forklift based on toyotaforklift.com
d. Power cycling equipment costs \$150,000 per unit according to an industry expert. 22 power cycling units needed. Data acquisition hardware costs \$15,000 per unit according to an industry expert. 11 data acquisition units needed.
e. Estimated to cost \$500/kW according to the developer
f. Estimated to cost \$100/kWh according to the developer

Transportation

To acquire and sell the batteries they must be transported to and from the facility. The batteries were collected as modules from the OEM [37], [38]. Li-ion batteries are classified as Class 9 hazardous materials [54], therefore, the batteries needed to be fully covered by individual non-metallic inner packaging to comply with Part 49 of the Code of Federal Regulations. Reusable packaging was assumed to cost $200 per module and be replaced every 5 years. The weight limit to transport standalone Li-ion batteries is 333 kg unless additional requirements are met [54]. This analysis assumed the additional requirements were met or the regulation will be changed in the future so that a class 8 freight truck can be filled to its gross weight limit of 36,287 kg [55]. The average discounted transportation costs were $90 thousand (k) annually, and details of the transportation costs are shown in Table A6.

Table A6. Transportation parameters.

Cost Name	Grid Services	Energy Shuffle	Repurpose
Fuel Cost [a]	$5,616/year	$9,936/year	$9,936/year
Driving Cost [b]	$3,952/year	$6,992/year	$6,992/year
Insurance Cost [c]	$10,000/year	$10,000/year	$10,000/year
Maintenance Cost [d]	$1,560/year	$2,760/year	$2,760/year
Packaging [e]	$244,800	$244,800	$244,800
Loading & unloading [f]	$10,400/year	$18,400/year	$18,400/year
Trip Distance	200 miles	200 miles	200 miles
Trips [g]	52/year	92/year	92/year
Average total yearly discounted cost [h]	$90,235	$106,795	$106,795

a. $0.54/mile spent on diesel fuel according to thetruckerreport.com
b. $0.36/mile to pay the driver and $0.02/mile for permits, licenses, and tolls according to thetruckerreport.com.
c. Estimated to be over $6,500 per year according to thetruckerreport.com. Assumed $10,000 per year-truck to be conservative.
d. $0.12/mile to for repairs and maintenance. $0.03/mile to replace tires according to thetruckerreport.com
e. Packaging in each truck assumed to cost $200 per module. Replace packaging every 5 years.
f. Assumed to take 6 hours to load a truck and 4 hours to unload a truck. Labor rate of $20/hour assumed.

g. Assumes max cargo weight of 27,216 kg and module weight of 22.2 kg to have 1,224 modules per trip. Total trips needed determined by the number of modules needed to be transported to have the facility at full refurbishing capacity. This accounts for viable product.
h. Calculated as discounted cost to account for packaging costs every 5 years

Reconditioning facility operation

Once the batteries were transported to the facility, they underwent an inspection consistent with the UL 1974, Standard for Evaluation for Repurposing Batteries [172]. The batteries were then transported to the reconditioning area or storage area. For reconditioning, the batteries were placed in an adapter tub connected to the DC-DC converter. The batteries underwent reconditioning for several days using the energy from charge and discharge cycles for grid services. Cell level SOH balancing was monitored and controlled by the DC-DC converter and decentralized controllers. Once the cells in the battery module had an optimized standard deviation of cell SOH, the battery module was removed from the adapter tub, transported to the packaging area, prepared for shipping, and placed in the storage area until the next outgoing shipment.

Table A7. Breakdown of yearly labor costs.

Cost Name	**Grid Services**	**Energy Shuffle**	**Repurpose**
Forklift [a, b]	$110,902	$198,630	$198,630
Inspect [b, c]	$268,619 [d]	$481,108 [d]	$85,734 [e]
Characterize [b, c]	-	-	$85,734 [f]
Bin [c]	-	-	$980,792 [g]
Package [c]	$336,990 [h]	$603,561 [h]	$603,564 [h]
Test [c]	-	-	$113,168 [i]
Subtotal Variable Labor	$716,511	$1,283,302	$2,067,621
Taxes [j]	$55,530	$99,456	$160,241
Total Variable Labor	$772,040	$1,382,758	$2,227,861
Clerical [k]	$34,040	$34,040	$34,040
Facility Manager [l]	$105,480	$105,480	$105,480
Sales Engineer [m]	$103,900	$103,900	$103,900
Reconditioning Monitors [c]	$181,069 [n]	$181,069 [n]	-
Supervisors	-	-	$193,020 [o]
Subtotal Fixed Labor	$424,489	$424,489	$436,440
Taxes [j]	$32,898	$32,898	$33,824

Total Fixed Labor	$457,387	$457,387	$470,264
Total	$1,229,427	$1,840,146	$2,698,126

a. Estimated a forklift operator can transport 24 modules/hour. Each module is transported five times by the forklift in the facility. Forklift operator has a wage of $17.24/hour according to USBLS for material moving machine operators.
b. Labor used for non-viable product
c. Technician labor rate of $20.69/hour according to USBLS 2019 occupation code 51-9061
d. Estimated one person spends 25 minutes to inspect one module
e. Inspect 10 modules with 45 minutes of labor
f. Characterize 10 modules with 45 minutes of labor
g. One person spends 13 minutes/kWh to grade, sort, and place the cells
h. Estimated one person spends 32 minutes to wire, close, fasten, and inspect one module
i. Estimated one hour of labor is required to test 10 modules
j. 6.2% Social Security, 1.45% Medicare, and 0.1% Employment Training Tax
k. $34,040/year according to USBLS for a General Office Clerk
l. $105,480/year according to USBLS for an Industrial Production Manager
m. $103,900/year according to USBLS for a Sales Engineer
n. One reconditioning monitor working for 24-hours every day of the year
o. Three supervisors each with a salary of $64,340 according to USBLS job code 51-1011

Table A8. Target ESS scenario input changes.

Input	**Grid Services**	**Energy Shuffle**	**Repurpose**	**New Li-ion**		**Units**
				2025	**2035**	
Reconditioning Cycles [a]	200	200	-	-	-	cycles
Acquisition Cost	21.50 [b]	21.50 [b]	21.50 [b]	140 [c]	105 [c]	$/kWh-nameplate
DC-DC Converter/BMS [a]	250	250	-	-	-	$/kW
Adapter Tub [a]	50	50	-	-	-	$/kWh-nameplate
Testing Equipment [a]	-	-	1,718,750	-	-	$
Trip Distance [d]	100	100	100	-	-	miles
Labor Task Time [a]	-25%	-25%	-25%	-	-	% reduction
Warranty [a]	1%	1%	1%	-	-	% of resale price
Depth of Discharge	60% [e]	60% [e]	60% [e]	-	-	%
ESS Costs [f]	-23%	-23%	-23%	-23%	-	% reduction
ESS Operating Costs [f]	8	8	8	8	8	$/kW-year

a. Target reductions from learning
b. Reduction in acquisition price assumed to be 18% [38] of new electric vehicle battery price. New electric vehicle battery price is assumed to be $120/kWh in 2025 [7].
c. Cost reduction based on projections by Mongird et al. (2019) [63] for new grid Li-ion batteries in 2025 and 2035.
d. Reduced trip distance is assumed for a widespread adoption of second life batteries.
e. Upper range of depth of discharge estimate by Neubauer et al. (2015) [38].

f. Cost reductions based on capital and operational projections by Mongird et al. (2019) [63] for Li-ion batteries in 2025.

Table A9. ESS cost breakdown for a 4-MW system. Approximated from Fu et al. (2018) [49].

Area Name	**Power Applications**	**Energy Applications**
Inverter [a]	$280,000	$280,000
Structural Balance of System [b]	$76,000	$208,000
Electrical Balance of System [c]	$324,000	$576,000
Installation Labor and Equipment [d]	$248,000	$368,000
EPC Overhead [e]	$104,000	$192,000
Sales Tax [f]	$115,313	$332,993
Land [g]	$16,680	$16,680
Grid Permitting [h]	$295,000	$295,000
Interconnection [i]	$120,000	$120,000
Contingency [j]	$59,499	$159,030
Developer Overhead [k]	$59,499	$159,030
EPC/Developer Net Profit [l]	$99,166	$265,050
Producer Price Index [m]	-0.4%	-0.4%
Total	$1,790,681	$2,961,073

a. $70/kW
b. $19/kWh for 1 C-rate, $13/kWh for 0.25 C-rate
c. $81/kWh for 1 C-rate, $36/kWh for 0.25 C-rate
d. $62/kWh for 1 C-rate, $23/kWh for 0.25 C-rate
e. $26/kWh for 1 C-rate, $12/kWh for 0.25 C-rate
f. 7.5% of installation costs
g. $4.17/kW
h. $295,000 per system
i. $30/kW
j. 3% of installation costs
k. 3% of installation costs
l. 5% of installation costs
m. Producer Price Index for electric transmission and control was 166.5 in January 2018 and 165.9 in January 2019 [50].

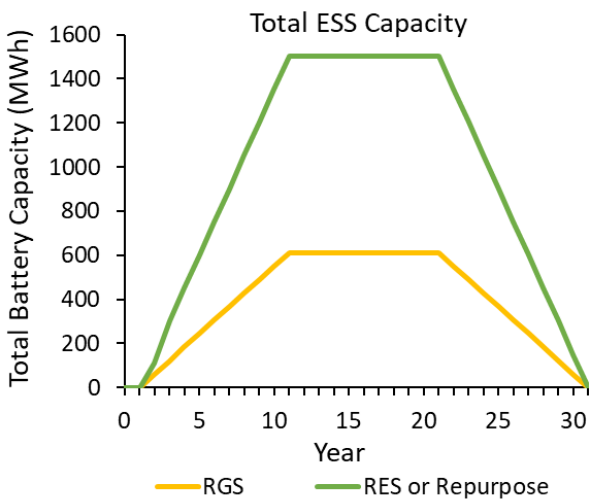

Figure A1. Total ESS capacity from years 0 through 30 for recondition with grid services (RGS), recondition through energy shuffle (RES), and repurpose. RES and repurpose have the same total ESS capacity.

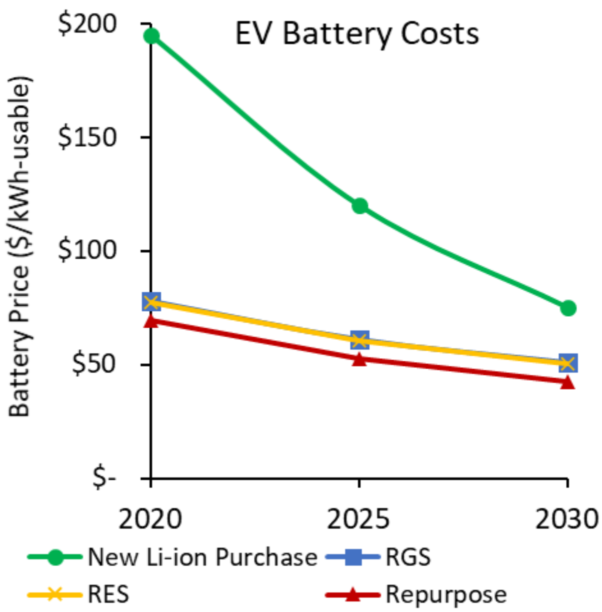

Figure A2. Projected electric vehicle battery prices from 2020 to 2030 for new Li-ion batteries [7] and second life batteries. Second life batteries include recondition with grid services (RGS), recondition through energy shuffle (RES), and repurpose. Second life batteries are assumed to have an acquisition cost of 18% of the price of a new electric vehicle battery [38].

Energy Arbitrage

The potential revenue from energy arbitrage was derived from 1-year (2018) of historical CAISO RTM Location Marginal Pricing (LMP) data obtained from CAISO OASIS [43]. The data was cleaned to remove nodes with missing pricing data. In total there were 9,452 nodes analyzed. To determine the potential revenue based on the pricing data, an algorithm was developed to optimize the revenue from the LMPs. The algorithm used the constraints and properties relevant to an ESS. The maximum capacity was for 2 hours of storage which corresponded to a maximum charge and discharging rate of 0.5-C. The roundtrip efficiency (Eff) was 90%. The constraints consisted of differences between charge and discharge LMPs and state of charge (SOC) as shown below.

$$LMP_{Discharge} * Eff > LMP_{Charge} \qquad \text{(A1)}$$

$$0\% \leq SOC \leq 100\% \qquad \text{(A2)}$$

The algorithm was written such that the revenue was maximized. The system size was assumed to be small enough to not change the LMP. The output of the algorithm gave the annual grid profits and mean number of cycles per day from each node. The mean number of cycles per day among nodes was determined to be 3.35 and was used for the RGS scenario. From these results, the 75th percentile of revenue (48.87 $/kWh-year) was used. It was assumed that only 70% of the potential revenue (34.21 $/kWh-year) could be captured due to imperfect price forecasting [173]. Thus, the grid profits per cycle (G) were determined by the annual grid profits (P), cycles per day (C), and usable capacity (U) as shown below.

$$G = \frac{P*U}{C*365} \quad \text{(A3)}$$

APPENDIX B

Supplemental Techno-economic Analysis Methodology

The *LCOC* was iteratively (due to *income tax*) computed to get a net present value of zero using Equation B8 with inputs from Equations B1-B7. Equation B1 computes the yearly (*y*) *revenue* using the *LCOC* and yearly *utilization* of the chargers.

$$(Revenue)_y = LCOC * (Utilization)_y \qquad \text{(B1)}$$

The depreciation schedule for the capital costs was determined using the 5-year Modified Accelerated Cost Recovery System (*MACRS*) rate for procurement and credit card reader costs as well as the 10-year MACRS for installation costs [157]. The *salvage values*, which impact *depreciation* (Equation B2), of the capital were assumed to be 10% for procurement, 0% for installation, and 0% for credit card readers. Salvage values were assumed to cancel out decommissioning costs.

$$Depreciation_y = (Capital\ Cost) * (1 - Salvage\ Value) * (MACRS\ Rate)_y \qquad \text{(B2)}$$

The *taxable income* was computed in Equation B3 using the yearly *revenue* (Eq. B1), *operational cost, electricity cost, depreciation* (Eq. B2)*, loan interest,* and any *carried over negative taxable income* from the previous year.

$$Taxable\ Income_y = (Revenue)_y - (Operational\ Cost)_y - (Electricity\ Cost)_y - (Depreciation)_y - (Loan\ Interest)_y + (Carried\ Over\ Negative\ Taxable\ Income)_{y-1} \qquad \text{(B3)}$$

The yearly income tax was computed using Equation B4 with that year's *taxable income* (Eq. B3) and *income tax rate* (26%). A negative taxable income resulted in zero income tax.

$$Income\ tax_y = (Taxable\ Income)_y * (Income\ Tax\ Rate) \qquad \text{(B4)}$$

The yearly *discount factor* was computed using Equation B5 using the *internal rate of return* which depends on the ownership model (Res.: 3%; Util.: 6%; PrC.: 10%).

$$Discount\ Factor_y = 1/(1 + Internal\ Rate\ of\ Return)^y \qquad \text{(B5)}$$

Next, the discounted expenses were calculated in Equation B6 using the capital costs paid upfront by the investor (*Capital Costs by Investor*), *loan payment, operational cost, electricity cost, income tax* (Eq. B4), *sales tax* (4.5%), and *discount factor* (Eq. B5).

$$Discounted\ Expenses = \sum_0^{y=30}\Big[(Capital\ Costs\ by\ Investor)_y + (Loan\ Payment)_y + (Operational\ Cost)_y + (Electricity\ Cost)_y + (Income\ Tax)_y\Big] * (Sales\ Tax) * (Discount\ Factor)_y \qquad \text{(B6)}$$

Then in Equation B7 the net present value (NPV) was set to zero by calculating the discounted revenue needed to equal the *discounted expenses*. The discounted revenue used the *LCOC*, *discount factor* (Eq. B5), and *utilization*.

$$NPV = 0 = \left\{\sum_1^{30} (Discount\ Factor)_y * (Utilization)_y\right\} * LCOC - (Discounted\ Expenses) \qquad \text{(B7)}$$

Finally, the *LCOC* was solved for in Equation B8 by rearranging Equation B7.

$$LCOC = (Discounted\ Expenses) \,/\, \left\{\sum_1^{30} (Discount\ Factor)_y * (Utilization)_y\right\} \qquad \text{(B8)}$$

Charger Utilization

The processed MUD data included 586K L2 charging sessions at 4.3K ports in 27 states (Figure B1) and 1.3K DCFC charging sessions at 13 DCFC ports in 4 states (Figure B2). The data were collected from October 2019 to October 2021. The charging schedule (Figure B3) for each charger type was simulated from the EV WATTS data by using each session’s start time, charge duration, and power.

The Level 1 charger utilization simulation had the following assumptions:

- Used once per day
- Have a session power of 1.5-kW (L2 max: 6.6-kW; L1 max: 1.9-kW)
- Charge duration was limited to be no greater than the dwell time
- Charging session energy was limited to be no greater than the L2 charging session energy

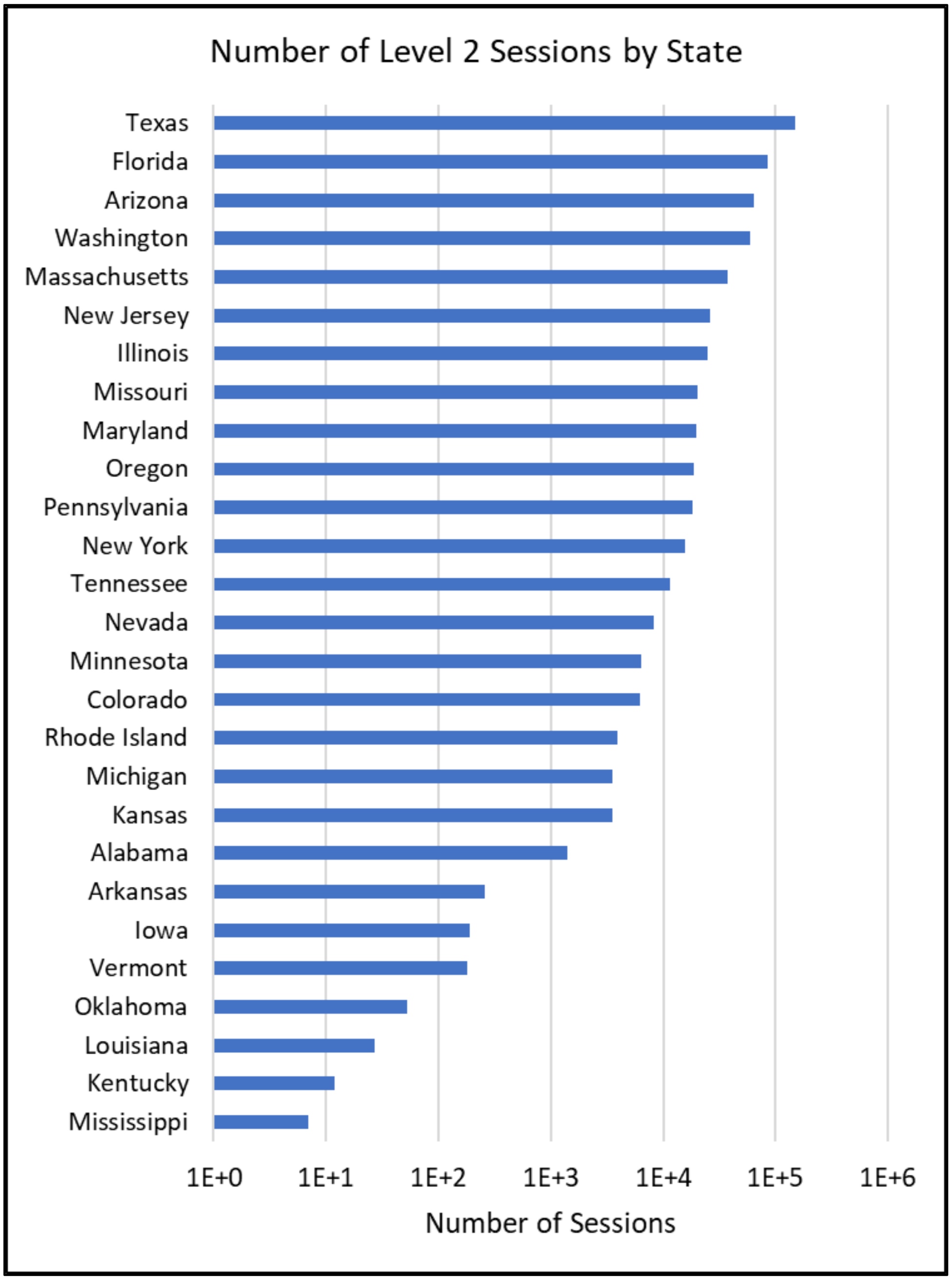

Figure B1. Number of Multi-Unit Dwelling Level 2 sessions by state.

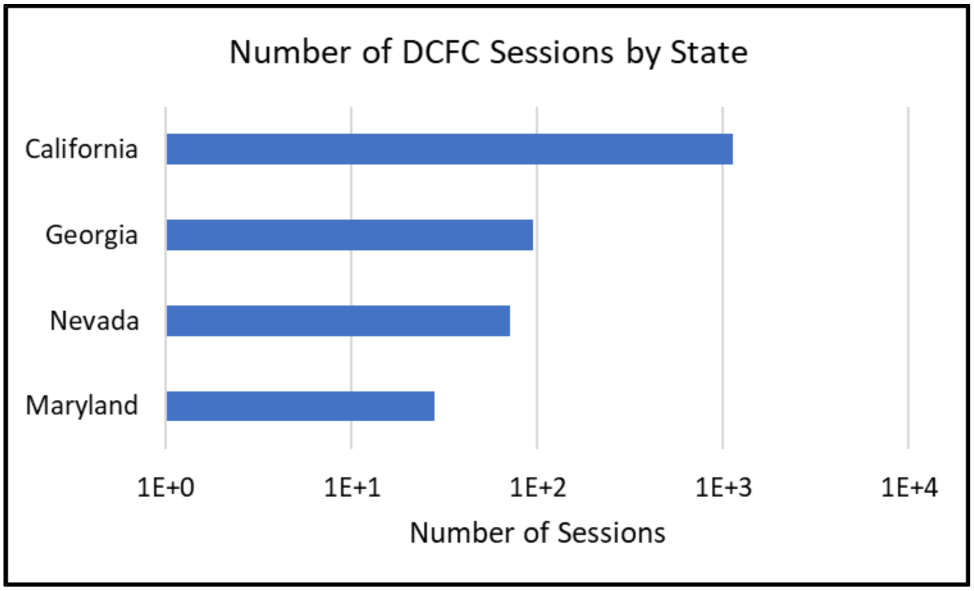

Figure B2. Number of Multi-Unit Dwelling DCFC sessions by state.

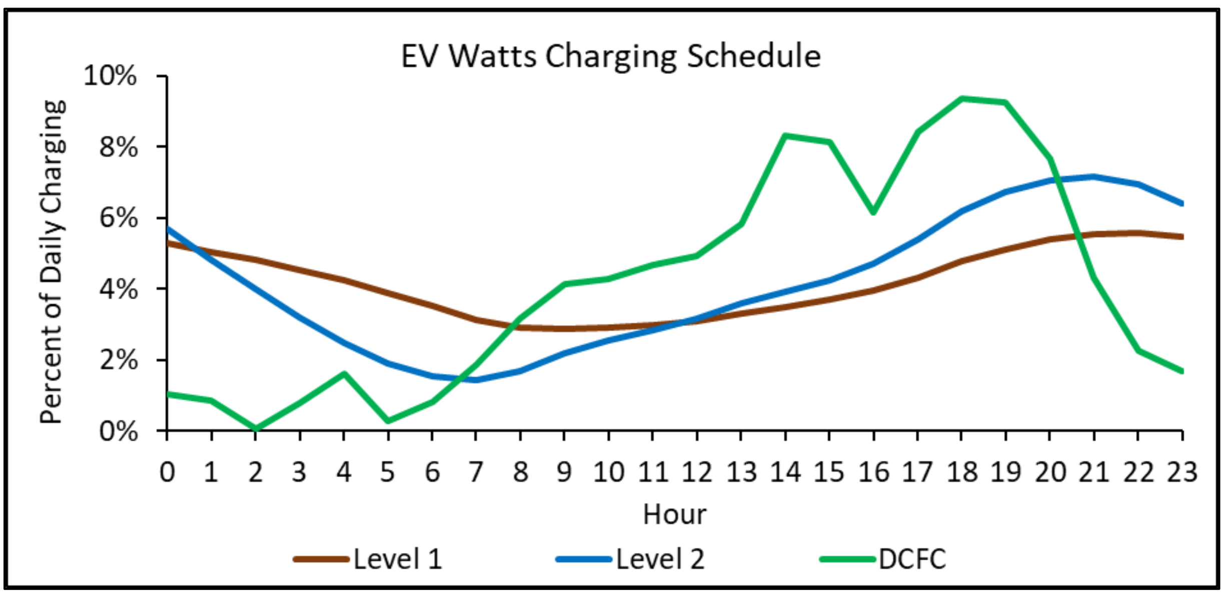

Figure B3. Average hourly charging profile for Level 1, Level 2, and DCFC at multi-unit dwellings from the EV Watts dataset.

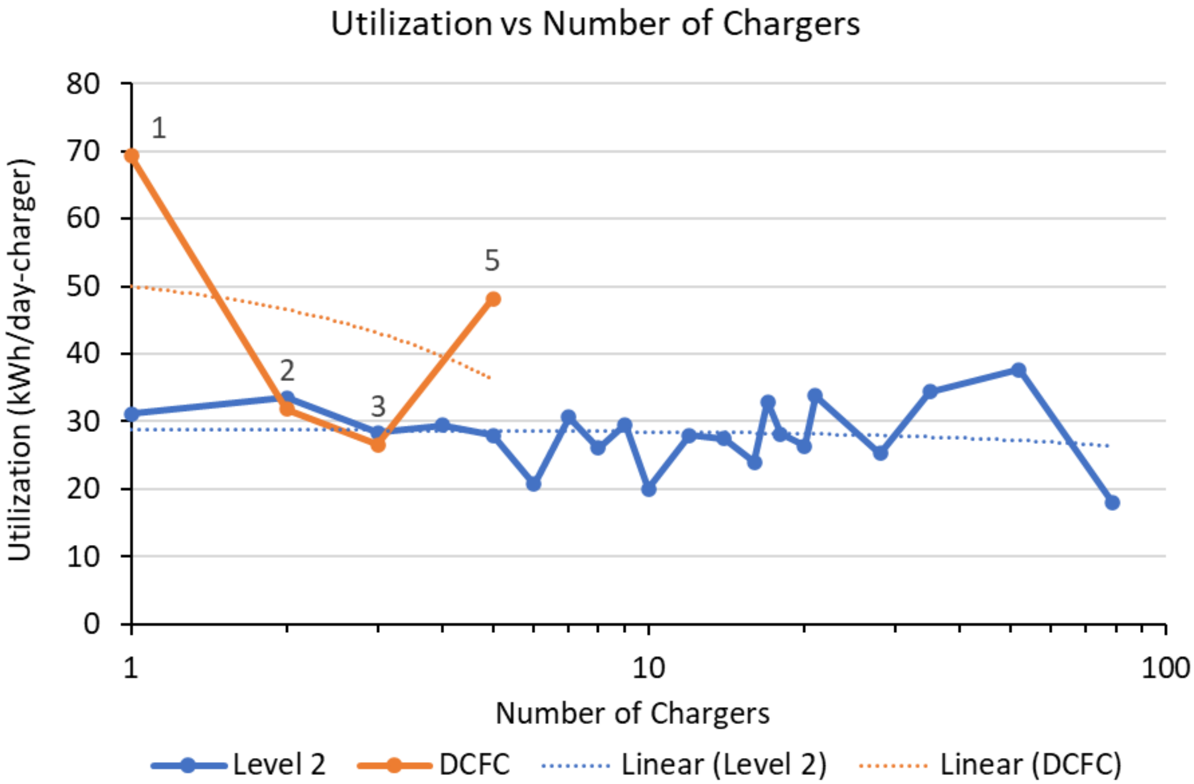

Figure B4: Utilization for Level 2 and DCFC as a function of the number of chargers at the Multi-Unit Dwelling hub.

The baseline scenario leverages utilization parameters from the processed EV WATTS charging data collected intermittently from October 2019 through October 2021 [91] to determine the LCOC based on current market conditions. However, the utilization for current market conditions may not be representative of the ordinary utilization since the period of data collection coincided with the COVID-19 pandemic. Surprisingly, the total daily energy consumption of L2 chargers (Figure B5) has a 17% higher median (by state) utilization during the pandemic than preceding the pandemic (before March 11, 2020).

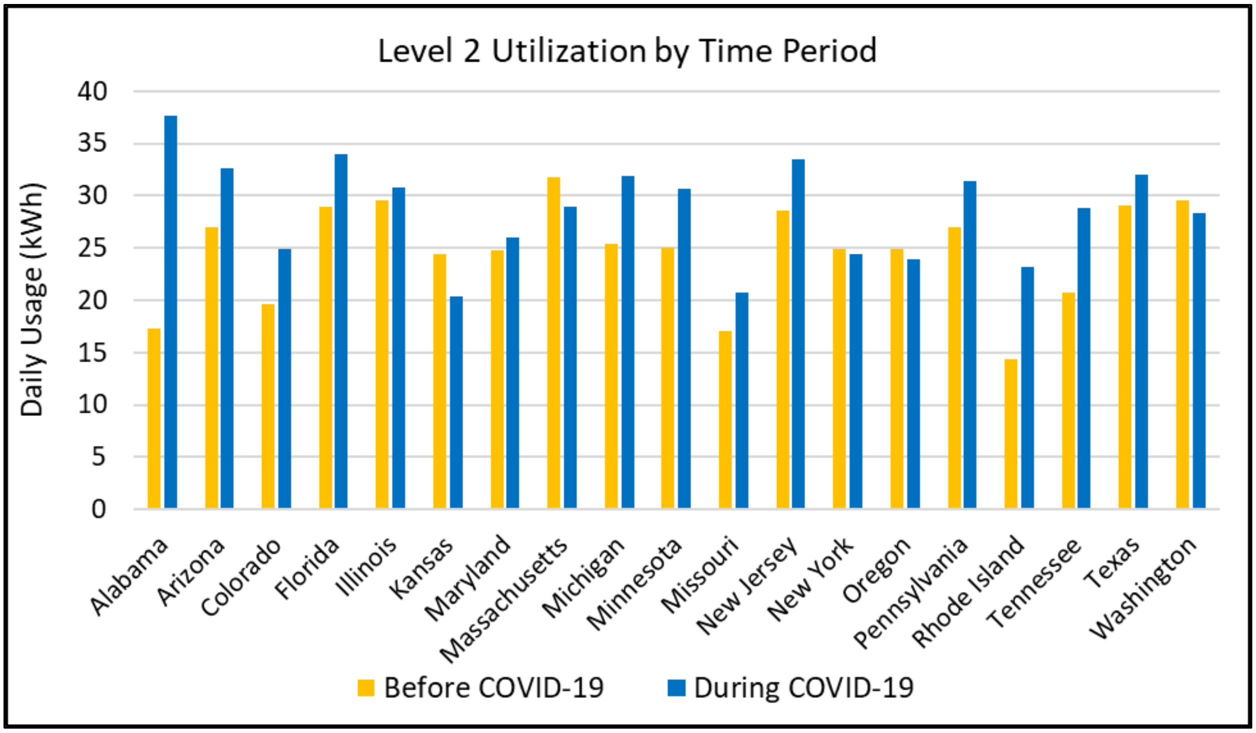

Figure B5. Utilization of Multi-Unit Dwelling Level 2 chargers in states Before COVID-19 and During Covid-19.

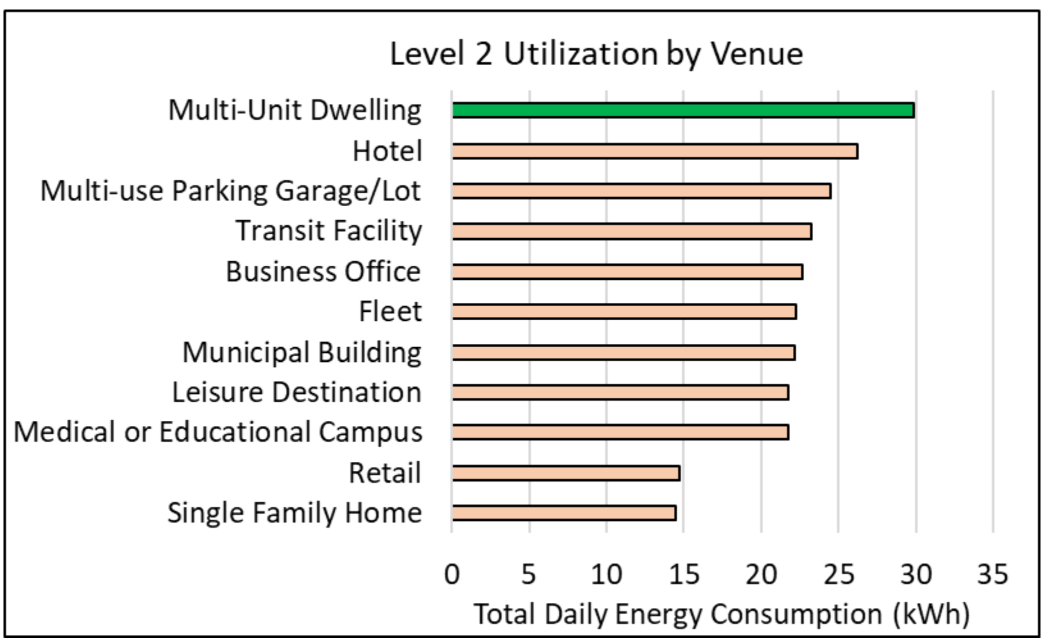

Figure B6. Total daily energy consumption of level 2 chargers at different venues.

Electricity Costs

The different commercial electricity schedule characteristics of the focus locations were:

- Illinois had moderate electricity rates (0.080 $/kWh) and low demand charges (7.8 $/month-kW) [174].
- New York had low electricity rates (0.026 $/kWh) and high demand charges (19 $/month-kW) [175].
- California had time-of-use pricing with high electricity rates (0.086-0.14 $/kWh) and high demand charges (16-34 $/month-kW) [96], representing an upper bound on electricity costs.

Residential Schedules

Table B1. Residential electricity schedules used to calculate electricity costs for all states.

State	**Full Name**	**Utility Name with Link**
Alabama	Alabama Power Co: Plug-In Electric Vehicle (EV)	Alabama Power Co
Alaska	Chugach Electric: Residential Service (Flat)	Chugach Electric
Arizona	Arizona Public Service: Residential Time of Use (Saver Choice) TOU-E (TOU)	Arizona Public Service
Arkansas	Entergy Arkansas: General Purpose Residential Service (RS) Single Phase (Flat)	Entergy Arkansas
California	Southern California Edison: TOU-EV-1 Domestic Time-of-Use Electric Vehicle Charging (TOU)	Southern California Edison
Colorado	Public Service Co of Colorado: Residential Energy Time Of Use (Schedule RE-TOU) (TOU)	Public Service Co of Colorado
Connecticut	NSTAR Electric Co Connecticut: Greater Boston Residential R-1 (A1) (Flat)	NSTAR Electric Co Connecticut
Delaware	Delmarva Power: Residential Service (Flat)	Delmarva Power
District of Columbia	Potomac Electric Power Co: Residential - Schedule R (Flat)	Potomac Electric Power Co
Florida	Florida Power & Light Co: RS-1 Residential Service (Flat)	Florida Power & Light Co
Georgia	Georgia Power: Schedule TOU-PEV-8 - Plug-in Electric Vehicle (EV)	Georgia Power
Hawaii	Hawaiian Electric Co: Schedule "R" Residential Service - Single Phase (Flat)	Hawaiian Electric Co
Idaho	Idaho Power Co: Schedule 1 - Residential Service (Flat)	Idaho Power Co

Illinois	Commonwealth Edison Co: BES - Residential Multi Family Without Electric Space Heat Delivery Class (Flat)	Commonwealth Edison Co
Indiana	Duke Energy Indiana: RS - Residential Service (Flat)	Duke Energy Indiana
Iowa	MidAmerican Energy Co: RATE RST - RESIDENTIAL TIME-OF-USE SERVICE (TOU)	MidAmerican Energy Co
Kansas	Kansas City Power & Light Co: Residential Standard Service (Schedule RS) (Flat)	Kansas City Power & Light Co
Kentucky	Kentucky Utilities: Residential Service (Flat)	Kentucky Utilities
Louisiana	Entergy Louisiana: Residential and Farm Service - Single Phase (RS-L) (Flat)	Entergy Louisiana
Maine	Central Maine Power Co: A-TOU Residential Service Time-of-Use (TOU)	Central Maine Power Co
Maryland	Baltimore Gas & Electric Co: Residential Optional Time of Use (Schedule RL) (TOU)	Baltimore Gas & Electric Co
Massachusetts	NSTAR Electric Co Massachusetts: Greater Boston Residential R-1 (A1) (Flat)	NSTAR Electric Co Massachusetts
Michigan	DTE Electric: Residential Time of Day Full Service (TOU)	DTE Electric
Minnesota	Northern States Power Co: Residential Service - Overhead Standard (A01) (Flat)	Northern States Power Co
Mississippi	Mississippi Power Co: Residential Electric Service (R-57) Single-Phase (Flat)	Mississippi Power Co
Missouri	Union Electric Co: 1(M) Residential Service Rate (Flat)	Union Electric Co
Montana	NorthWestern Energy: Rate 10: Residential Electric (Flat)	NorthWestern Energy
Nebraska	Nebraska Public Power District: Residential Service (Flat)	Nebraska Public Power District
Nevada	Nevada Power Co: ORS-TOU Optional Residential Service Time of Use (TOU)	Nevada Power Co
New Hampshire	NSTAR Electric Co New Hampshire: Greater Boston Residential R-1 (A1) (Flat)	NSTAR Electric Co New Hampshire
New Jersey	Public Service Electric & Gas Co: RS - Residential Service (Flat)	Public Service Electric & Gas Co
New Mexico	Public Service Co of New Mexico: 1A (Residential Service) (Flat)	Public Service Co of New Mexico
New York	Consolidated Edison Co - SC-1—Residential & Religious Service [Westchester]. (Flat)	Consolidated Edison Co
North Carolina	Duke Energy Carolinas: RS (Residential Service) (Flat)	Duke Energy Carolinas
North Dakota	Northern States Power Co: Residential Time of Day Service (D02/D04) Standard (TOU)	Northern States Power Co
Ohio	Columbus Southern Power Co: Residential Service: SCHEDULE R-R (Flat)	Columbus Southern Power Co
Oklahoma	Oklahoma Gas & Electric: R-1 (Residential Service) (Flat)	Oklahoma Gas & Electric
Oregon	Portland General Electric Co: Residential Service (Rate 7) (Flat)	Portland General Electric Co
Pennsylvania	PECO Energy Co: Residential Service (R) (Flat)	PECO Energy Co

Rhode Island	The Narragansett Electric Co: A-16 (Residential Service) (Flat)	The Narragansett Electric Co
South Carolina	Duke Energy Carolinas: Residential Service Time-of-Use (R-TOUD-55) Single Phase (TOU)	Duke Energy Carolinas
South Dakota	Otter Tail Power Co: Residential Service (Rate Code 101) (Flat)	Otter Tail Power Co
Tennessee	Nashville Electric Service: RS Residential Service (Over 4000kWh) (Flat)	Nashville Electric Service
Texas	Oncor Electric Delivery Co: Residential (by Green Mountain Energy Company) (Flat)	Oncor Electric Delivery Co
Utah	PacifiCorp - Utah: Schedule 1 (Residential Service - Single Phase) (Flat)	PacifiCorp - Utah
Vermont	Green Mountain Power Corp: Rate 01 Residential Service (Flat)	Green Mountain Power Corp
Virginia	Virginia Electric & Power Co: Residential Schedule 1 (Flat)	Virginia Electric & Power Co
Washington	Puget Sound Energy: 7 (Residential Service - Single Phase) (Flat)	Puget Sound Energy
West Virginia	Appalachian Power Co: Schedule RS: Residential Service (Flat)	Appalachian Power Co
Wisconsin	Wisconsin Electric Power Co: Residential (Single-Phase) Rg 1 (Flat)	Wisconsin Electric Power Co
Wyoming	PacifiCorp - Wyoming: 2 Residential Service Single Phase (Flat)	PacifiCorp - Wyoming

Commercial Schedules

Table B2. Commercial electricity schedules used to calculate electricity costs for all states.

State	Full Name	Utility Name with Link
Alabama	Alabama Power Co: BEVT Business Electric Vehicle - Time of Use (EV, any)	Alabama Power Co
Alaska	Chugach Electric: Large General Secondary Service Rates (Flat, >20 kW)	Chugach Electric
Arizona	Arizona Public Service: Small General Service (E-32 S) Primary (Flat, 20-100 kW)	Arizona Public Service
Arkansas	Entergy Arkansas: Small General Service (SGS) (Flat, <100 kW)	Entergy Arkansas
California	Southern California Edison: TOU-GS-2 Time-of-Use General Service—Demand Metered (TOU, 20-200 kW)	Southern California Edison
Colorado	Public Service Co of Colorado: Transmission Time Of Use (Schedule TTOU) (TOU, >25 kW)	Public Service Co of Colorado
Connecticut	NSTAR Electric Co: Western Massachusetts Primary General Service G-2 (Flat, <350 kW)	NSTAR Electric Co

Delaware	Delmarva Power: Medium General Service - Secondary (Flat, 30-300 kW)	Delmarva Power
District of Columbia	Potomac Electric Power Co: General Service Primary Service - Schedule GS3A (Flat, 25-100 kW)	Potomac Electric Power Co
Florida	Florida Power & Light Co: GSD-1 (General Service Demand) (Flat, 25-500 kW)	Florida Power & Light Co
Georgia	Georgia Power: Time of Use-High Load Factor Schedule TOU-HLF-10 (TOU, >30 kW)	Georgia Power
Hawaii	Hawaiian Electric Co: SCHEDULE EV-C COMMERCIAL ELECTRIC VEHICLE CHARGING SERVICE PILOT - Demand Service (EV, any)	Hawaiian Electric Co
Idaho	Idaho Power Co: Schedule 7 - Small General Service (Flat, <1000 kW)	Idaho Power Co
Illinois	Commonwealth Edison Co: BES-Small Load Delivery Class (Secondary) (Flat, <100 kW)	Commonwealth Edison Co
Indiana	Duke Energy Indiana: CS - Commercial Service (Flat, <75 kW)	Duke Energy Indiana
Iowa	MidAmerican Energy Co: RATE GET - GENERAL ENERGY TIME-OF-USE SERVICE (Commercial) (TOU, <200 kW)	MidAmerican Energy Co
Kansas	Kansas City Power & Light Co: Medium General Service (Schedule MGS) (0-199 kW) Primary (Flat, <200 kW)	Kansas City Power & Light Co
Kentucky	Kentucky Utilities: General Service (Single Phase) (Flat, <50 kW)	Kentucky Utilities
Louisiana	Entergy Louisiana: Small General Service (GS-L) Three Phase (Flat, <500 kW)	Entergy Louisiana
Maine	Central Maine Power Co: MGS-P-TOU Medium General Service - Primary - Time-Of-Use (Three Phase) (TOU, 20-400 kW)	Central Maine Power Co
Maryland	Baltimore Gas & Electric Co: Schedule GS General Service Small (TOU, <60 kW)	Baltimore Gas & Electric Co
Massachusetts	NSTAR Electric Co: Western Massachusetts Primary General Service G-2 (Flat, <350 kW)	NSTAR Electric Co
Michigan	Consumers Energy Co: General Service - Primary, CVL 1 (Rate GP) (Flat, <100 kW)	Consumers Energy Co
Minnesota	Northern States Power Co - Minnesota: General Service (A14) Primary Voltage (Flat, 25-1000 kW)	Northern States Power Co - Minnesota
Mississippi	Mississippi Power Co: General Service Electric Heating - High Voltage (GSEH-HV-12) Three-Phase (Flat, >25 kW)	Mississippi Power Co
Missouri	Union Electric Co: 2(M)Small General Service - Three Phase (Flat, <100 kW)	Union Electric Co
Montana	NorthWestern Corporation: GSEDS-1 Primary Non-Demand (Flat, <1000 kW)	NorthWestern Corporation
Nebraska	Nebraska Public Power District: General Service Three-Phase (Flat, <200 kW)	Nebraska Public Power District
Nevada	Nevada Power Co: GS-1 (Small General Service) (Flat, <50 kW)	Nevada Power Co

New Hampshire	Public Service Co of NH: General Service Three Phase (Flat, <100 kW)	Public Service Co of NH
New Jersey	PECO Energy Co: GS-PD (Primary-Distribution Power) Procurement Class-2 (Flat, <100 kW)	PECO Energy Co
New Mexico	Public Service Co of NM: 2B Small Power Service - TOU (TOU, <50 kW)	Public Service Co of NM
New York	Consolidated Edison Co-NY Inc SC-9—General Large Low Tension Service [Westchester] (Flat, 10-1500 kW)	Consolidated Edison Co - NY
North Carolina	Progress Energy Carolinas: Medium General Service Schedule (MGS-58) Three Phase (Flat, 30-1000 kW)	Progress Energy Carolinas
North Dakota	Northern States Power Co - North Dakota: Small General Time-of-Day kWh Metered Service (A16) (TOU, <1000 kW)	Northern States Power Co - North Dakota
Ohio	Columbus Southern Power Co: General Service - Low Load Factor, Primary Voltage: SCHEDULE GS-2 (Flat, 10-50 kW)	Columbus Southern Power Co
Oklahoma	Oklahoma Gas & Electric Co: GS-1 (General Service) (Flat, <400 kW)	Oklahoma Gas & Electric Co
Oregon	Portland General Electric Co: Large Non-Residential Service, Three Phase (Rate 83) (TOU, 30-200 kW)	Portland General Electric Co
Pennsylvania	PECO Energy Co: General Service Polyphase Service (GSA) Class 2 (Flat, <100 kW)	PECO Energy Co
Rhode Island	The Narragansett Electric Co: G-02 (General C & I Rate) (Flat, 10-200 kW)	The Narragansett Electric Co
South Carolina	Progress Energy Carolinas: Small General Service TOU (Schedule SGS-TOU-58) (TOU, 30-1000 kW)	Progress Energy Carolinas
South Dakota	Otter Tail Power Co: General Service Primary (Rate 403) (Flat, 20-80 kW)	Otter Tail Power Co
Tennessee	Nashville Electric Service: TGSA - 1 - General Power Time-of-Day (TOU, <50 kW)	Nashville Electric Service
Texas	Oncor Electric Delivery Co: Small Non- Residential LSP POLR(GREATER THAN 10KW) (Flat, >10 kW)	Oncor Electric Delivery Co
Utah	PacifiCorp - Utah: Schedule 6 (General Service - Distribution Voltage) (Flat, 35-1000 kW)	PacifiCorp - Utah
Vermont	Green Mountain Power Corp: Rate 08: General Service Three Phase (Flat, <200 kW)	Green Mountain Power Corp
Virginia	Virginia Electric & Power Co: GS-2T Time-of-Use (TOU, 30-500 kW)	Virginia Electric & Power Co
Washington	Puget Sound Energy: 24 (General Service - Three Phase) (Flat, <50 kW)	Puget Sound Energy
West Virginia	Appalachian Power Co - West Virginia: Schedule GS TOD: General Service Time-of-Day (Primary) (TOU, 10-150 kW)	Appalachian Power Co - West Virginia
Wisconsin	Wisconsin Electric Power Co: General Secondary (Three-Phase) Cg 1 (Flat, <10000 kW)	Wisconsin Electric Power Co
Wyoming	PacifiCorp - Wyoming: 28 (General Service - Three Phase Primary) (Flat, 20.5-1000 kW)	PacifiCorp - Wyoming

Single-Family Homes

The scenarios for the single-family home have the following six assumptions: 1) MUD resident ownership model without credit card readers and taxes, 2) Illinois, New York, or California service locations 3) procurement cost of 490 $/charger [15] and installation cost of 1.7K $/charger [16], 4) one L2 charger at the site, 5) single-family home utilization (Figure B6), and 6) no fixed charge.

MUD Levelized Cost of Charging

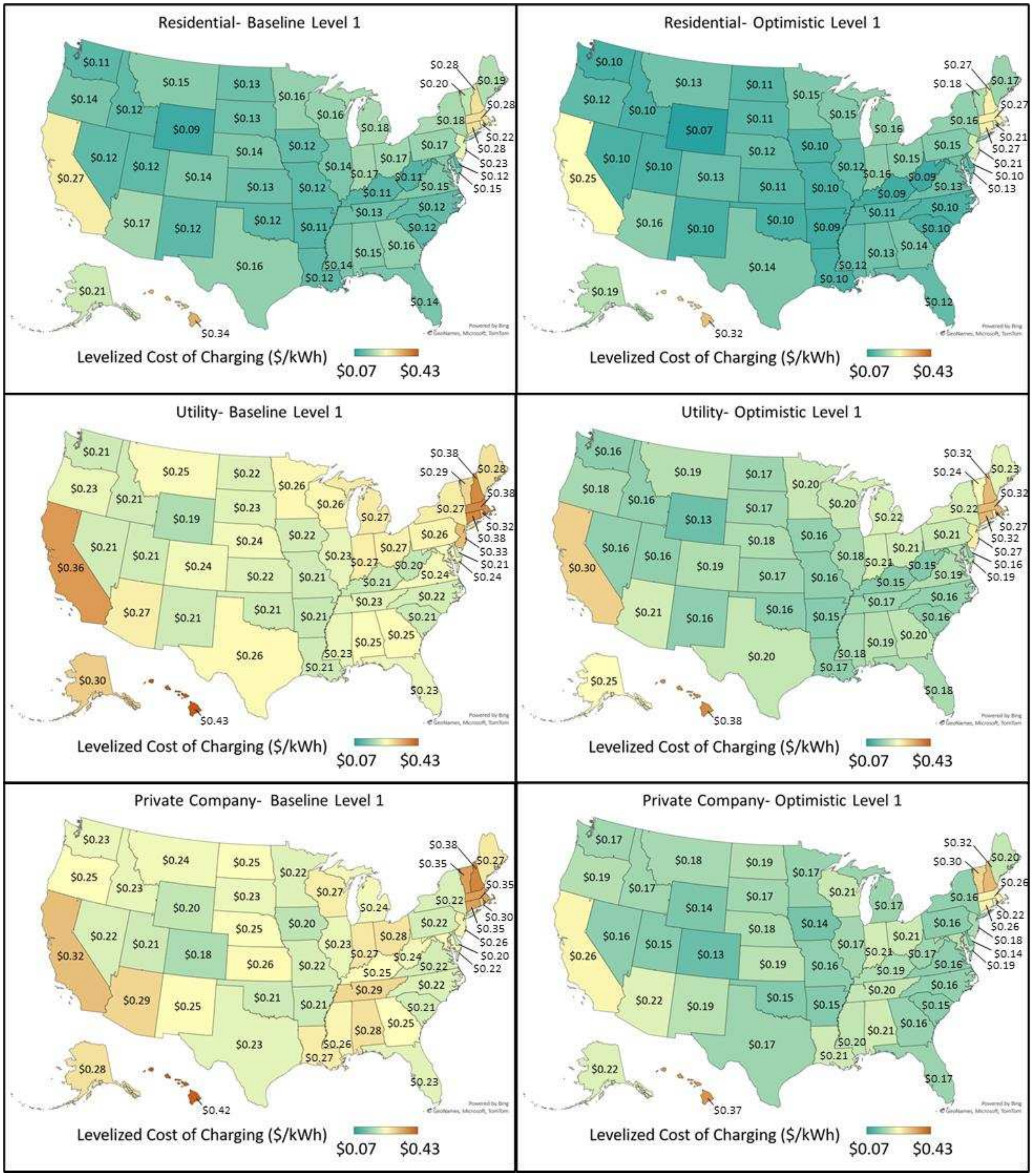

Figure B7. Baseline and optimistic levelized cost of charging (LCOC) for Level 1 (L1) stations in 50 U.S. states at Multi-Unit Dwellings under residential (Res.), utility (Util.), and private company (PrC.) ownership models. The gasoline equivalent cost ranges from $0.38 to $0.60 per kWh (Figure B9).

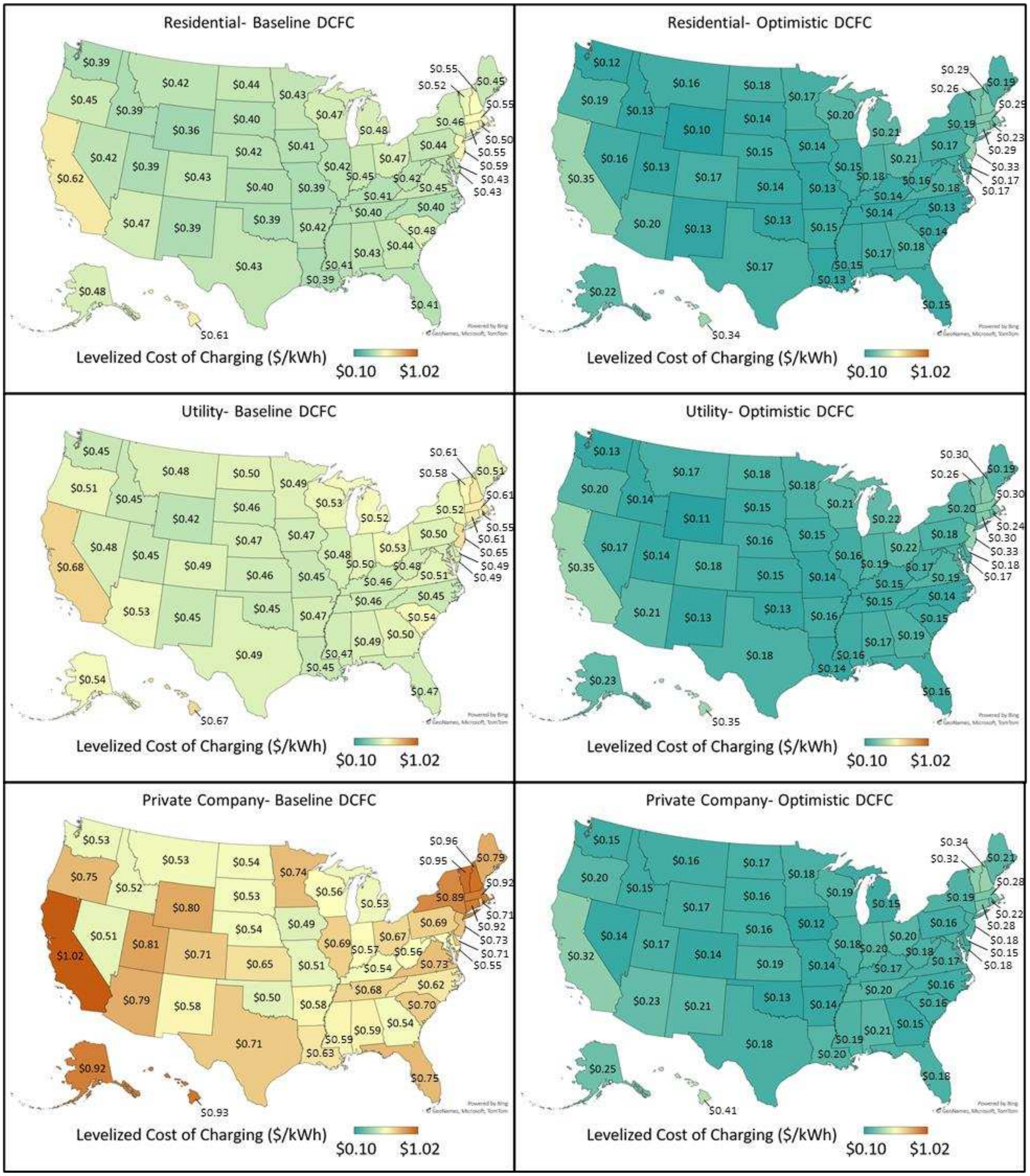

Figure B8. Baseline and optimistic levelized cost of charging (LCOC) for Direct Current Fast Charging (DCFC) stations in 50 U.S. states at Multi-Unit Dwellings under residential (Res.), utility (Util.), and private company (PrC.) ownership models. The gasoline equivalent cost ranges from $0.38 to $0.60 per kWh (Figure B9).

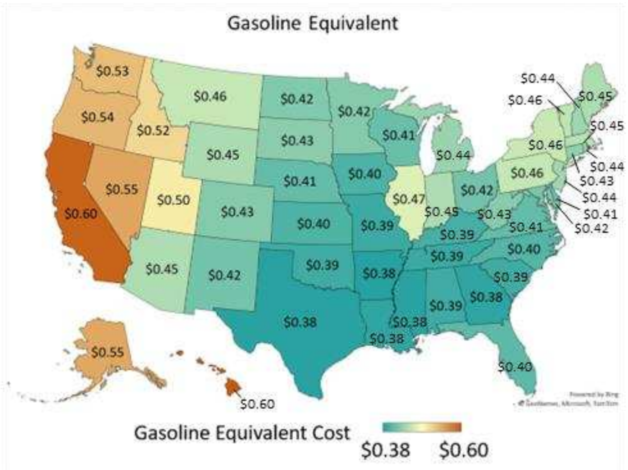

Figure B9. Gasoline equivalent cost per kWh in the United States on September 2, 2022 [104].

Sensitivity Analysis

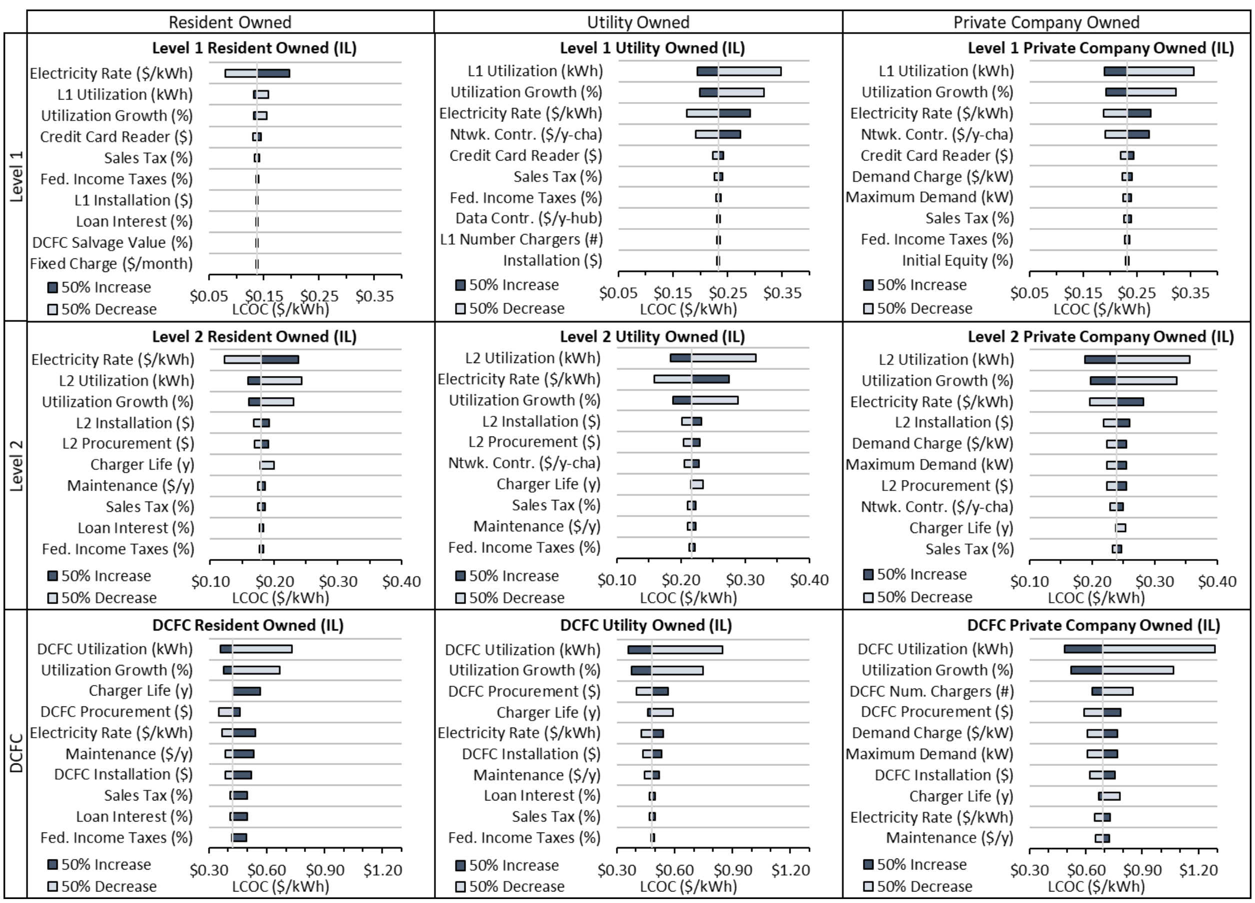

Figure B10. Sensitivity of techno-economic analysis (TEA) model inputs for a Multi-Unit Dwelling (MUD) charging hub in Illinois (IL) with baseline scenarios: Level 1 (L1), Level 2 (L2), and Direct Current Fast

Charging (DCFC) stations; and resident, utility, and private company ownership models. Abbreviations: year (y), federal (Fed.), network (Ntwk.), contract (Contr.), charger (cha.), number (num.).

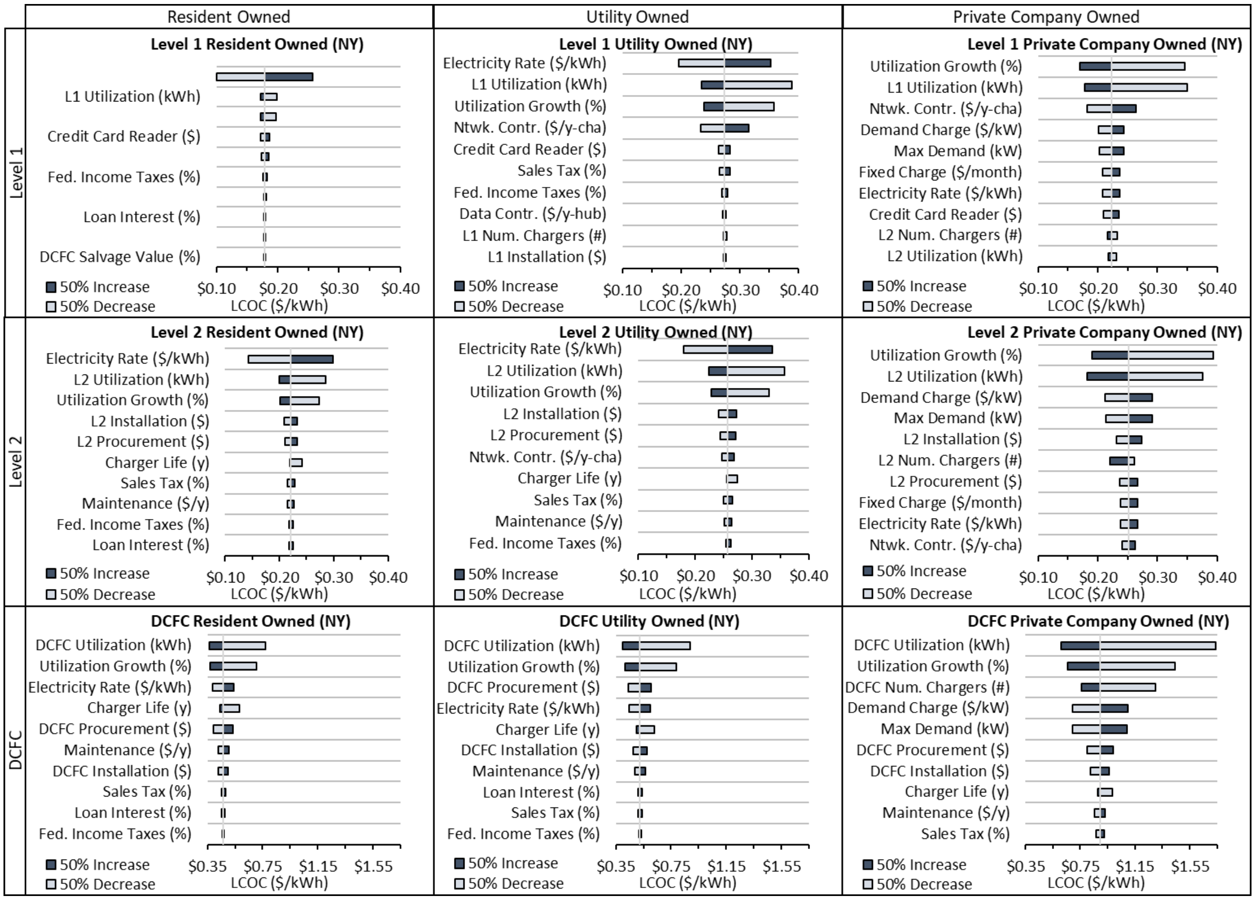

Figure B11. Sensitivity of techno-economic analysis (TEA) model inputs for a Multi-Unit Dwelling (MUD) charging hub in New York (NY) with baseline scenarios: Level 1 (L1), Level 2 (L2), and Direct Current Fast Charging (DCFC) stations; and resident, utility, and private company ownership models. Abbreviations: year (y), federal (Fed.), network (Ntwk.), contract (Contr.), charger (cha.), number (num.).

Cambium Implementation Into GREET

The Cambium data had hourly grid mix projections for every day of the year, every 2 years, on a state basis from 2020 through 2050; the aggregated U.S. mix was also included. Before being imported into GREET, the Cambium grid mix was converted into the mean hourly mix for 2020, 2025 (interpolated), 2030, 2035 (interpolated), 2040, 2045 (interpolated), and 2050. In total, 8232 Cambium grid mix scenarios were individually run in GREET and recorded to determine the BEV fuel-cycle GHG emissions for each scenario; the scenarios were from each combination of the time-of-day (24 hours), geographical location (48 states & 1 U.S. average), and year (2020 to 2050 with 5-year increments). Hourly BEV fuel-cycle GHG emissions were then coupled with the MUD charging site's schedule (Figure B1) to determine the fuel-cycle GHG emissions of each of the 5-year increments (2020-2050).

Cambium Grid Resources

The grid resources by year projected by NREL Cambium were be binned into the following GREET categories:

- Residual Oil: oil-gas-steam
- Natural Gas: natural gas combined cycle, natural gas combined cycle with carbon capture & storage, and natural gas combustion turbine
- Coal: coal and coal with carbon capture & storage
- Nuclear: nuclear
- Biomass: biomass
- Others: behind the meter PV, concentrated solar power, utility-scale PV, geothermal, hydro, offshore wind, onshore wind, hydro storage, battery storage, and Canadian imports.

Fuel-cycle Results

An average passenger size BEV's hourly fuel-cycle GHG emissions for Illinois, New York, and California grid mixes are determined for the years 2020 and 2050. The respective grid mix (BEV: hour & year) and vehicle parameters (BEV & Gas CV: year) are embodied in the fuel-cycle GHG emissions on a per mile basis for a BEV and gasoline CV in Figure B12. The gasoline CV fuel-cycle GHG emissions are based on a national average passenger size gasoline CV in 2020 and 2050. The BEVs are shown to have lower fuel-cycle GHG emissions than gasoline CVs every hour of the day in 2020 and 2050. The hours with low GHG emissions are due to electricity generation from low GHG emitting resources such as renewables (2 gCO_{2e}/kWh), nuclear (6 gCO_{2e}/kWh), and biomass (53 gCO_{2e}/kWh). These results are consistent with previous studies [27,28].

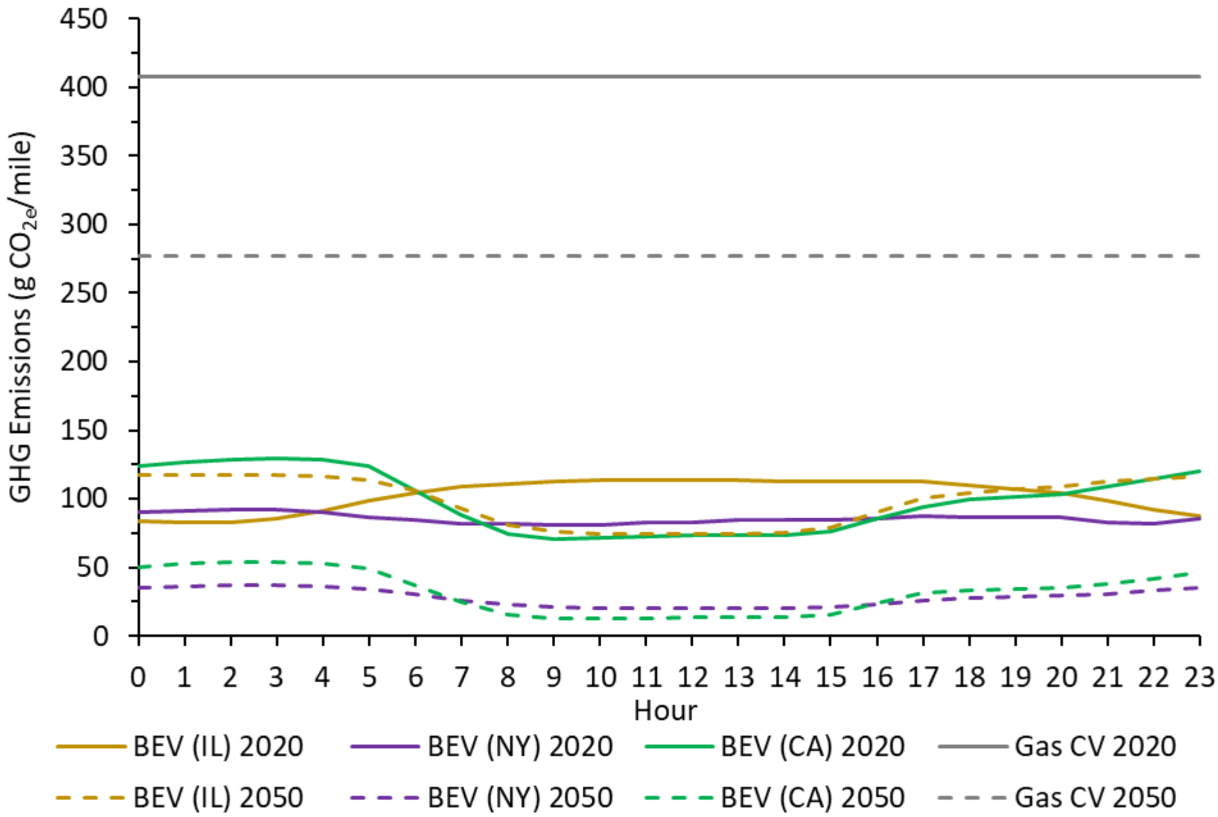

Figure B12. Hourly battery electric vehicle (BEV) fuel-cycle greenhouse gas (GHG) emissions for annual averages in 2020 and 2050 for Illinois (IL), New York (NY), and California (CA) grid mixes. The BEV fuel-cycle GHG emissions are compared to a 2020 and 2050 gasoline conventional vehicle (Gas CV) in the United States. Abbreviations: Carbon Dioxide Equivalent (CO_{2e}), gram (g).

The BEV fuel-cycle GHG emissions vary by both hour and year with the latter having a larger impact for California and New York (Figure B12). In 2020 the BEV fuel-cycle GHG emissions range between 82-114 gCO_{2e}/mi in Illinois, 81-92 gCO_{2e}/mi in New York, and 71-129 gCO_{2e}/mi in California. In comparison, the 2050 BEV fuel-cycle GHG emissions range between 63-117 gCO_{2e}/mi in Illinois, 20-37 gCO_{2e}/mi in New York, and 13-54 gCO_{2e}/mi in California. Thus, the hourly fuel-cycle GHG emissions are reduced from 2020 to 2050 in New York and California by 49-64 gCO_{2e}/mi (-76% to -59%) and 58-75 gCO_{2e}/mi (-82% to -58%), respectively. In Illinois, however, the hourly BEV fuel-cycle GHG emissions in 2020 differ from 2050 by -35 to +39 gCO_{2e}/mi (-42% to +35%) meaning fuel-cycle GHG emissions can be higher in 2050 than in 2020 depending on the time-of-day. Considering that the BEV fuel economy improves from 103 MPGGE in 2020 to 166 MPGGE in 2050 (+61%), the 2050 Illinois grid mix has higher GHG emissions per unit of energy (kWh) by using more natural gas (2020: 17-21%; 2050: 41-73%) and less nuclear (2020: 51-58%; 2050: 0%). Additionally, the gasoline CV reduces emissions by 131 gCO_{2e}/mi (-47%) from 2020 (26 MPGGE) to 2050 (38 MPGGE) due to an improved fuel economy. Thus, from 2020 to 2050 the gasoline CV has a higher nominal reduction to fuel-cycle GHG emissions than the BEV in all three locations, but a lower relative change to fuel-cycle GHG emissions than the BEV in California and New York. Furthermore, the fuel-cycle GHG emissions reduction from BEVs by time-of-day relative to gasoline CVs in 2020 is 72-80% in Illinois, 77-80% in New York, and 68-83% in California; and in 2050 is 58-73% in Illinois, 87-93% in New York, and 80-95% in California. Based on the variability of fuel-cycle GHG emissions reductions by time-of-day and location, the time and location at which the BEV charges will substantially impact the fuel-cycle GHG emissions. The time-of-day is shown to be especially important to grid GHG emissions in Illinois and California but makes little difference in New York, since New York interchanges low GHG emitting resources (nuclear & renewables) during 2020 and small interchanges (Δ <12%) between renewables and natural gas in 2050. This variability underscores the need to understand when and where the BEVs are charging so the appropriate GHG emissions are assigned to them. Moreover, in states with high hourly variability, the BEV charging schedule could be optimized to only charge at the time-of-day when grid GHG emissions are lowest.

In California the emissions are lowest during the daytime (8am-3pm) in 2020 and 2050 when the mix is comprised of more renewables (Ren) (2020: 25-58%; 2050: 60-90%) and less natural gas (NG) (2020: 35-64%; 2050: 10-43%); that is also true for Illinois in 2050 (Ren: 18-49%; NG: 43-71%). Contrastingly, the GHG emissions in Illinois are lowest at nighttime (8pm-3am) in 2020 when the mix is comprised of more renewables (8-14%), more nuclear (51-58%), less coal (11-18%), and less natural gas (17-21%). At a given service location, the optimal times to charge may also depend on the price of electricity from time-of-use rates. Therefore, the optimal times to charge could be determined from both an economic and environmental perspective and get more complicated if a carbon tax is involved. For this limited analysis, however, the total fuel-cycle GHG emissions are calculated by coupling the hourly fuel-cycle GHG emissions with the hourly MUD charging schedule (Figure B3).

Total Cost of Ownership

The custom inputs entered into AFLEET for each TCO scenario are:

- 173K vehicle miles travelled (VMT) over a 15-year period [100].
- Fuel efficiency [100] (BEV: 132 MPGGE; Gas CV: 34 MPGGE) that accounted for an 85% BEV charging efficiency and 155 MPGGE BEV fuel economy.
- LCOC from the TEA for each gasoline CV (3) and BEV (54) scenario. The MUD LCOC was assumed to be the BEV's LCOC hence public and workplace charging costs were not included.
- Medium sized vehicle price in 2020 (Gas CV: $28K; BEV: $35K [103]) that translated to a depreciation value of $25K per gasoline CV and $31K per BEV.

  Default inputs in AFLEET include:

- Maintenance and repair (Gas CV: $32K; BEV: $20K)
- Insurance (Gas CV: $16K-$23K; BEV $18K-$26K)
- License and registration (Gas CV: $320-$2.1K; BEV $320-$3.5K)

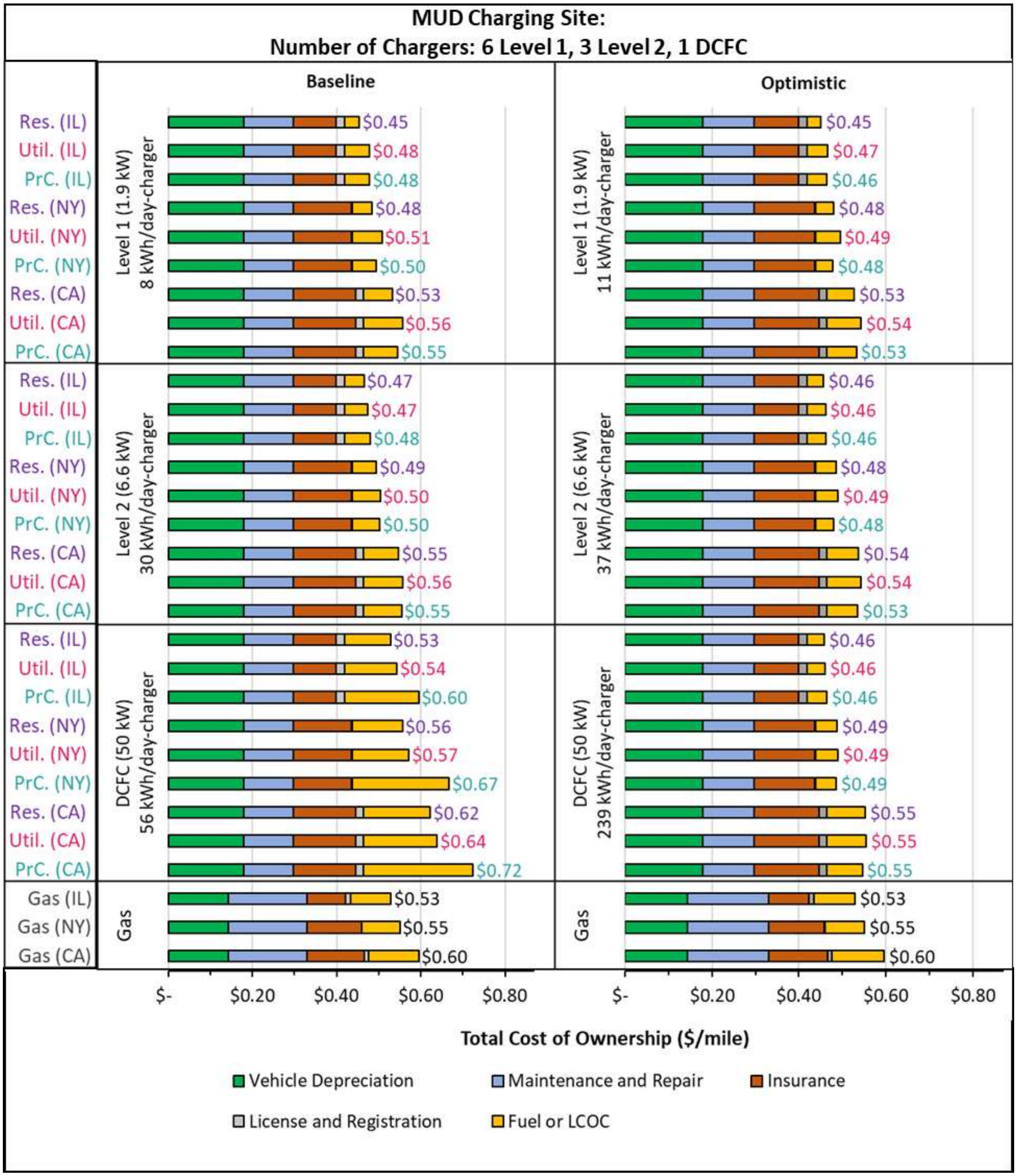

Figure B13. Breakdown of the baseline and optimistic total cost of ownership for a Level 1, Level 2, and DCFC station at a Multi-Unit Dwelling (MUD) in Illinois (IL), New York (NY), and California (CA) for resident (Res.), utility (Util.), and private company (PrC.) ownership models. The total cost of ownership for a gasoline conventional vehicle in Illinois, New York, and California is also included for comparison.

APPENDIX C

Supplementary Text

This section provides instructions on how to open and operate the interactive figures. The interactive figures include Figs. 1-4 and figs. S8-S9. Another short set of instructions are also included within the notebook. The static figures can be downloaded from Data C1 if you prefer not to use the interactive figures.

Step 1: Select the Link to the Google Colab Notebook

Please click the following link to go to the Google Colab Notebook:

https://colab.research.google.com/drive/12nsObq1nqsj1W7OY4caAuYccnlXMIhGx?usp=sharing

You may be prompted to sign-in to your google account if you are not already. Sign-in to your google account to access the notebook.

Step 2: Run the Notebook

To run the notebook, go to the "**Runtime**" ribbon and press "**Run all**". Expect about a 60 second runtime. Note that a warning will pop-up and the code can be viewed by expanding the headers. The script imports the zip folders that contain the images into the notebook workspace, but nothing is downloaded to the computer. Please press "Run Anyway".

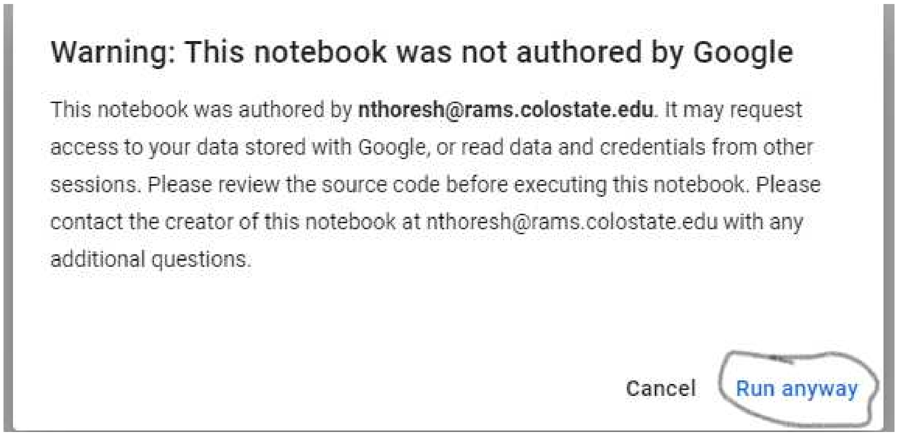

Step 4: View the Figures

Each figure is viewed by expanding the section under the figure's header. The header section is expanded by clicking the arrow to the left of the header.

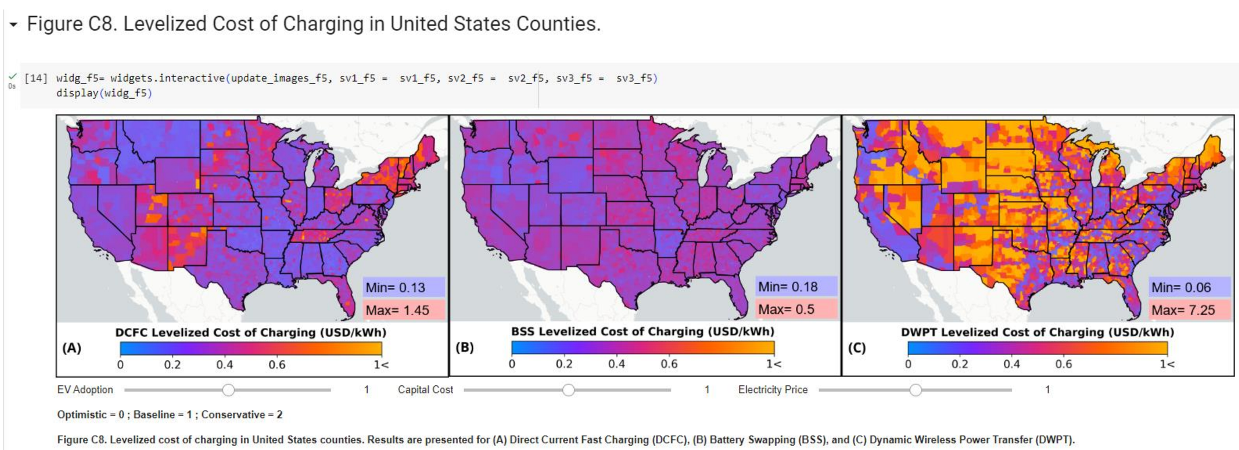

Step 5: Adjust the Scenarios

The figure shown is updated based on scenarios selected with the slider bars. The values of the slider bars are 0 for optimistic, 1 for baseline, and 2 for conservative.

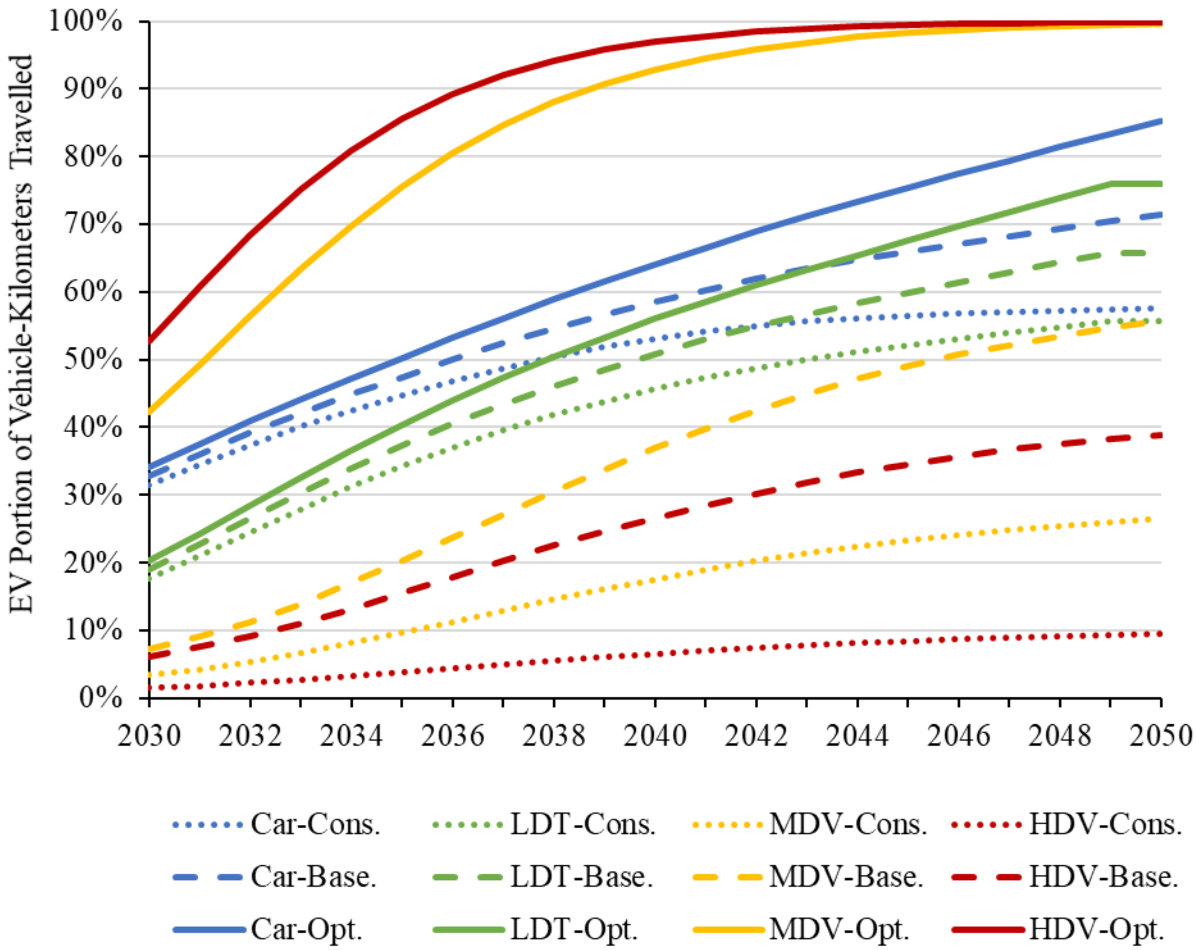

Figure C1. Electric vehicle (EV) adoption scenarios for modeled vehicles. Optimistic (Opt.), baseline (Base.), and conservative (Cons.) adoption rates are presented for electric passenger cars (Car), Light Duty Trucks (LDT), Medium-duty Vehicles (MDV), and Heavy-Duty Vehicles (HDV) [110,117].

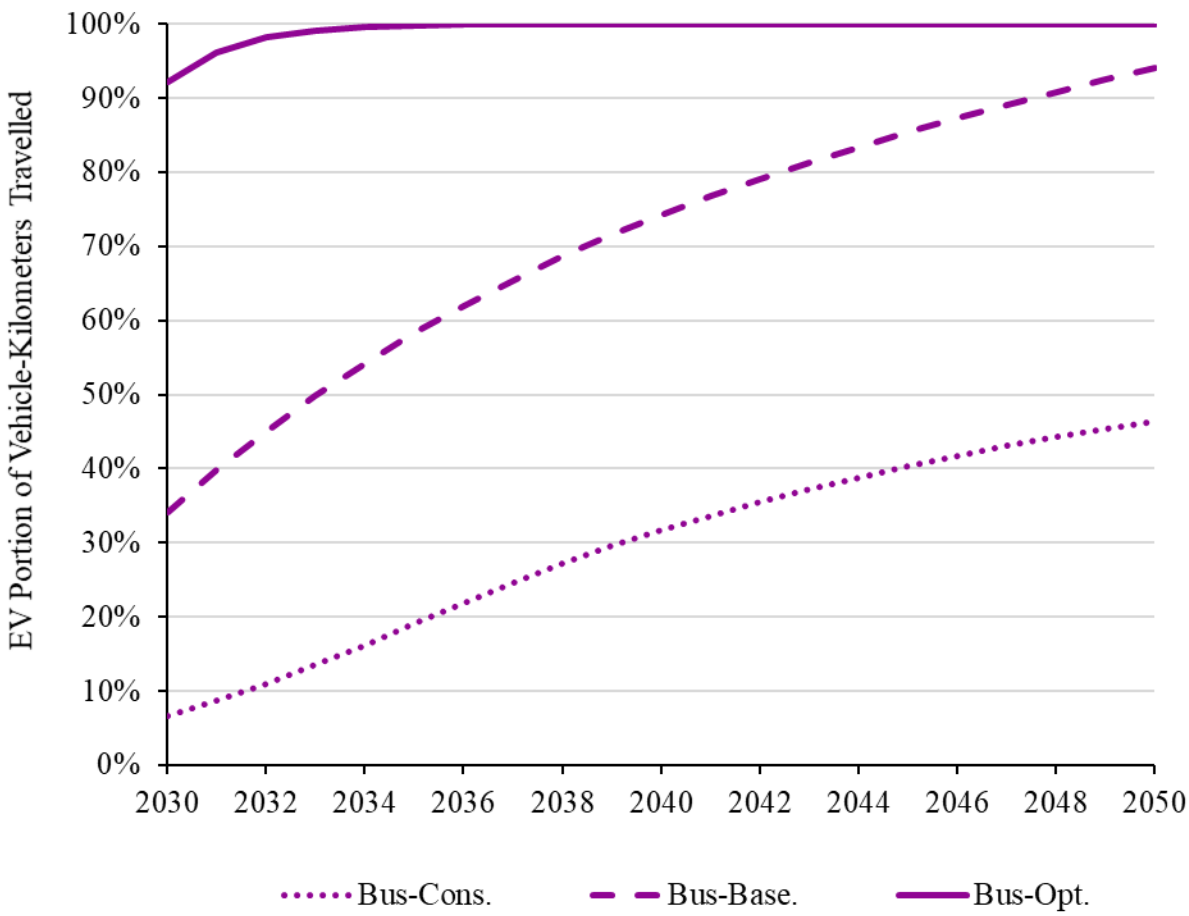

Figure C2. Electric vehicle adoption scenarios for buses. Adoption curves are presented for optimistic (Opt.), baseline (Base.), and conservative (Cons.) scenarios [117].

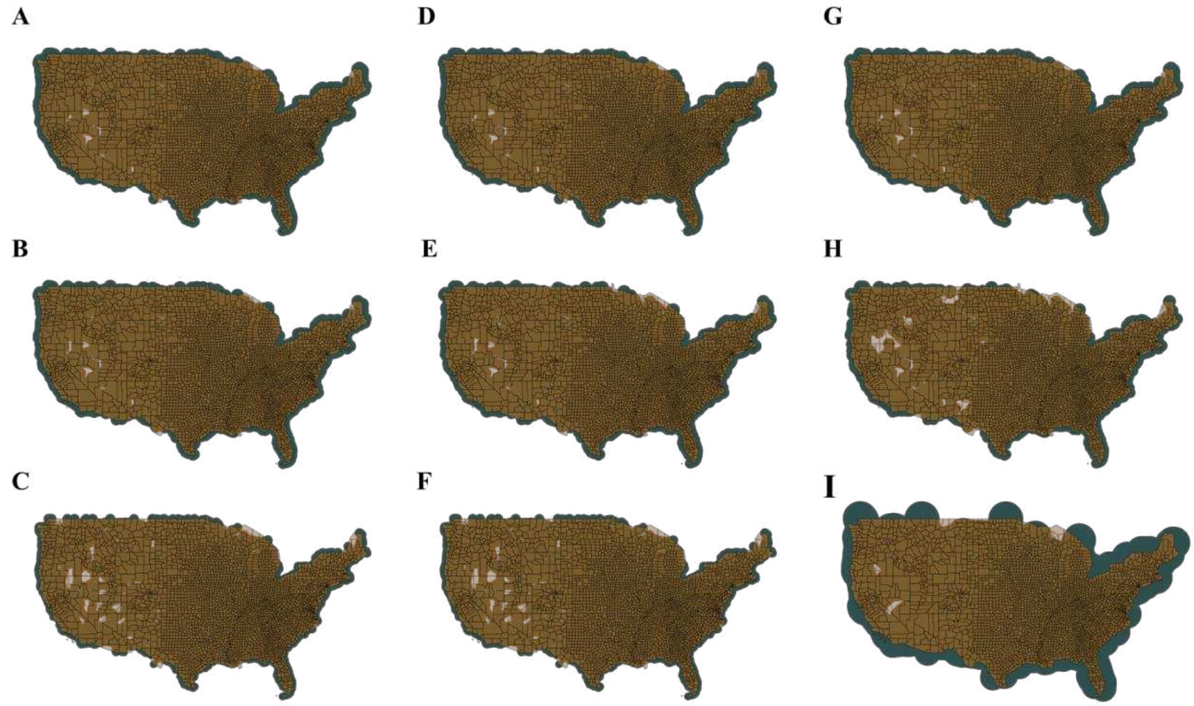

*Figure C3. Charging infrastructure deployment coverage. Coverage is shown by the darkened color for (**A-C**) optimistic, (**D-F**) baseline, and (**G-I**) conservative electric vehicle adoption scenarios with deployment for (**A, D, G**) Direct Current Fast Charging, (**B, E, H**) Battery Swapping, and (**C, F, I**) Dynamic Wireless Power Transfer. A coverage radius of 80 kilometers (50 miles) is used for each Direct Current Fast Charging and Battery Swapping site. Dynamic Wireless Power Transfer roads have a 56 kilometer (35-mile) radius for optimistic and baseline deployment scenarios. The radius for conservative Dynamic Wireless Power Transfer roadways is 214 kilometers (133 miles), which represents the shortest range among electric vehicle categories.*

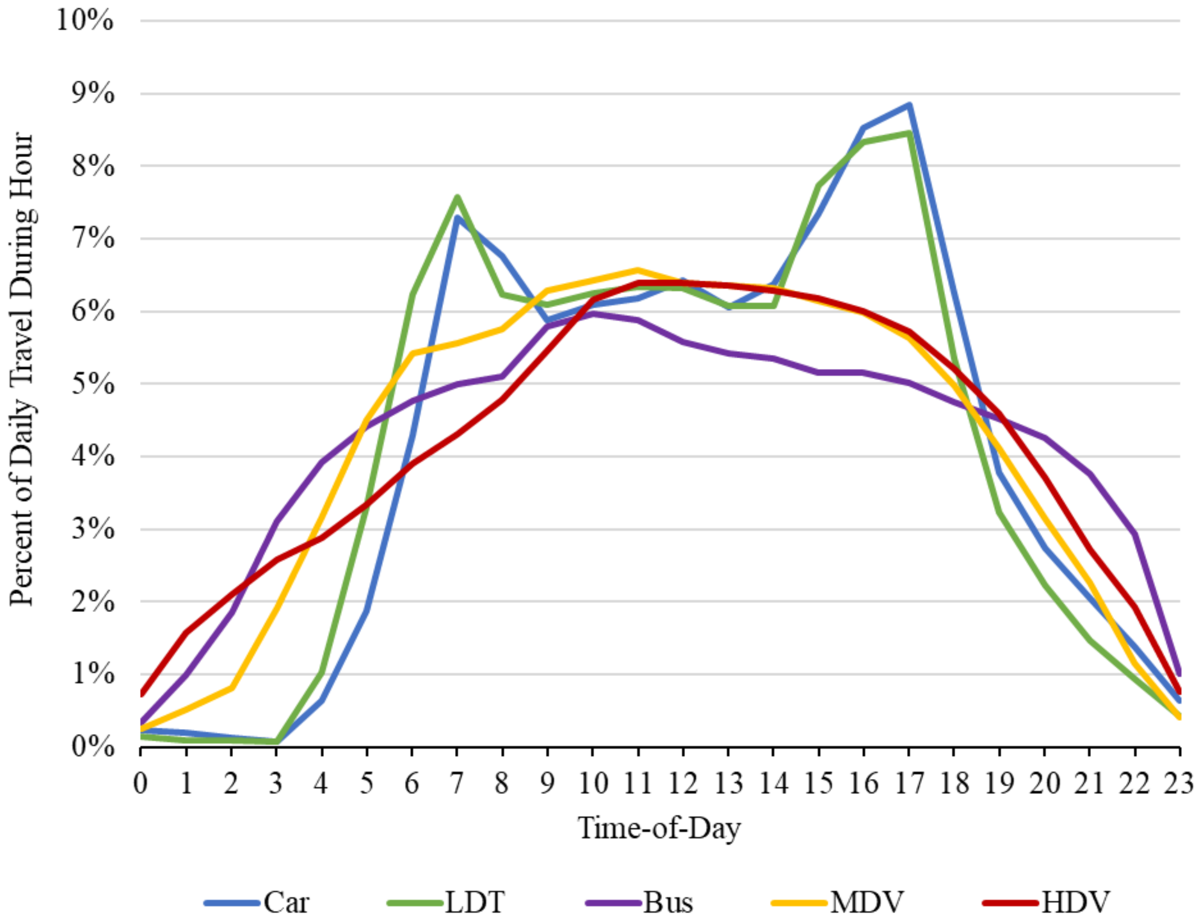

Figure C4. Portion of daily vehicle travel during each hour of the day. Results are shown for passenger cars (Car), Light Duty Trucks (LDT), buses (Bus), Medium-duty Vehicles (MDV), and Heavy-Duty Vehicles (HDV) [132,133].

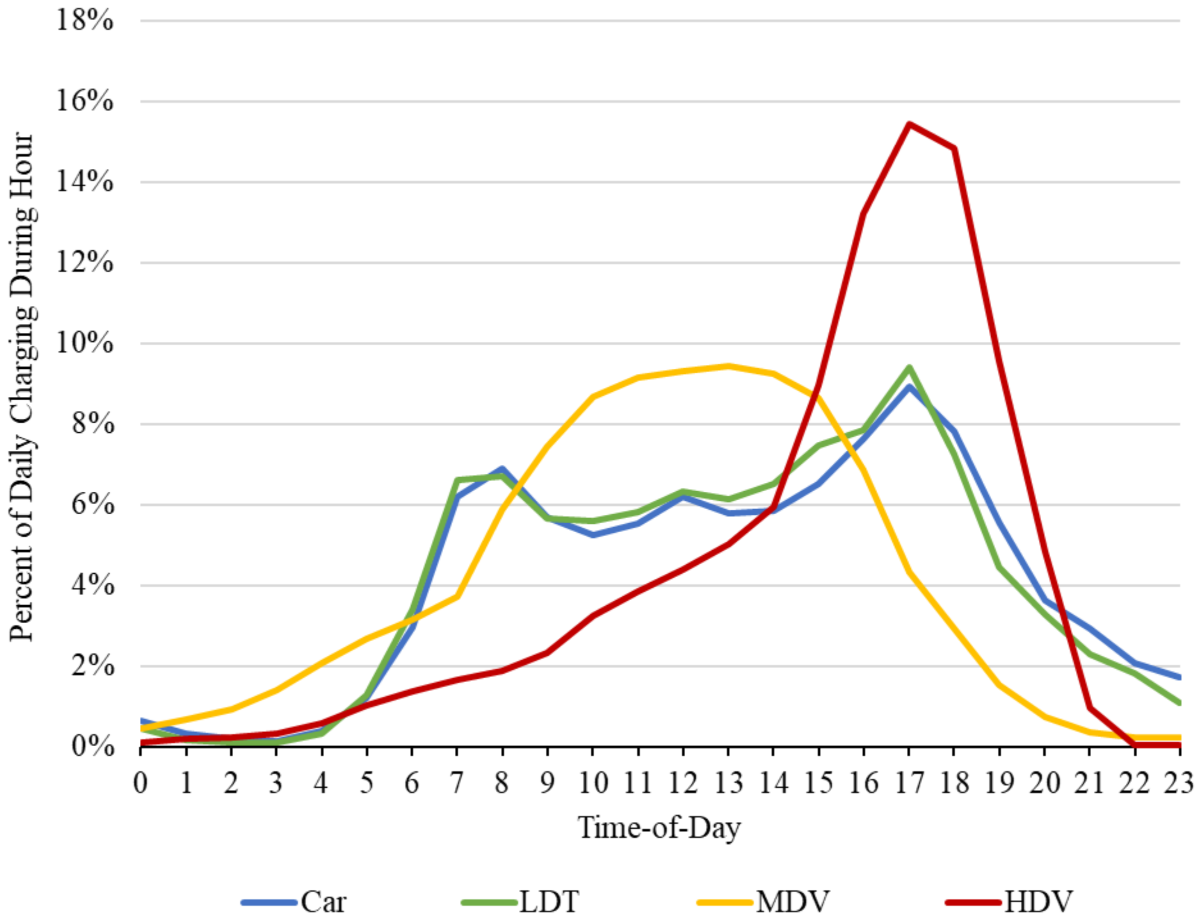

Figure C5. Portion of daily direct current fast charging during each hour of the day. Results are shown for passenger cars (Car), Light Duty Trucks (LDT), Medium-duty Vehicles (MDV), and Heavy-Duty Vehicles (HDV) [132,133].

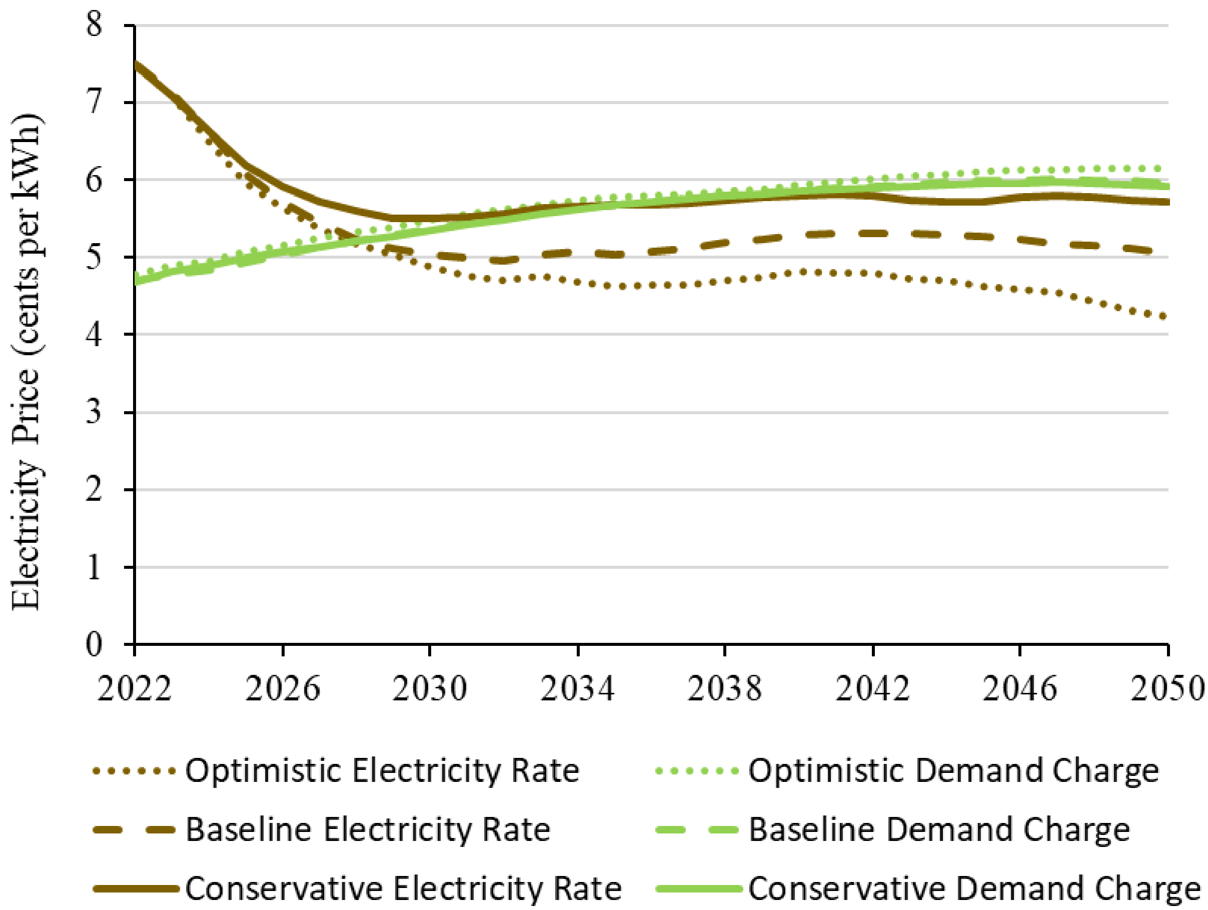

Figure C6. Forecasted electricity prices from 2022 to 2050. Optimistic, baseline, and conservative scenarios are presented for a set of electricity rates (energy) and corresponding demand charges (power) [155].

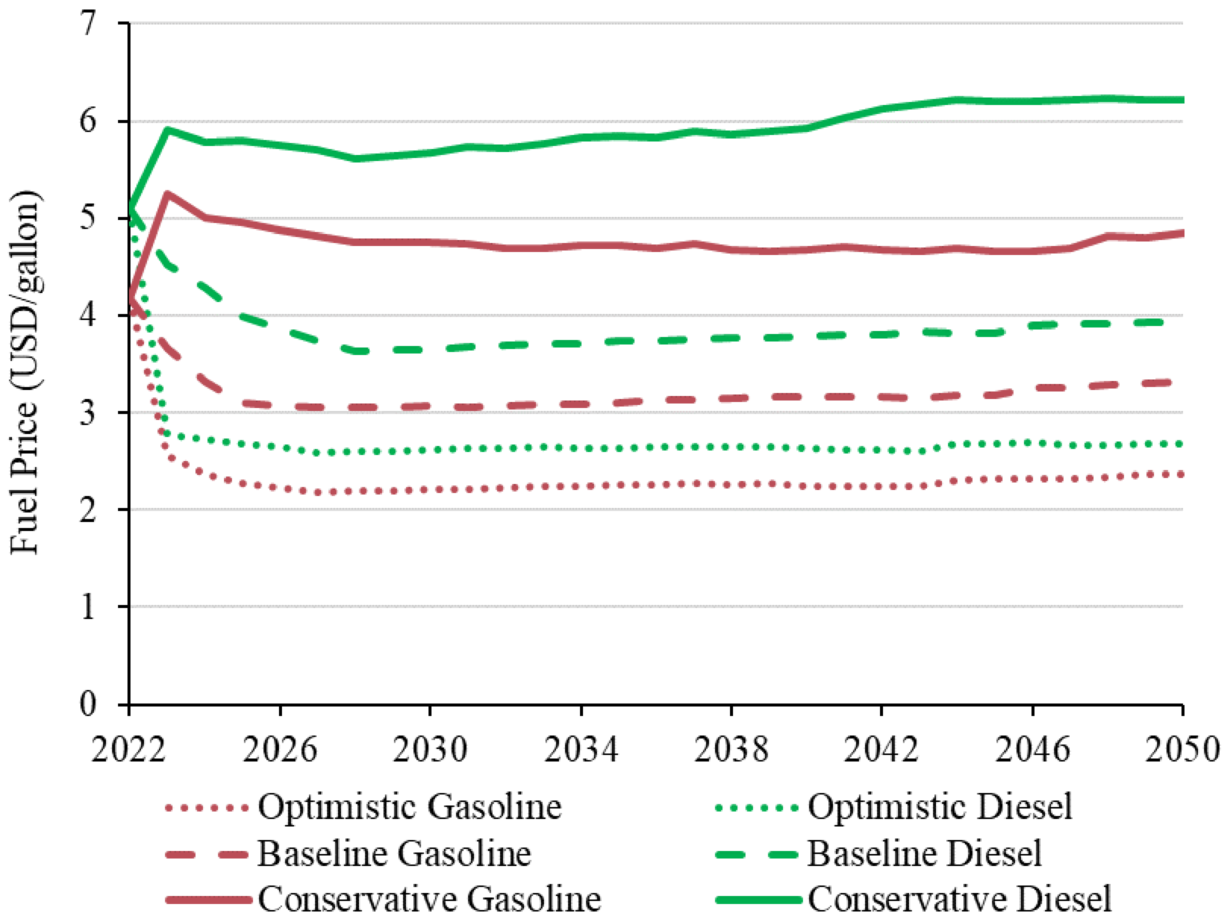

Figure C7. Forecasted fuel prices from 2022 to 2050. Optimistic, baseline, and conservative scenarios are presented for gasoline and diesel fuel [155].

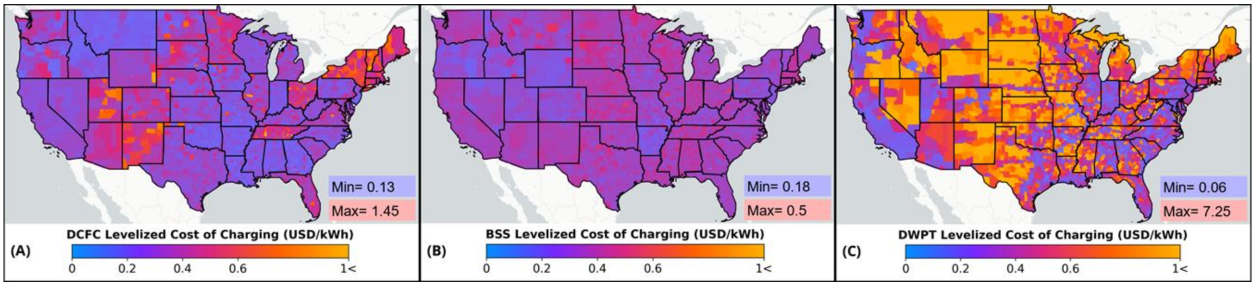

*Figure C8. Levelized cost of charging in United States counties. Results are presented for (**A**) Direct Current Fast Charging (DCFC), (**B**) Battery Swapping (BSS), and (**C**) Dynamic Wireless Power Transfer (DWPT). The baseline scenarios are shown in this static figure with all scenarios shown in the interactive figure or Data C1.*

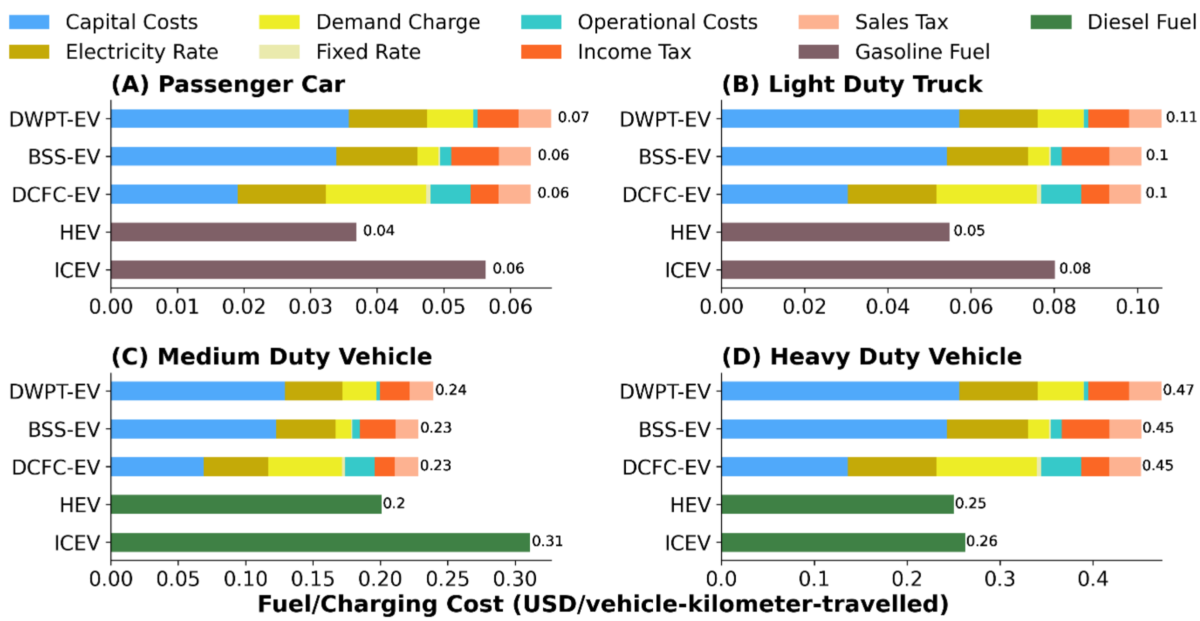

*Figure C9. Breakdown of the charging/fuel cost. Average costs in the contiguous United States are shown for electric vehicles charged via Direct Current Fast Charging (DCFC-EV), Battery Swapping (BSS-EV), and Dynamic Wireless Power Transfer (DWPT-EV). Results are compared to an average internal combustion engine vehicle (ICEV) and hybrid electric vehicle (HEV) fueled by gasoline or diesel for the vehicle categories of (**A**) passenger car, (**B**) light-duty truck, (**C**) medium duty vehicle, and (**D**) heavy duty vehicle. The baseline scenarios are shown in this static figure with all scenarios shown in the interactive figure or Data C1.*

Table C1. Vehicle operating ranges and battery sizes for medium duty vehicles (MDVs) and heavy duty vehicles (HDVs). Abbreviations: kilometer (km), mile (mi), vehicle kilometer travelled (VKT), kilowatt-hour (kWh).

Primary Operating Range [127]	**Operating Distance**	**Portion of MDV VKT** [127]	**Portion of HDV VKT** [127]	**MDV Battery Size**	**HDV Battery Size**	**MDV Portion Public Charging**	**HDV Portion Public Charging**
Off-road	0 km	0.89%	2.7%	90 kWh	90 kWh	0%	0%
Under 80 km (50 mi)	40 km	79%	23%	90 kWh	90 kWh	0%	0%
81 to 161 km (50-100 mi)	121 km	13%	14%	180 kWh	270 kWh	0%	0%
162 to 322 km (101-200 mi)	241 km	3.7%	12%	180 kWh	360 kWh	12%	11%
323 to 805 km (201-500 mi)	563 km	1.8%	19%	450 kWh	810 kWh	5.3%	14%
806 km (501 mi) or more	889 km	1.7%	30%	720 kWh	990 kWh	4.0%	33%

*Table C2. Parameters used for charging systems and vehicles. Capital and operational costs for Direct Current Fast Charging (DCFC), Battery Swapping Stations (BSS), and Dynamic Wireless Power Transfer (DWPT) systems, along with Total Cost of Ownership (TCO) parameters for the modeled passenger car (car), light-duty truck (LDT), medium-duty vehicle (MDV), and heavy-duty vehicle (HDV) as well as electric vehicle (EV), hybrid electric vehicle (HEV), and internal combustion engine vehicle (ICEV). The table shows values for (**A**) optimistic, (**B**) baseline, and (**C**) conservative scenarios in 2022 United States Dollars (USD). Abbreviations: thousand (k), kilowatt (kW), kilowatt-hour (kWh), vehicle kilometers travelled (VKT).*

Parameter	**Value**	**Units**
Direct Current Fast Charging		
150-kW Procurement	(**A**) 103k, (**B**) 119k, (**C**) 136k [15]	USD/charger
350-kW Procurement	(**A**) 174k, (**B**) 189k, (**C**) 204k [15]	USD/charger
150-kW Installation (chargers/site)	59k (1), 47k (2), 35k (3-5), 23k (6+) [141]	USD/charger
350-kW Installation (chargers/site)	82k (1), 65k (2), 48k (3-5), 32k (6+) [141]	USD/charger
Maintenance	5% of procurement [156]	%/charger-year
Network Contract	229 [15]	USD/charger-year
Data Contract	165 [15]	USD/charger-year
Battery Swapping Station		
7.7-kW Procurement	(**A**) 3.4k, (**B**) 3.7k, (**C**) 4.1k [15]	USD/charger
50-kW Procurement	(**A**) 27k, (**B**) 38k, (**C**) 49k [15]	USD/charger
7.7-kW Installation	2.9k [141]	USD/charger

50-kW Installation	22k [141]	USD/charger
Battery Cabinet	175 [176]	USD/kWh-nameplate
Automated Storage and Retrieval System	(**A**) 48k, (**B**) 95k [177], (**C**) 143k	USD/BSS
Building	3.1k [178]	USD/square-meter
Maintenance	5% of procurement [156]	%/charger-year
Dynamic Wireless Power Transfer		
Rural Implementation	(**A**) 0.94M [24], (**B**) 2.7M [114,119], (**C**) 3.9M [119]	USD/lane-km
Urban Implementation	(**A**) 2.2M [24], (**B**) 4.2M [114,119], (**C**) 5.4M [114,119]	USD/lane-km
Replacement Inverter	487k [119]	USD/km
Total Cost of Ownership		
EV Price without Battery	25k (car), 32k (LDT), 100k (MDV), 150k (HDV) [25]	USD/vehicle
EV Battery Price	(**A**) 90, (**B**) 118, (**C**) 150 [118]	USD/kWh-nameplate
EV Battery Full-size	70 (car) [158], 112 (LDT), 122 (MDV), 549 (HDV)	kWh/vehicle
EV Battery Short Range	13 (car), 21 (LDT), 48 (MDV), 94 (HDV)	kWh/vehicle
HEV Selling Price	36k (car), 51k (LDT), 101k (MDV), 190k (HDV) [25]	USD/vehicle
ICEV Selling Price	33k (car), 45k (LDT), 93k (MDV), 179k (HDV) [25]	USD/vehicle
EV Maintenance	0.07 (car), 0.08 (LDT), 0.10 (MDV), 0.11 (HDV) [102]	USD/VKT
HEV Maintenance	0.10 (car), 0.11 (LDT), 0.11 (MDV), 0.12 (HDV) [102]	USD/VKT
ICEV Maintenance	0.11 (car), 0.15 (LDT), 0.15 (MDV), 0.13 (HDV) [102]	USD/VKT
Annual VKT	20k (car), 17k (LDT), 20k (MDV), 96k (HDV) [163]	VKT/vehicle-year
ICEV Fuel Economy	51 (car), 36 (LDT), 11 (MDV), 13 (HDV) [100]	VKT/gallon
HEV Fuel Economy	77 (car), 52 (LDT), 17 (MDV), 14 (HDV) [100]	VKT/gallon

Table C3. Breakdown of the baseline scenario's urban roadway civil cost for dynamic wireless power transfer. The values are in 2022 United States Dollars (USD).

Parameter	**Value (thousand USD per lane-km)**
Electrical	727 [114]
Pavement Removal	106 [114]
Traffic Control	112 [114]
Signage	12 [114]
Soft Cost	820 [114]
Pavement	552 [114]
Install materials	69 [114]
Subtotal	2398
Contingency	10% [114]
Total	2638

Table C4. Average gasoline and diesel fuel prices from 2022 in United States Dollars (USD).

Parameter	**Regular Gasoline (USD/gallon)** [104]	**Diesel (USD/gallon)** [104]
Alabama	3.121	4.148
Arkansas	3.091	3.975
Arizona	3.939	4.439
California	4.924	5.598
Colorado	3.938	4.668
Connecticut	3.322	4.668
Delaware	3.263	4.105
District of Columbia	3.511	4.734
Florida	3.325	4.416
Georgia	3.263	4.292
Iowa	3.25	3.935
Idaho	3.679	4.489
Illinois	3.658	4.306
Indiana	3.404	4.456
Kansas	3.091	3.918
Kentucky	3.17	4.127
Louisiana	3.1	4.05
Massachusetts	3.3	4.757
Maryland	3.303	4.217
Maine	3.429	5.179
Michigan	3.548	4.421
Minnesota	3.32	4.052
Missouri	3.056	3.904
Mississippi	3.018	4.026
Montana	3.274	4.219
North Carolina	3.256	4.174
North Dakota	3.276	4.327
Nebraska	3.291	4.043
New Hampshire	3.264	4.777
New Jersey	3.304	4.32
New Mexico	3.424	4.162
Nevada	4.344	4.694
New York	3.466	4.996
Ohio	3.41	4.319
Oklahoma	3.077	3.814
Oregon	3.91	4.714
Pennsylvania	3.634	4.841
Rhode Island	3.292	4.713
South Carolina	3.18	4.071
South Dakota	3.346	4.144
Tennessee	3.159	4.078
Texas	3.079	3.868
Utah	3.85	4.433

Virginia	3.236	4.273
Vermont	3.443	4.591
Washington	4.247	5.027
Wisconsin	3.338	3.937
West Virginia	3.421	4.442
Wyoming	3.433	4.526

Table C5. Annual license and registration costs. Costs are for cars, light-duty trucks (LDTs), medium-duty vehicles (MDVs), and heavy-duty vehicles (HDVs) in United States Dollars (USD).

State	Car (USD) [25]	LDT (USD) [25]	MDV (USD) [25]	HDV (USD) [25]
Alabama	50	50	586	816
Arizona	160	205	210	930
Arkansas	20	24	130	1350
California	133	378	1325	2119
Colorado	173	198	1788	2105
Connecticut	178	176	281	1520
Delaware	40	40	877	709
District of Columbia	72	155	125	340
Florida	23	33	589	995
Georgia	20	20	365	400
Idaho	53	51	517	3202
Illinois	151	151	1698	2790
Indiana	21	30	811	1351
Iowa	153	214	1060	1695
Kansas	43	52	132	1727
Kentucky	21	21	704	1445
Louisiana	10	30	348	494
Maine	35	35	638	835
Maryland	135	162	596	1288
Massachusetts	30	30	840	1200
Michigan	97	141	975	1277
Minnesota	55	55	865	1760
Mississippi	29	21	1663	2872
Missouri	57	57	63	1720
Montana	115	102	415	315
Nebraska	21	21	138	933
Nevada	33	33	986	1360
New Hampshire	31	43	557	1240
New Jersey	49	69	162	841
New Mexico	40	55	172	172
New York	24	39	334	968
North Carolina	39	57	871	963
North Dakota	66	126	632	1059
Ohio	36	36	740	1351
Oklahoma	81	79	653	954

Oregon	132	132	220	320
Pennsylvania	38	38	882	1688
Rhode Island	48	58	140	1044
South Carolina	40	40	844	1600
South Dakota	65	95	873	1311
Tennessee	27	27	898	1334
Texas	51	51	180	840
Utah	77	68	420	660
Vermont	76	76	271	1910
Virginia	31	36	600	980
Washington	68	88	771	1832
West Virginia	52	52	755	980
Wisconsin	85	100	1135	2578
Wyoming	183	240	60	60

Table C6. Annual insurance costs for a car, light-duty truck (LDT), medium-duty vehicle (MDV), and heavy-duty vehicle (HDV). Cost is per thousand United States Dollars (USD) of vehicle value.

State	**Car (USD)** [25]	**LDT (USD)** [25]	**MDV (USD)** [25]	**HDV (USD)** [25]
Alabama	43.00	43.00	59.00	61.75
Arizona	35.75	35.75	35.00	51.25
Arkansas	53.25	53.25	63.00	64.75
California	53.75	53.75	68.00	61.00
Colorado	50.75	50.75	42.00	52.50
Connecticut	40.50	40.50	97.25	73.75
Delaware	39.25	39.25	99.75	85.25
District of Columbia	36.00	36.00	55.00	56.75
Florida	39.25	39.25	74.00	84.50
Georgia	43.75	43.75	87.25	89.50
Idaho	38.00	38.00	39.50	39.00
Illinois	40.75	40.75	44.25	59.75
Indiana	36.00	36.00	48.50	48.25
Iowa	40.75	40.75	32.25	38.50
Kansas	57.25	57.25	38.25	44.00
Kentucky	58.75	58.75	66.25	67.25
Louisiana	53.00	53.00	113.25	101.75
Maine	29.50	29.50	54.75	59.75
Maryland	35.50	35.50	63.75	69.50
Massachusetts	34.75	34.75	31.25	73.75
Michigan	66.50	66.50	51.25	59.75
Minnesota	39.75	39.75	55.50	55.50
Mississippi	45.75	45.75	20.50	20.25
Missouri	54.25	54.25	44.00	51.00
Montana	52.75	52.75	37.25	41.25
Nebraska	49.75	49.75	36.00	37.50

Nevada	43.00	43.00	61.25	73.25
New Hampshire	32.50	32.50	39.25	49.50
New Jersey	32.25	32.25	119.25	87.75
New Mexico	38.50	38.50	42.00	42.25
New York	41.25	41.25	101.00	73.50
North Carolina	26.50	26.50	42.75	46.00
North Dakota	50.00	50.00	37.00	40.00
Ohio	31.75	31.75	40.75	43.00
Oklahoma	55.75	55.75	53.75	58.00
Oregon	34.75	34.75	48.75	48.75
Pennsylvania	44.75	44.75	43.25	54.00
Rhode Island	51.75	51.75	80.75	74.75
South Carolina	36.25	36.25	54.00	58.00
South Dakota	68.25	68.25	38.50	39.00
Tennessee	55.00	55.00	55.00	59.75
Texas	41.75	41.75	60.50	62.75
Utah	31.50	31.50	52.50	48.25
Vermont	39.25	39.25	39.75	41.75
Virginia	30.75	30.75	57.25	57.00
Washington	32.25	32.25	48.75	55.00
West Virginia	46.00	46.00	67.25	63.50
Wisconsin	39.75	39.75	38.50	40.00
Wyoming	56.25	56.25	28.25	31.00

Table C7. State level income and sales tax rates. Sales taxes rates are an average of the combined county and state rates.

State	**Income Tax** [146]	**Sales Tax** [145]
Alabama	6.5%	9.2%
Arizona	4.9%	8.4%
Arkansas	5.3%	9.5%
California	8.8%	8.8%
Colorado	4.6%	7.8%
Connecticut	7.5%	6.4%
Delaware	8.7%	0.0%
District of Columbia	8.3%	6.0%
Florida	5.5%	7.0%
Georgia	5.8%	7.3%
Idaho	5.8%	6.0%
Illinois	9.5%	8.8%
Indiana	4.9%	7.0%
Iowa	5.5%	6.9%
Kansas	4.0%	8.7%
Kentucky	5.0%	6.0%
Louisiana	3.5%	9.5%

Maine	3.5%	5.5%
Maryland	8.3%	6.0%
Massachusetts	8.0%	6.3%
Michigan	6.0%	6.0%
Minnesota	9.8%	7.5%
Mississippi	5.0%	7.1%
Missouri	4.0%	8.3%
Montana	6.8%	0.0%
Nebraska	5.6%	6.9%
Nevada	0.0%	8.2%
New Hampshire	7.5%	0.0%
New Jersey	6.5%	6.6%
New Mexico	4.8%	7.8%
New York	6.5%	8.5%
North Carolina	2.5%	7.0%
North Dakota	3.6%	7.0%
Ohio	0.0%	7.2%
Oklahoma	4.0%	9.0%
Oregon	6.6%	0.0%
Pennsylvania	9.0%	6.3%
Rhode Island	7.0%	7.0%
South Carolina	5.0%	7.4%
South Dakota	0.0%	6.4%
Tennessee	6.5%	9.5%
Texas	0.0%	8.2%
Utah	4.9%	7.2%
Vermont	8.5%	6.2%
Virginia	6.0%	5.8%
Washington	0.0%	9.3%
West Virginia	6.5%	6.5%
Wisconsin	7.9%	5.4%
Wyoming	0.0%	5.2%

Table C8. Breakdown of vehicle emissions. The global warming potential is given for multiple vehicle types: electric vehicles (EV), hybrid electric vehicles (HEVs), and internal combustion engine vehicles (ICEVs); and vehicle categories: car, light-duty truck (LDT), medium-duty vehicle (MDV), and heavy-duty vehicle (HDV). Abbreviations: Carbon Dioxide Equivalent (CO_{2e}), metric tonne (t), gram (g), vehicle kilometer traveled (VKT).

Parameter	**Car** [100]	**LDT** [100]	**MDV** [100]	**HDV** [100]
Embodied Vehicle Emissions				
EV Full-Size Battery	5.7 tCO_{2e}/ battery-life	9.0 tCO_{2e}/ battery-life	11 tCO_{2e}/ battery-life	37 tCO_{2e}/ battery-life
EV Reduced Battery	1.0 tCO_{2e}/ battery-life	1.7 tCO_{2e}/ battery-life	5.3 tCO_{2e}/ battery-life	9.0 tCO_{2e}/ battery-life

EV Other Components	5.0 tCO_{2e}/life	8.4 tCO_{2e}/life	34 tCO_{2e}/life	74 tCO_{2e}/life
HEV	6.1 tCO_{2e}/life	10 tCO_{2e}/life	38 tCO_{2e}/life	83 tCO_{2e}/life
ICEV	6.2 tCO_{2e}/life	10 tCO_{2e}/life	37 tCO_{2e}/life	81 tCO_{2e}/life
Feedstock and Fuel Emissions				
HEV	26 g-CO_{2e}/VKT	39 g-CO_{2e}/VKT	123 g-CO_{2e}/VKT	156 g-CO_{2e}/VKT
ICEV	40 g-CO_{2e}/VKT	57 g-CO_{2e}/VKT	191 g-CO_{2e}/VKT	164 g-CO_{2e}/VKT
Operating Emissions				
HEV	112 g-CO_{2e}/VKT	166 g-CO_{2e}/VKT	597 g-CO_{2e}/VKT	757 g-CO_{2e}/VKT
ICEV	171 g-CO_{2e}/VKT	243 g-CO_{2e}/VKT	924 g-CO_{2e}/VKT	793 g-CO_{2e}/VKT

Table C9. Breakdown of Direct Current Fast Charging infrastructure emissions. Abbreviations: Carbon Dioxide Equivalent (CO_{2e}), metric tonne (t).

Parameter	**Value (t-CO_{2e}/charger)**
Charger Pedestal	7.1 [165,167]
150-kW Power Cabinet	2.4
350-kW Power Cabinets	4.9
Implementation	7.9 [168]
Construction	1.4 [166]
Total 150-kW	19
Total 350-kW	21

Table C10. Breakdown of one power cabinet's global warming potential. Abbreviations: Carbon Dioxide Equivalent (CO_{2e}), kilogram (kg).

Material	**Emissions Rate (kg-CO_{2e}/kg)**	**Weight (kg)**	**Total GWP (kg-CO_{2e})**
Steel	1.1 [165]	847	915
Copper	0.82 [165]	327	267
Fiberglass	8.8 [165]	45	400
Aluminum	7.3 [165]	115	844
Ferrite	2.0 [165]	6	12
Total		1340	2439

Table C11. Breakdown of Battery Swapping (BSS) infrastructure emissions. Abbreviations: Carbon Dioxide Equivalent (CO_{2e}), kilogram (kg), kilowatt-hour (kWh).

Parameter	**Value**	**Units**
7.7-kW Charger Pedestal	312 [165,179]	kg-CO_{2e}/charger
50-kW Charger Pedestal	4673 [165,180]	kg-CO_{2e}/charger
7.7-kW Construction	200 [166]	kg-CO_{2e}/charger
50-kW Construction	1380 [166]	kg-CO_{2e}/charger
Automated Supply and Retrieval System	346 [165]	kg-CO_{2e}/BSS
Building	36 [165]	kg-CO_{2e}/square-meter
Car Battery	5348 [100]	kg-CO_{2e}/battery

LDT Battery	8961 [100]	kg-CO_{2e}/battery
MDV Battery	10694 [100]	kg-CO_{2e}/battery
HDV Battery	36865 [100]	kg-CO_{2e}/battery
Battery Cabinet	270 [165,181]	kg-CO_{2e}/kWh

Table C12. Breakdown of Dynamic Wireless Power Transfer infrastructure emissions. Abbreviations: Carbon Dioxide equivalent (CO_{2e}), metric tonne (t), kilometer (km).

Parameter	**Value (t-CO_{2e}/lane-km)**
Electronic Components [169]	
Transformer	18.58 [165]
AC/DC Converter	16.10 [165]
Shelter	0.11 [165]
Super-Capacitors Box	0.01 [165]
Control Power Supply	0.38 [165]
Coil	2.90 [165]
Connectors	0.06 [165]
Capacitors	2.06 [165]
Power Electronics Board	0.53 [165]
Housing	0.55 [165]
Connectors	0.06 [165]
Distribution lines	25.19 [165]
Pavement	
Concrete	3388.35 [114,165]
Reinforcement bars	63.20 [114,165]
Transportation	
Electronic Components	0.54 [165,169]
Pavement	21.19 [165,169]
Equipment	0.43 [165,169]
Construction	
Milling	0.36 [165,169]
Sweeping	0.02 [165,169]
Paver	0.32 [165,169]
Total	3540.95

Table C13. Emissions factors for Cambium (2022) resources. All values are in kilograms of Carbon Dioxide equivalent per kilowatt-hour. Unknown values are either set equal to zero or equal to the value from other regions. Abbreviations: oil-gas-steam (o-g-s), natural gas combined cycle (gas-cc), natural gas combustion turbine (gas-ct), hydropower (hydro), onshore wind (wind-ons), offshore wind (wind-ofs), concentrating solar power (csp), utility scale photovoltaics (upv), behind-the-meter photovoltaics (distpv), pumped hydro storage (phs), bioenergy with carbon capture and storage (beccs), renewable energy combustion turbine (re-ct), coal with carbon capture and storage (coal-ccs), natural gas combined cycle with carbon capture and storage (gas-cc-ccs), Midwest Reliability Organization (MRO), Northeast

Power Coordinating Council (NPCC), Reliability First Corporation (RFC), SERC Reliability Corporation (SERC), Texas Reliability Entity (TRE), Western Electricity Coordinating Council (WECC).

Cambium (2022) Resource [182]	**MRO** [165]	**NPCC** [165]	**RFC** [165]	**SERC** [165]	**TRE** [165]	**WECC** [165]
nuclear	0.0066	0.0066	0.0066	0.0066	0.0066	0.0066
coal	1.25	1.24	1.21	1.28	1.23	1.23
o-g-s	1.27	1.18	1.22	1.03	1.10	1.86
gas-cc	0.44	0.44	0.43	0.46	0.43	0.42
gas-ct	0.68	0.66	0.64	0.74	0.64	0.60
hydro	0.0054	0.0054	0.0054	0.0054	0.0054	0.0054
geothermal	0.067	0.067	0.067	0.067	0.067	0.067
biomass	0.041	0.041	0.041	0.041	0.041	0.041
wind-ons	0.015	0.015	0.015	0.015	0.015	0.015
wind-ofs	0.016	0.016	0.016	0.016	0.016	0.016
csp	0.047	0.047	0.047	0.047	0.047	0.047
upv	0.068	0.068	0.068	0.068	0.068	0.056
distpv	0.071	0.071	0.071	0.071	0.070	0.059
phs	0.029	0.029	0.029	0.029	0.029	0.029
battery	0.0017	0.0017	0.0017	0.0017	0.0017	0.0017
beccs	0	0	0	0	0	0
re-ct	0	0	0	0	0	0
coal-ccs	0	0	0	0	0	0
gas-cc-ccs	0	0	0	0	0	0
canada	0.40	0.42	0	0	0	0.45

Data C1

Below are the links to the direct download of the static figures. The figure downloads are separated such that they are less than 25-MegaBytes each, however, the cumulative file size is about 250-MegaBytes. Note that it is recommended to try to use the interactive figures instead (Supplementary Text), so the figures can be viewed seamlessly and do not need to be downloaded.

Figure 13. Total change in cost due to electric vehicle (EV) adoption.
*County level results are presented for the change in total cost of ownership due to the transition from internal combustion engine vehicles (ICEVs) to EVs (**A-C**) as a percentage and (**D-F**) in billions (B) of 2022 United States Dollars (USD). Each map corresponds to EVs charged via (**A, D**) Direct Current Fast Charging (DCFC), (**B, E**) Battery Swapping (BSS), and (**C, F**) Dynamic Wireless Power Transfer (DWPT). The numbers in the file names correspond to [EV adoption; capital cost; electricity price; fuel price] with scenario values of 1 for optimistic, 2 for baseline, and 3 for conservative.*

Link to download (**A**): https://drive.google.com/uc?export=download&id=1nJmobH9Qd-90CJuT-bTWdylGh5BGitre;
Link to download (**B**): https://drive.google.com/uc?export=download&id=1LZOzT7VuXOwvpx-cXcLSGsWohA_G4gFb;
Link to download (**C**):
https://drive.google.com/uc?export=download&id=1Wf_YZiZ0vaZMTOAEo8tTxsSgdkICfP1D;
Link to download (**D**):
https://drive.google.com/uc?export=download&id=1uM5sNUrRfZe0qhPtHK0SER5BaWzfeZm;
Link to download (**E**):
https://drive.google.com/uc?export=download&id=1388qQJqZHnyNtrs39pc8jtlQ3NAT4XVO;
Link to download (**F**): https://drive.google.com/uc?export=download&id=1-RSfxkWh8CJmNqMHBy75OMAvT-_Mq8r3

Figure 14. Breakdown of the 10-year total cost of ownership.
*Results are presented for an average (**A**) passenger car, (**B**) light-duty truck, (**C**) medium duty vehicle, and (**D**) heavy duty vehicle in the contiguous United States. The vehicle types include electric vehicles charged via Direct Current Fast Charging (DCFC-EV), Battery Swapping (BSS-EV), and Dynamic Wireless Power Transfer (DWPT-EV). The EVs are compared to an average internal combustion engine vehicle (ICEV) and hybrid electric vehicle (HEV) from each vehicle category. The numbers in the file names correspond to [EV adoption; capital cost; electricity price; fuel price] with scenario values of 1 for optimistic, 2 for baseline, and 3 for conservative. Link to download:*

https://drive.google.com/uc?export=download&id=1Yv6dAYRmojcg2pb34xJMT6QRQeNOKDRF.

Figure 15. Total change to global warming potential (GWP) from electric vehicle (EV) adoption.
*The maps are for the change in GWP of on-road vehicle transportation in United States counties by switching from internal combustion engine vehicles (ICEVs) to EVs charged via (**A, D**) Direct Current Fast*

*Charging (DCFC), (**B, E**) Battery Swapping (BSS), and (**C, F**) Dynamic Wireless Power Transfer (DWPT). The results are presented as (**A-C**) a percentage and (**D-F**) in billions (B) of kilograms (kg) of Carbon Dioxide equivalent. The numbers in the file names correspond to [EV adoption; electricity mix] with scenario values of are 1 for optimistic, 2 for baseline, and 3 for conservative.*

Link to download (**A-C**):
https://drive.google.com/uc?export=download&id=1dFxwqK2lNXCIedRstfVl4Qq890OXVbHx;
Link to download (**D-F**):
https://drive.google.com/uc?export=download&id=1ozqPKqDPLVwX4An0BrPQLg6aJx8ZrSuq.

Figure 16. Breakdown of the lifetime global warming potential.
Results are for an average (A) passenger car, (B) light-duty truck, (C) medium duty vehicle, and (D) heavy duty vehicle in the contiguous United States. The vehicle scenarios include electric vehicles (EVs) charged via Direct Current Fast Charging (DCFC-EV), Battery Swapping (BSS-EV), and Dynamic Wireless Power Transfer (DWPT-EV). Results are compared to an internal combustion engine vehicle (ICEV) and hybrid electric vehicle (HEV) from each vehicle category. The numbers in the file names correspond to [EV adoption; electricity mix] with scenario values of 1 for optimistic, 2 for baseline, and 3 for conservative. Link to download:
https://drive.google.com/uc?export=download&id=12ZT3IIvbezkXq3mK8Avu88x_GuD3e7zh.

Figure C8. Levelized cost of charging in United States counties.
*Results are presented for (**A**) Direct Current Fast Charging (DCFC), (**B**) Battery Swapping (BSS), and (**C**) Dynamic Wireless Power Transfer (DWPT). The numbers in the file names correspond to [EV adoption; capital cost; electricity price] with scenario values of 1 for optimistic, 2 for baseline, and 3 for conservative. Link to download:*
https://drive.google.com/uc?export=download&id=1XFjSzAZtMryOgmuoiAtGBG_-HjzJpUXw.

Figure C9. Breakdown of the charging/fuel cost.
Average costs in the contiguous United States are shown for electric vehicles charged via Direct Current Fast Charging (DCFC-EV), Battery Swapping (BSS-EV), and Dynamic Wireless Power Transfer (DWPT-EV). Results are compared to an average internal combustion engine vehicle (ICEV) and hybrid electric vehicle (HEV) fueled by gasoline or diesel for the vehicle categories of (A) passenger car, (B) light-duty truck, (C) medium duty vehicle, and (D) heavy duty vehicle. The numbers in the file names correspond to [EV adoption; capital cost; electricity price; fuel price] with scenario values of 1 for optimistic, 2 for baseline, and 3 for conservative. Link to download:
https://drive.google.com/uc?export=download&id=1bTR6pbAy-k6UabRSWS5rR4U7sfW1y7jd.